Bioengineering Devices for the Treatment of Hearing Dysfunctions

Samuel Mark Flaherty

2020

Supervised by

Dr Andrei N. Lukashkin

University of Brighton

School of Pharmacy and Biomolecular Sciences
Centre for Regenerative Medicine and Devices

A thesis submitted to fulfil the requirements of the University of Brighton for the degree of Doctor of Philosophy, June 2021

Declaration of Originality

I declare that the research contained in this thesis, unless otherwise formally indicated within the text, is the original work of the author. The thesis has not been previously submitted to this or any other university for a degree and does not incorporate any material already submitted for a degree.

Samuel Mark Flaherty

Monday 28th June 2021

Acknowledgements

I would like to thank my supervisors Dr. Andrei N. Lukashkin, Professor Ian J. Russell and Dr. Victoria A. Lukashkina for their guidance, patience and continued support during my PhD studies. I am grateful for the time they generously spent supervising me during this degree. Andrei, I will miss our late evening chats that always made me laugh during times of stress and hardship.

I would like to thank James Hartley for his technical expertise and for building the set ups we all use today. May you rest in peace.

I give thanks to Dr. Jacqueline Mayer and the bioresources team for their technical assistance, general support and friendship. I also thank the students who worked with me and assisted where needed.

I thank my parents, Simon Flaherty and Jane Flaherty for their never-ending support and love, whom without, I would not have been able to pursue my adventure into scientific research. I thank my siblings for their care, support and friendship during my studies. I thank my grandparents for their guidance and support throughout my education.

I would like to thank my friends, in particular Daniel Holley, for their support, friendship and laughter.

And last but not least, I would like to thank my partner and best friend, Clarice Head, for staying by my side through it all. Thank you for always being there to offer advice, for listening to my endless worries and for your continued love. Without you, I would be truly lost.

Preface

The work presented in this thesis is the work of Samuel M. Flaherty under the supervision of Andrei N. Lukashkin, Ian J. Russell and Victoria A. Lukashkina.

This thesis is a collection of six chapters and one appendix. Chapter one is a general introduction into mammalian hearing, in which the anatomy, mechanics and medical literature of the auditory system are explored. Chapter two describes the materials and methods used in the *in vivo* experiments.

Chapters three, four and five are results sections, written in a scientific paper format, with an abstract, introduction, results and discussion. Chapter three explores the passive diffusion of an arbitrary substance along the cochlear spiral utilising measurements of auditory nerve compound action potential (CAP) thresholds and mathematical modelling. This work was published in the Frontiers, Delivering Therapeutics to the Inner Ear journal, volume 16, article 161, on the 26th April 2019 (Sadreev *et al*., 2019) and the format altered to fit the style of this thesis. The supplementary data has been moved to the results section in chapter three and the appendix, which provides detailed derivations of diffusion along the long axis of a tube with decreasing diameter, has been moved to the last pages of this thesis.

Chapter four looks to determine the efficiency of round window stimulation, of the guinea pig cochlea, using mechanically displacing probes which partially occlude the round window membrane (RWM). Chapter five describes a novel method of drug delivery in the guinea pig cochlea by means of inaudible RWM micro vibrations in an attempt to enhance drug distribution to the cochlear apex. This work was published in Taylor & Francis, Drug Delivery journal, volume 28, issue 1, on the 26th June 2021 and the format altered to fit the style of this thesis.

Chapter six comprises a conclusion of the findings presented in this thesis and suggestions of further work to advance the findings described.

University of Brighton

Samuel Mark Flaherty

Bioengineering Devices for the Treatment of Hearing Dysfunctions

Abstract

Approximately 466 million people, as of 2020, suffer with hearing loss of some degree (Deafness and hearing loss, 2020). Ranging from mild to severe, auditory complications can affect one's ability to communicate, learn and interpret environmental stimuli.

This work looks to provide experimental findings to further understand how the bioengineering of hearing devices can offer auditory rehabilitation to patients with sensorineural, conductive and mixed hearing loss. We explore the fundamental issues with passive intracochlear drug diffusion and the inability to administer drugs to the most apical regions of the cochlea without external assistance. We used sodium salicylate, which inhibits the cochlear amplifier, to determine the path of diffusion by recording compound action potentials thresholds across a wide frequency range in guinea pigs. We conclude that passive diffusion of an arbitrary substance through the round window membrane (RWM) leads to the formation of large substance concentration gradients along the cochlea.

It is known that mechanical stimulation of the RWM, at frequencies similar to that of incoming sound, excites the cochlea. To further explore the efficiency and mechanism of round window stimulation, we designed mechanical displacement probes with different diameters, that partially occlude the round window membrane, to determine cochlear stimulation efficiency. We conclude that round window stimulation can be optimised for maximum cochlear excitation and without the requirement for ossicular chain mobility.

Methods of drug delivery to the entire cochlear spiral are limited. We describe a novel method of cochlear drug delivery, by means of inaudible RWM micro vibrations, which enhance drug-perilymph mixing. We provide a proof of concept that vibrating the RWM at a low frequency, enhances intracochlear drug distribution without impairing hearing.

Table of Contents

List of Figures

List of Tables

Abbreviations:

BAHA: Bone Anchored Hearing Device
BCD: Bone Conduction Device
BLB: Blood Labyrinth Barrier
BM: Basilar Membrane
CAP: Compound action potential
CI: Cochlear Implant
CM: Cochlear Microphonic
CNS: Central Nervous System
DPOAE: Distortion Product Otoacoustic Emission
ECG: Electrocardiogram
EP: Endocochlear Potential
HL: Hearing Loss
IHC: Inner Hair Cell
IM: Intramuscular
IP: Intraperitoneal
MET: Mechanoelectrical Transducer
OHC: Outer Hair Cell
OW: Oval Window
RW: Round Window
RWM: Round Window Membrane
SC: Subcutaneous
SFOAE: Stimulus Frequency Otoacoustic Emission
SM: Scala Media
SP: Summating Potential
SPL: Sound Pressure Level
SNHL: Sensorineural Hearing loss
SSNHL: Sudden Sensorineural Hearing Loss
ST: Scala Tympani
SV: Scala Vestibuli
TEOAE: Transient Evoked Otoacoustic Emission
TM: Tectorial Membrane

Nomenclature

A = Amplitude of displacement of oscillatory motion m

A_{R} = Freely moving area of the round window membrane mm^2

B = Probe amplitude of velocity measured using a laser vibrometer ms^{-1}

f = Frequency stimulation and frequency of oscillatory motion Hz/ kHz

F = Outer hair cell force

FR = Force reduction generated by the outer hair cells

G = Open loop gain of the cochlear amplifier obtained when there is no positive or negative feedback in the system dB

H = Feedback gain of the cochlear amplifier dB

$i\omega q$ = Probe acceleration mm/s^2

k_c = Clearing coefficient drug clearance from the cochlear fluids to surrounding vasculature and compartments

k_d = Diffusion coefficient of passive diffusion referring to salicylate diffusing along the cochlear length

l = Scala tympani length mm

ρ = Fluid density

$P_{inBlock}(x)$ = The sound pressure level required to produce a response from the auditory nerve when the cochlear amplifier is completely blocked.

P_{M} = The average alternating far-field pressure Pa

P_{N} = Near-field pressure Pa

q = Volume velocity/ flow rate mm^3/s

r = Radii of cochlear scala tympani mm

S = Round window membrane stiffness

$S\ (x)$ = Cross sectional area of scala tympani, where x is basilar membrane length mm

t = Time of drug application minutes

V = Velocity of the system ms^{-1}

$Vmax$ = Maximum reaction velocity of prestin saturation

x = Length of the basilar membrane used to illustrate cochlear length mm

ω = Angular velocity of the system. Also written as $2\pi f$ s^{-1}

α = The gain constant

Chapter One

General Introduction

1.1 The Anatomy and Mechanics of the Mammalian Ear

The mammalian ear is a complex sensory organ functioning as an auditory and vestibular apparatus. It is anatomically divided into three fundamental parts: the outer, middle, and inner ears. The outer ear comprises of the auricle, or pinna, providing a sound collecting surface concentrating vibrations into the external auditory meatus, or auditory canal. The middle ear contains the smallest bones of the human body, the ossicular chain, utilised to propagate sound vibrations from the surrounding air into the fluid of the inner ear labyrinth. It is the inner ear which contains the organ of hearing, the cochlea, and the vestibular system (semicircular canals, saccule and utricle) which mediates balance. Figure 1.1 provides an overview of the human ear (Hallowell and Silverman, 1970).

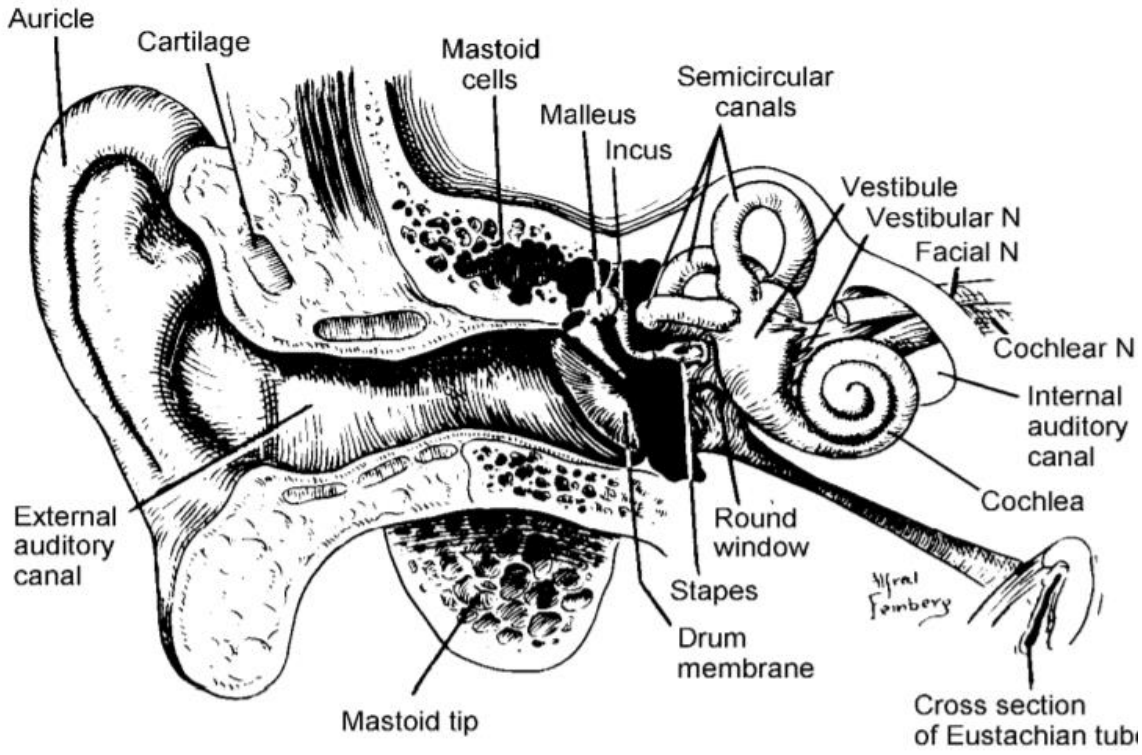

Figure 1.1. The human ear. An overview of the human ear displaying all three fundamental parts. The outer ear begins at the pinna and ends at the tympanic membrane. The middle ear starts at the tympanic membrane, includes the eustachian tube, and finishes at the entrances to the cochlea, the oval and round windows. The inner ear consists of the organ of hearing, the cochleae, and the semicircular canals which mediate balance. (from Hallowell and Silverman, 1970).

The cochlea amplifies mechanical pressure waves and transduces them into corresponding neural signals which are processed by the central nervous system (CNS). Alterations to the periphery of the ear can result in conductive or sensorineural hearing loss (SNHL) and a neurosensory prosthesis, such as a cochlear implant (CI), is required to re-establish the auditory sense. Such devices are not perfect and acoustic rehabilitation is poor. New research has promise for an optimised auditory prosthesis to improve the lives of partial or profoundly deaf individuals which is the subject of the thesis.

1.1.1 The Outer and Middle Ear

The soft and cartilaginous tissue pinna of the outer ear display diverse shapes and sizes across all mammalian species. On the pinna are depressions, the deepest being the concha located at the apex of the auditory canal, which together provide a unique structure. The pinnae functions to localise, collect and direct soundwaves into the external auditory meatus. Mammalian hearing is binaural allowing directional sound perception due to interaural time differences and acoustic intensity. For example, a sound wave approaching the right of the head will strike the right ear before the left thus the perceived auditory stimulus is on the right. However, when sounds approach from the front or behind, above or below, the pinnae enable greater directional acoustic differentiation. By means of sound wave deflection-scattering and frequency manipulation, the external ear allows for acoustic modulation providing directional sound perception and source distance. Soundwaves striking the pinnae are then concentrated, or funnelled, into the concha and then into the auditory canal (Pickles, 2008).

Sound pressure waves travel through the auditory canal of the outer ear stimulating the tympanic membrane and the middle ear ossicular bones. Figure 1.2 displays the sound transmission pathway in mammalian hearing (Fettiplace, 2017). Malleus, the first middle ear bone, is bound to the tympanic membrane via the ‘handle of malleus’. The malleus displaces in response to sound vibrations and propagates the vibrations throughout the middle ear. The malleus displaces the incus and stapes, the second and third ear bones, which are joined by synovial joints transferring the vibrations to the fenestra vestibuli (oval window).

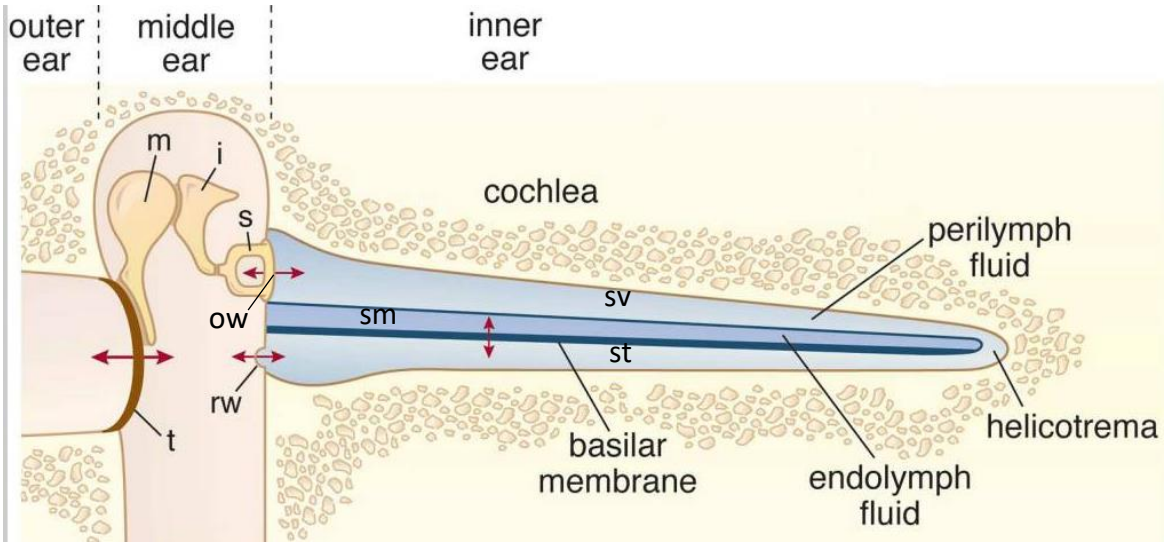

Figure 1.2. Outer, middle, and inner ear. Schematic of uncoiled cochlea displaying the sound transmission pathway from the eardrum to the cochlea. Sound waves vibrate the tympanum (t) and then propagate to the ossicular chain (Malleus: m, Incus i, Stapes: s). The footplate of the stapes behaves like a piston on the oval window (ow) generating pressure waves, in the cochlear fluid, which displace the BM. Pressure is relieved by the round window (rw). The scala vestibuli (sv) and scala tympani (st) contain cochlear fluid and are linked by the helicotrema which acts as a low-pass filter. (Adapted from Fettiplace, 2017).

The stapedial annular ligament binds the stapes and oval window allowing the nanometric displacement of the membranous opening of the cochlea. Below the ossicular chain is the eustachian tube used to equalise the pressure of the middle ear relative to that of the outer ear. Displacement of the OW membrane sends pressure waves into the perilymph and endolymph fluids of the inner ear. The mechanical structure of the outer and middle ear allows for the efficient transfer of sound vibrations from the air to the cochlear fluids over a wide frequency range.

Located in the middle ear, below the ossicular chain, is the eustachian tube, approximately 36mm in length, 12mm making up a shorter bony region and a 24mm cartilaginous region, which base is inserted under the rhinopharynx lateral wall mucosa. The area between the bony and cartilaginous regions behaves similarly to a valve and regulates air intake. The eustachian tube has three major functions; gas exchange and pressure equalisation; mucus clearance from

the middle ear; and prevention of sound or fluid reflux from the nasopharynx (Sade & Ar, 1997). In healthy adults, the eustachian tube remains closed until the cartilaginous portion is momentarily pulled open, during swallowing or yawning, by the soft palate tensor muscle and the soft palate elevator muscle (paratubal muscles) (Poe *et al*., 2000). During periods of paratubal muscle activation, air moves from the nasal pharynx to the middle ear, allowing pressure equalisation between the environmental air and the tympanic cavity air. This mechanism protects the ear by preventing sudden pressure changes, preserving mucosa and allowing the ossicular chain vibrations to be unhindered. Secretions also drain via the action of paratubal muscles to prevent their build up. Secretions leave the middle ear and drain into the nasopharynx. The 'valve' prevents fluids entering the middle ear from the nasopharynx.

Compromised eustachian tube function is a major cause of Otitis Media – a build-up of fluid in the middle ear. An occlusion to the eustachian tube results in poor middle ear ventilation, increasing the absorption of nitrogen, generating negative pressure (Sáenz *et al*., 2005). Otitis media can also be caused by upper airway infections and allergic reactions of the nasal mucosa (Sáenz, *et al*., 2005).

1.1.2 Impedance Transformer

The structure of the middle ear serves a specific task, not only in propagating soundwaves, but also matching the impedance of the air to that of the intracochlear fluids. Materials and substances differ in their response to sound and how effectively they may transfer sound energy. For example, a compressible medium, such as air, has an exact sound pressure that will generate higher velocities of particle movement of that medium, when compared to a denser medium, such as water, where particle movement will be lower. This is known as impedance (Z) and can be quantitated using the formula $Z = p / v$, where (p) is sound pressure and (v) is particle velocity. The impedance of a medium describes how effective sound energy transfer will be for that medium.

Impedance matching of the outer, middle and inner ear media is crucial to ensure efficient sound energy transfer. The middle ear acts as an acoustic impedance transformer. Soundwaves hit the pinna and are channelled into the middle ear, via the auditory canal. From the relatively large surface area of the pinna, sound energy is channelled into a relatively smaller area, the eardrum. This process increases the sound pressure at the tympanic membrane, when compared

to the open air surrounding the head. The ossicular chain of the middle ear couples this sound energy to the cochlea through the OW. The tympanic membrane has a comparatively larger area and lower impedance to that of the much smaller, higher impedance OW. The middle ear apparatus transfers vibrations efficiently from the outer ear to the OW of the cochlea utilising three principals:

1. The area of the tympanic membrane is larger than that of the stapes footplate in the cochlea. The forces collected over the tympanic membrane are therefore concentrated onto a smaller area, increasing the pressure at the OW. The pressure is increased by the ratio of the eardrum and OW areas. This is the most important factor in achieving the impedance transformation.
2. The rigidly attached malleus and incus producing a lever action that increases the force and decreases the velocity at the stapes. This is a comparatively small factor in the impedance match.
3. The tympanic membrane has a conical shape, therefore as the membrane moves in and out, it buckles so that the arm of the malleus moves less than the surface of the membrane. This increases the force and decreases the velocity, although is a comparatively small factor.

Overall, the three principals act to reduce the loss of sound energy, through its reflection, by means of matching the impedance of air and intracochlea fluids. By matching the impedance of the two media, sound energy can be effectively transferred to the cochlea initiating compressive waves in the fluids of the cochlea during OW displacement.

1.1.3 The Cochlea

Situated deep in the temporal bone of humans, 10 mm wide and 5mm from base to apex, is the most complex sensory organ of the body, the cochlea. In a transverse section of the cochlea, the prominent feature is the cochlea duct, a longitudinal division into three separated scalae which spiral together along the length of the cochlea displaying a constant spatial relation. The two outer scalae, vestibuli and tympani, are separated from the central scala media isolating the intracochlear fluids which is essential for ionic distribution. The scala vestibuli is partitioned from the scala media via Reissner’s membrane above the scala media, and the

basilar membrane below separating the scala tympani (ST) (figure 1.3). The outer scalae are interconnected by the helicotrema at the cochlear apex and wrap around the scala media.

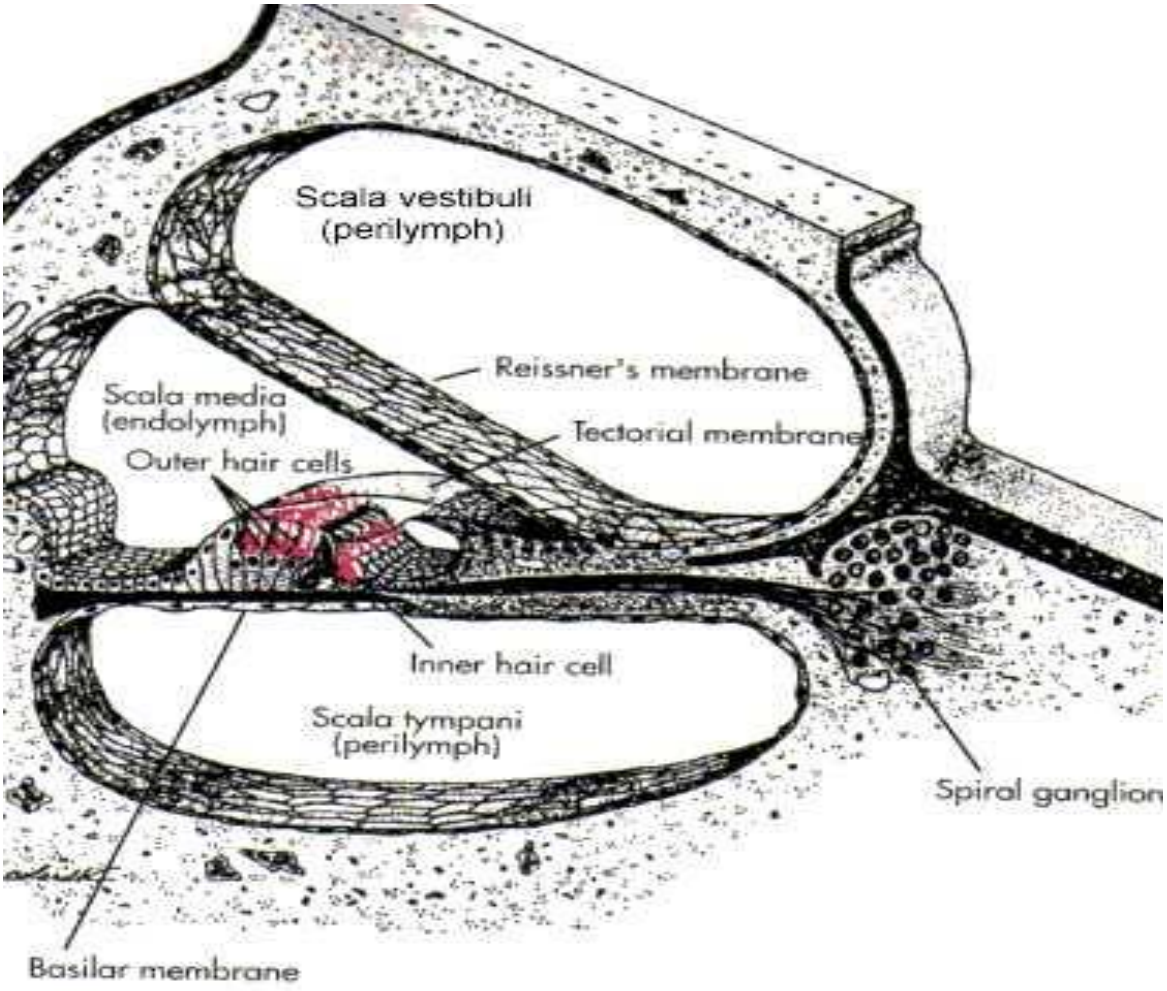

Figure 1.3 The Cochlea. A traverse cross-section of the cochlea. The red region in the Organ of Corti highlights the sensory outer (three rows) and inner (one row) hair cells. (From Nolte, 1993).

The organ of Corti is positioned within the scala media and mounted on top of the basilar membrane. The structurally intricate epithelium of the organ of Corti is characterised by four rows of specialised hair cells and by unique supporting cells - Pillar, Hansen's, Claudius' and Dieters' cells, which provide structural deformability and strength to withstand mechanical sound vibrations. The supporting cells of the organ of Corti, which lie adjacent to the hair cells, collectively function as an epithelium isolating the endolymph of the scala media from the perilymph of the outer scalae.

There are two openings into the cochlea from the middle ear, OW, also known as the fenestra ovalis, and the round window membrane (RWM) also known as the fenestra rotunda (positions shown in figure 1.2 and 1.4). The OW is a membrane of connective tissue which is coupled to the to the tympanic membrane, via the ossicular chain. The OW is surrounded by the annular ligament. The main role of the OW is to propagate sound into the cochlea thus vibrating the inner ear structures.

The RWM is comprised of three layers: the core of connective tissue, outer epithelium and inner epithelium (Carpenter *et* al., 1989; Goycoolea and Lundman, 1997). Collagen fibres, fibroblasts and elastic fibres make up the core of connective tissue, as well as blood and lymph vessels. The outer epithelium comprises of a single layer of epithelial cells which possess a moderate degree of osmophilia (Goycoolea and Lundman, 1997). The epithelial cells of the inner epithelium are squamous, characterising long lateral extensions and tight junctions, which results in stratification. The adult human RWM is usually thicker at the edges than the centre and has an average thickness of around 70µm (Sahni *et al*., 1987), whereas in rodents, it is

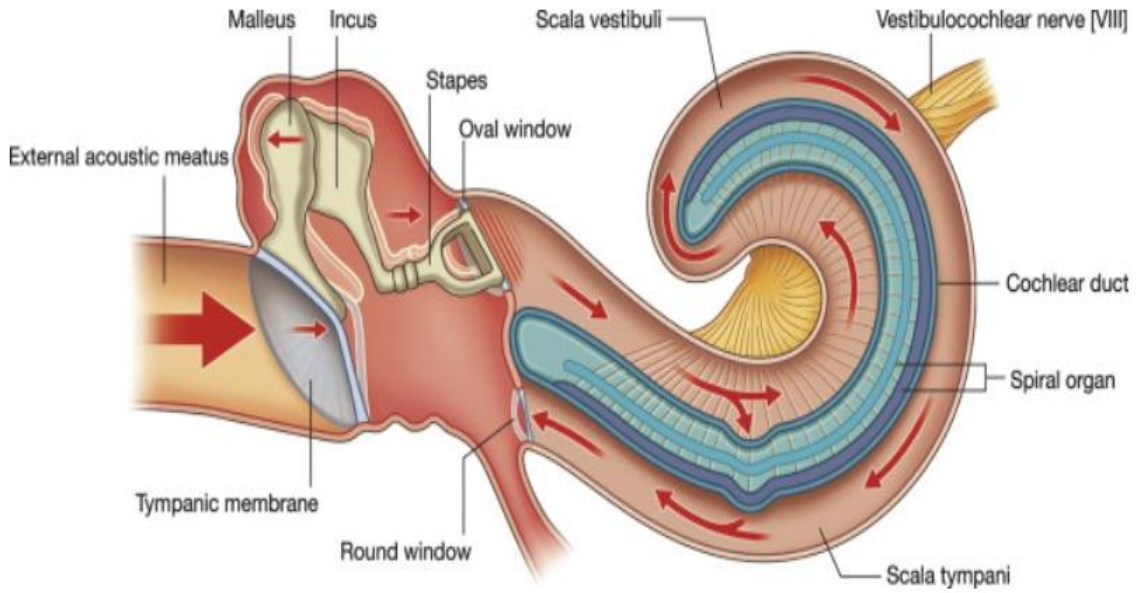

Figure 1.4. Round window location in the cochlea. A diagram showing the direction of fluid flow in conventional hearing. The oval window and round window lie in close proximity to one another and can both be accessed from the middle ear where the malleus, incus and stapes are located. *In situ*, the round window acts as a pressure relief value allowing the movement of the inner ear structures. (From Drake *et al*., 2005).

significantly smaller; 10-14µm for chinchillas (Goycoolea *et al*., 1987), 12µm for rats (Nordang *et al*., 2003) and 10-30µm for guinea pigs (Tanaka and Motomura, 1981).

In guinea pigs, the round window is elliptical in shape and slightly curved with an approximate: surface area of 1.18 mm^2, width of 0.75 mm and length of 1.1 mm (Ghiz *et al*., 2001; Wysocki *et al*., 2005). The human round window (RW) is almost circular in shape, with a surface area of around 2.29-2.58 mm^2 and diameter of approximately 1.8 mm (Okuno and Sando, 1988; Zhang and Gan, 2013).

The primary function of the RWM is to act as a pressure relief valve for the fluids of the cochlea and allowing the movement of the inner ear structures. The RWM is flexible and moves in response to the movement of the OW, during acoustic stimulation, allowing the displacement of the inner ear fluids. Culler *et al* demonstrated in 1935 that a compromised RWM resulted in impaired cochlea activity and thus partial or profound deafness (Culler *et al.*, 1935). RWM complications, such as immobilization, thickening and congenital malformation will result in impaired hearing (Borrmann and Arnold, 2007; Linder *et al*., 2003; Martin *et al*., 2002). These observations outline the physiological importance of the RWM and its contribution to the hearing system. Damage to the RWM, such as membrane perforation, will result in perilymph aspiration and a loss of normal pressure-releasing functionality (Goodhill, 1971).

1.1.4 Cochlear fluids

The two fluids of the cochlea have different ionic compositions and must be isolated. The scala media is filled with endolymph, a predominantly high K^+ and low Na^+ and Ca^{2+} solution, resembling intracellular fluid. In mammals, the accepted ionic concentrations (in mmol/L) are 157 K^+, 1 Na^+, 0.02 Ca^{2+}, 0.01 Mg^{2+}, 132 Cl^- and 30 HCO_3^- (Wangemann, 2006). The enveloping scalae contains perilymph which contains high Na^+ and Ca^{2+} concentrations and low K^+ concentration. The ionic concentrations of the perilymph, in mmol/L, are 4 K^+, 148 Na^+, 1.3 Ca^{2+}, 1 Mg^{2+}, 119 Cl^- and 21 HCO_3^- (Wangemann, 2006). The movement and distribution of ions by active ion pumps induces a large electrical difference, the endocochlear potential (EP), between the two compartments. The endolymph has an electric potential of +80 mV to +100 mV and the perilymph +5 mV in the scala vestibuli and +7 mV in the ST. The functional purpose of isolating the intracochlear fluids is to ensure the EP remains optimal for hair cell transduction. The EP is the main driving force of sensory mechanoelectrical

transduction and the disturbance to the transporting of ions can interfere with audition. A decrease in EP has been shown to reduce hair cell sensitivity, frequency selectivity and auditory nerve tuning curves (Brown *et al.,* 1983; Evans and Klinke, 1982).

The endolymph is generated by the stria vascularis, a functional three-layered specialised epithelium, which is located within cochlear duct laterally to Reissner's membrane and the basilar membrane. The main cell layers of the stria vascularis, the marginal cells which border the endolymph and the basal cells, interconnected with gap junctions facing the spiral ligament and exposed to perilymph, act as barriers but also facilitate endolymph production. Both cell layers are separated by an intrastrial space which is the channel of ionic distribution. When analysing the ionic composition of the endolymph and perilymph, it would be assumed that the high electric potential of the endolymph may be due to a K^+ potential gradient. However, the ionic composition of the endolymph is similar to that inside cells but the electric potential is much higher. Interestingly, the EP is not a result of ionic diffusion potentials but is sourced from the stria vascularis by means of energy consuming, ion-pumping processes. The main electrogenic ion pump maintaining the EP is an activated Na^+- K^+-ATPase pump located on the margin of the border cells of the stria vascularis (Johnstone and Sellick, 1972). Na^+- K^+-ATPase actively transports K^+, from the bloodstream, into the endolymph and Na^+ out of the endolymph. Evidence of this has been displayed from ion pump 'knockout' experiments. Johnstone and Sellick (1972) demonstrated that during stria vascularis anoxia, the inactive ion pumps caused the EP to diminish to zero after approximately 1-2 mins (Johnstone and Sellick, 1972). Furthermore, increasing the concentration of K^+ in the ST, utilising K^+-rich perfusates, decreases the K^+ gradient and the EP becomes more positive.

Perilymph production has two potential origins, from the cerebrospinal fluid which then migrates via the cochlear aqueduct, or is an ultrafiltrate of blood plasma, produced by capillaries in the walls of the perilymphatic space. It could be that perilymph is produced by both actions. There is a third fluid within the cochlea, termed cortilymph, which lies within the extracellular spaces of the organ of Corti. Cortilymph has the same ionic composition of perilymph however has a higher protein content and approximately 0 mV electric potential.

1.1.5 The organ of Corti

The organ of Corti facilitates the transduction of sound within the cochlea and is located in the scala media of the cochlea between the vestibular and tympanic ducts. Situated above the basilar membrane (BM) are inner hair cells (IHCs) and outer hair cells (OHCs), characterised by a mechanoreceptive organelle composed of 50-100 microvilli, termed stereocilia, protruding from the endolymphatic pole, which convert sound to an equivalent electrical waveform. The stereocilia are approximately 200 nm in diameter, in OHCs, and twice as large in IHCs (Fettiplace, 2017). The stereocilia are reinforced along their length by paracrystalline arrays of parallel β-and γ-actin filaments cross-linked with several actin-binding proteins, such as espin (Fettiplace, 2017). IHCs are situated close to the edge of the BM, near the spiral lamina, where the amplitude of the BM vibrations should be minimal (figure 1.5).

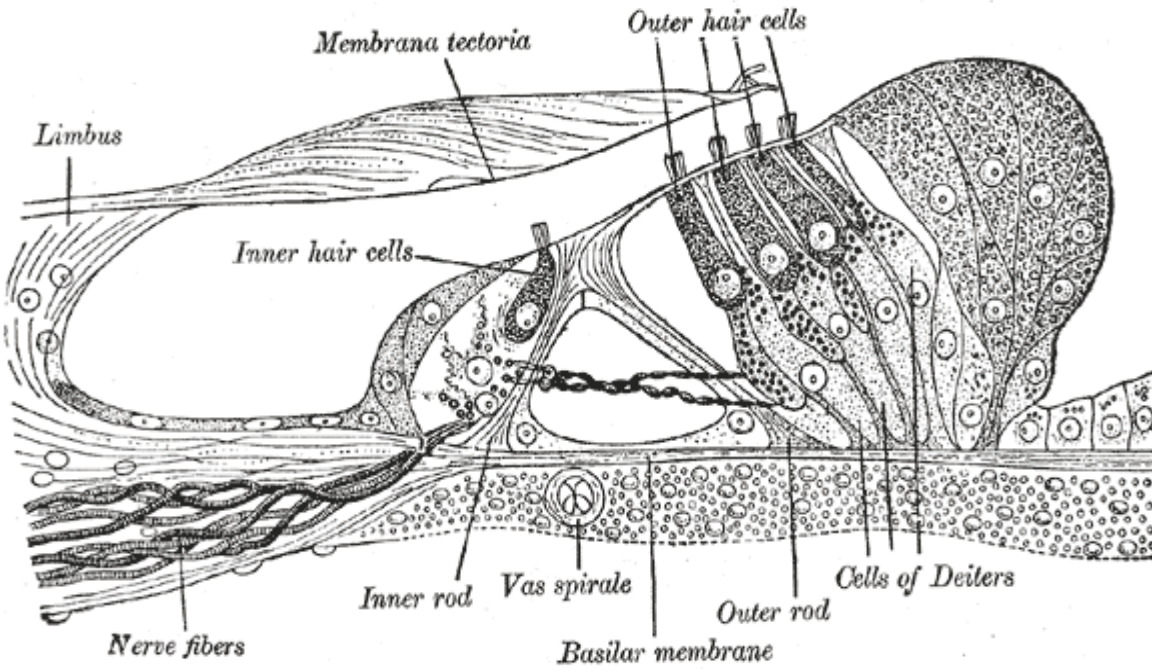

Figure 1.5. The organ of Corti. The organ of Corti displaying the sensory hair cells, TM, nerve fibres and surrounding supporting cells. Note, *in situ*, OHCs are embedded into the TM. (From White *et al.*, 2020).

The OHCs lie in the centre of the BM where vibration amplitudes would be maximal. Locational differences of the IHCs and OHCs suggests variation in cell function. IHCs are

sensory mechanoreceptive cells, which respond to fluid flow, by opening and closing mechanoelectrical transducer (MET) ion channels, resulting in the flow of K^+ and Ca^{2+} down

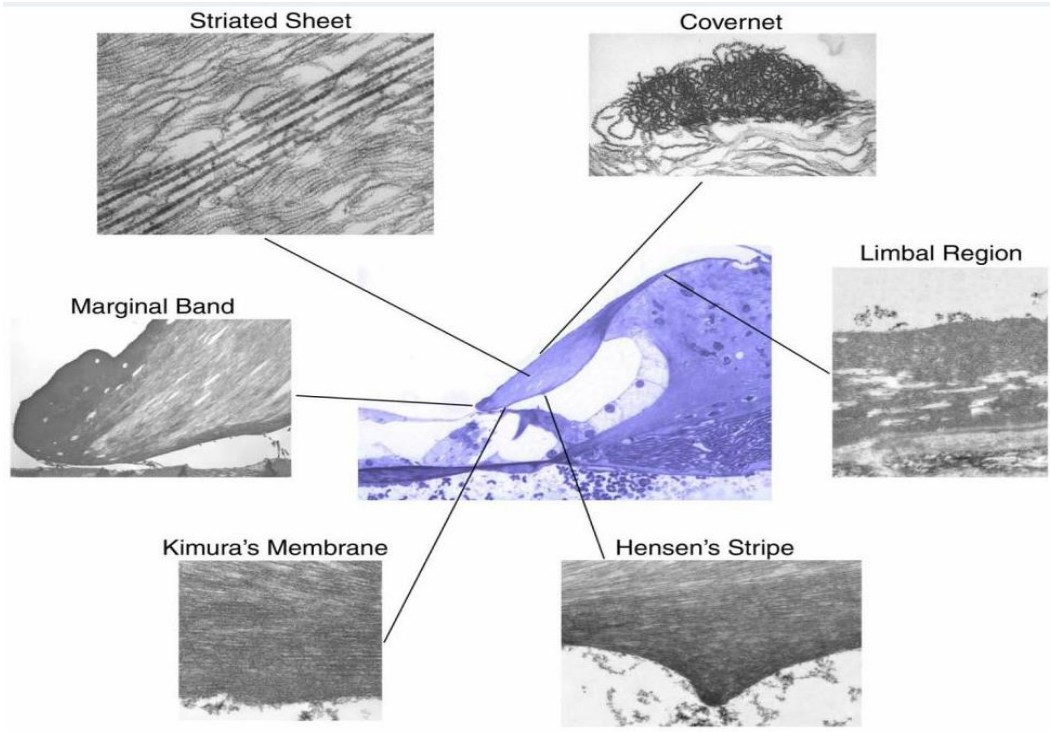

Figure 1.6. Tectorial membrane structure. A Toluidin blue stained section from the mouse cochlear duct (centre) and transmission electron micrographs (surrounding) showing the ultrastructure of the different regions and peripheral features of the TM. Arrows represent localised area of the described TM property. (Constructed from Legan *et al*., 2000).

their respective electrochemical gradients in the hair cells (Fettiplace, 2017). Overlying the hair cells is the tectorial membrane (TM), a gelatinous and fibrous ribbon-like strip (figure 1.6), which covers the organ of Corti, affixing to the tips of the OHCs.

The TM spirals along the length of the entire cochlea, attached along its medial side to the surface of the spiral limbus, stretching across the spiral sulcus (Richardson *et al*., 2008). The structure of the TM can be separated into five main parts (numbered). The central core is composed of 20 nm diameter collagen filaments that are embedded in an unusual, striated sheet-matrix (Hasko and Richardson, 1988). The striated sheet-matrix (1) is characterised by two types of fine-diameter (7-9 nm) filaments, which lie parallel within the plane of each sheet, and are linked along their length by staggered cross bridges (Hasko and Richardson, 1988). Properties of the TM surface include the covernet (2) – an anastomosing network of large

calibre fibrils that mainly run longitudinally over the upper surface of the TM. The marginal band (3) is a dense thickening of the lateral edge of the TM. The Kimura's membrane (4) is a thickening of the lower surface into which the hair bundles of the outer hair cells are imbedded. The Hansen's stripe (5) is a ridge that runs longitudinally along the lower surface of the TM adjacent to the hair bundles of the inner hair cells. See figure 1.6 for an overview of the TM structure.

The TM radial width and cross-sectional area increase from the basal to the apical end of the cochlea (Richardson *et al*., 2008). There is a radial gradient in collagen fibril packing density across the TM with a greater density in the limbal than the middle zone, but there are no gradients in collagen fibril density along the length of the TM (Weaver and Schweitzer, 1994). The collagen fibrils are oriented radially across the TM with an offset of ~15 degrees towards the apical end of the cochlea.

Connecting the organ of Corti and the central nervous system (CNS) are an array of afferent and efferent neurons. Afferent neurons can be divided into two types, type I and type II. Type I afferent neurons innervate the basal surfaces of IHCs and are stimulated in response to IHC stereocilia deflections. Each IHC has up to 30 afferent neuron terminals radially connected, with each fibre innervating an individual IHC. Type II afferent neurons are unmyelinated and represent 5-10 % of the afferent fibres in the auditory nerve. Forming synapses with OHCs, one type II afferent neuron can innervate up to 8-10 OHCs, but a single OHC can be connected to many type II neurons. The proposed role of these neurons is to behave as a part of a regulatory feedback system between the organ of Corti and the CNS.

1.1.6 Hair Cell Mechanoelectrical Transduction

Hair cells are stimulated by BM vibrations which initiate the mechanotransduction of acoustic stimuli into electrical impulses (Fettiplace, 2017; Hudspeth and Jacobs, 1979). OHCs are directly coupled to the overlying TM via their hair bundles and are stimulated by a 'shearing' motion between the organ of Corti and the TM in response to vibrations. The stereocilia of OHCs are structured in three V-shaped rows of graded height, with their distal tips inserted into compartments on the underside of the TM (Hudspeth and Jacobs, 1979). This connection could act as a tight mechanical coupling between the two structures but the significant purpose

of the V-shaped arrangement is not known. IHCs are not embedded in the TM and instead respond to fluid motion at their apical surfaces (Russell *et al*., 2007; Russell and Sellick, 1978).

The mechanoreceptive organelle of the hair cell is the hair bundle. Deflections of the hair bundle, caused by fluid flow (IHCs) or shearing between the TM and organ of Corti (OHCs) towards the tallest stereocilium, results in an increased membrane conductance for K^+ and Ca^{2+} (Hudspeth and Jacobs, 1979). The hair bundle is incredibly sensitive to mechanical stimuli; deflections of less than the diameter of an atom can induce mechanotransduction. Fine extracellular filaments extend from the tip of a shorter stereocilium to the lateral wall of its taller neighbour and are fundamental to mechanotransduction. The tip links are mechanically in series with an unidentified elastic element, referred to as a gating-spring (Kachar *et al*.,

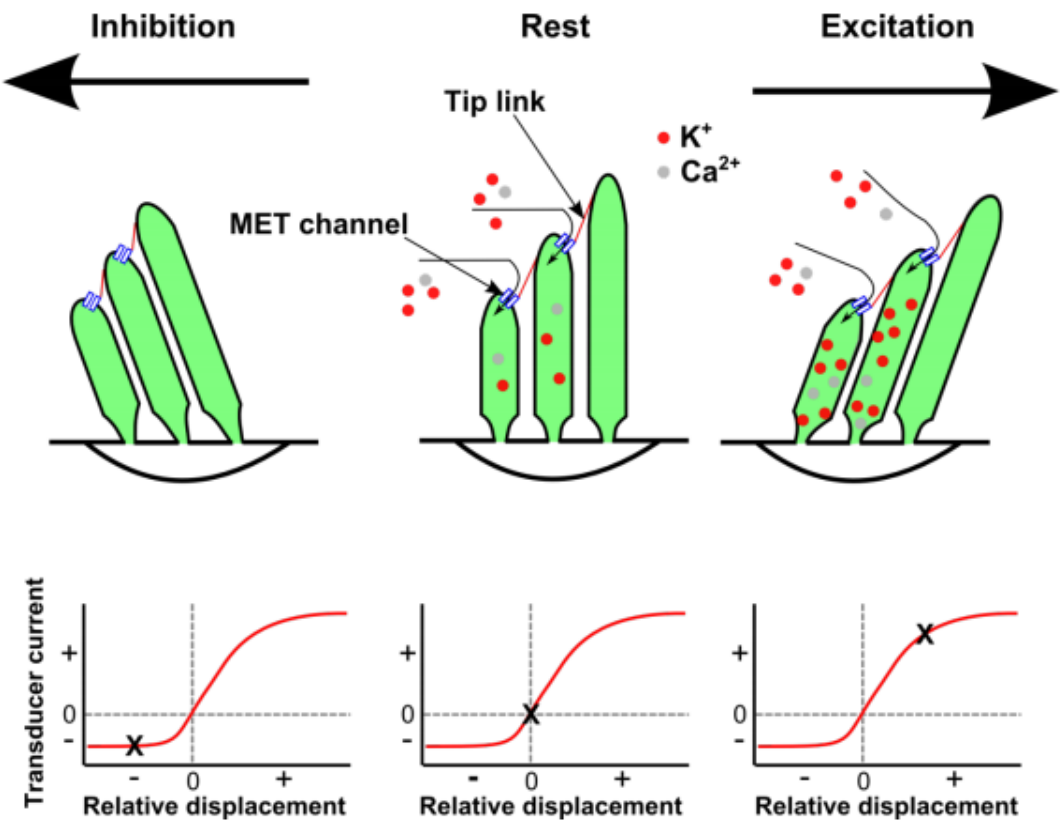

Figure 1.7. Hair bundle stereocilia displacement. Hair bundle displacement in excitatory direction causing a relative movement between stereocilia opening mechano-electrical transduction (MET) channels. Displacing the hair bundle in the opposite direction closes MET channels resulting in inhibition. (From Jones, 2012).

2000), which pulls on transduction channels, allowing K^+ and Ca^{2+} entry into the stereocilia (figure 1.7).

The fine extracellular filaments that connect the tips of the stereocilia to their taller neighbour enable the hair bundle to respond as a unit; stereocilia move as rigid rods, pivoting about their insertion points, with zero flexion (Crawford and Fettiplace, 1985; Howard and Ashmore, 1986). Basal tapering and extensive cross-linking of the bundles causes such movements, pivoting at their bases and touching at their tips. A significant resting tension is also present within the bundles as a consequence of the mechanical structural features. The main purpose of the hair cells is to convert sound energy into equivalent neural impulses. Basilar membrane oscillations induce hair bundle deflections; OHCs by the TM and IHCs by fluid motion. Deflection of the hair bundle triggers the opening of a nonselective cation channel, termed the transduction channel, induced by increasing the tension of the tip link. Deflection towards the tallest stereocilia opens channels and displacement towards the smallest stereocilia closes channels (Figure 1.7). Sideway movements have no effect. Opening of transduction channel causes an influx of K^+ and Ca^{2+} ions, located in the surrounding endolymph which covers the hair cells apical surface. The EP (+80 mV) enhances receptor current giving rise to a +150 mV electrical driving force for K^+ and Ca^{2+} entry. Depolarisation of the IHCs opens voltage gated Ca^{2+} channels, located close to basolateral synapses, elevating Ca^{2+} levels which triggers the release of a neurotransmitter at the glutamatergic synapses initiating signal propagation to afferent neurons.

Endolymphatic Ca^{2+} concentration is essential for normal auditory function, playing an important role in mechanotransduction and tip link structural preservation. As mentioned above, there is approximately 0.02 mmol/L of Ca^{2+} in the endolymph, which is miniscule when compared to the K^+ concentration (157 mmol/L). However, deviations from the normal Ca^{2+} concentrations can cause SNHL. Elevated endolymphatic Ca^{2+} concentrations block microphonic potentials and transduction currents generated by sensory cells and suppressed by reduced concentrations (Tanaka *et al*. 1980, Ohmori. 1985). Reduced endolymphatic Ca^{2+} concentrations are also linked with vitamin D deficiency and hyperthyroidism, two conditions associated with low plasma Ca^{2+} concentrations, resulting in hearing loss (Brookes, 1983; Ikeda *et al*., 1987).

Upon acoustic stimulation, hair bundles are deflected opening cation-selective transducer channels located at the tips of the stereocilia. Ca^{2+} enters the stereocilia through the transducer channels and acts in a negative feedback manner to reset the channel's operating range. This process is referred to as adaptation and involves multiple mechanisms (Fettiplace and Ricci, 2003). One component, termed fast adaptation, occurs in milliseconds and is thought to be caused by the direct binding of Ca^{2+} to an intracellular site of the mechanotransduction channel (Howard and Hudspeth, 1987; Cheung and Corey, 2006). Ca^{2+} enters the transducer channels, then closes them in milliseconds or less causing a decline in current that follows a deflection. It has also been postulated that the adaptive decline in current can generate oscillations at a frequency in the animals hearing range, suggesting potential contributions to the cochlear frequency tuning (Ricci *et al*., 1998). A second component, slow adaptation, which has been studied predominantly in the vestibular system, has been linked to activity of molecular motors (Howard and Hudspeth, 1987), composed of unconventional myosin molecules (Grati and Kachar, 2011), which interact in a Ca^{2+} dependant manner with actin filaments at the core of stereocilia. Slow adaptation also closes the transducer channels, but on a different timescale and by a different mechanism than the fast adaptation. A positive deflection of the hair bundle causes bundle relaxation in the direction of the stimulus, corresponding to a reduction in *gating-spring* tension (Howard and Hudspeth, 1987). It is thought that the slow-adaptation mechanism regulates resting tensions of the *gating-spring*. Assad and Corey (1992) demonstrated that decreasing the hair cell Ca^{2+} concentration increases the resting tension exerted by the motor, resulting in hair-bundle movement in the negative direction. The resting tension exerted by the motor is ~10 pN, which can increase to ~25 pN under low Ca^{2+} conditions (Jaramillo and Hudspeth, 1993).

To summarise, the adaptation mechanism restores transduction channel sensitivity by decreasing the response to a maintained stimulus. Furthermore, adaptation sets the resting tension of the transduction channel by setting an adequate resting tension, essential to position the channels near their most sensitive point. A consequence of this is that both positive and negative deflections change the current and the hair cell's transducer has no threshold (Hudspeth, 1992).

1.1.7 The cochlear amplifier

Most physiological sounds, such as speech and music, vary in frequency, amplitude and phase on a scale of milliseconds. The ear analyses sound, in real-time, by processing complex acoustic signals, translating temporal and amplitude information into auditory nerve activity. The human ear can differentiate between two acoustic tones which differ in frequency by approximately 0.2-0.5 % (Dallos and Cheatham, 1992), a characteristic dependent on the sharp tuning of the BM (Robles and Ruggero, 2001). Early measurements of auditory nerve fibre activity (Tasaki *et al*., 1954; Kiang *et al*., 1967) demonstrated that complex acoustic signals are sharply separated into spectral components at the periphery of the auditory system. However, in 1960, von Békésy carried out ground-breaking work revealing observations which contrasted earlier findings (von Békésy, 1960). He found that a travelling wave generated by pure tone excitation propagated along the BM with the wave amplitude gradually increasing. It was observed that, after a peak at a specific location, below the resonance, vibrations decay quickly along the BM. The location at which the peak occurred was dependent on the input tone frequency and was more basal, at high frequencies, and more apical, at low frequencies. Both findings of passive sharpening of frequency selectivity in the cochlea led to numerous hypotheses.

Cochlea nonlinearity was first suggested in 1971 (Rhode, 1971). Rhode demonstrated that the BM responded to sinusoidal stimuli with less frequency selectivity for higher level stimuli. Technological advancements aided the understanding of a nonlinear and active cochlea with much more evidence being published. The theory of active cochlear processes was proposed by Gold (1948) and evidenced by Kemp (1978) during work on tinnitus and otoacoustic emissions (OAEs). Measurements of evoked and spontaneous OAEs (Zurec. 1981) provided strong evidence of the presence of an active mechanism within the cochlea which pumps energy into the vibrations of the cochlear partition, providing frequency-sharpening. Primarily, the active processes function as an automatic gain control which allows the amplification of sounds that would otherwise be too weak to hear (Lyon, 1990; Lyon and Mead, 1988). BM responses differ, both qualitatively and quantitatively, in living ears when compared to dead ears. Figure 1.8 demonstrates the nonlinearity and the sharp tuning of the living cochlea, with higher gains at lower stimuli levels, which is not evident in dead ears.

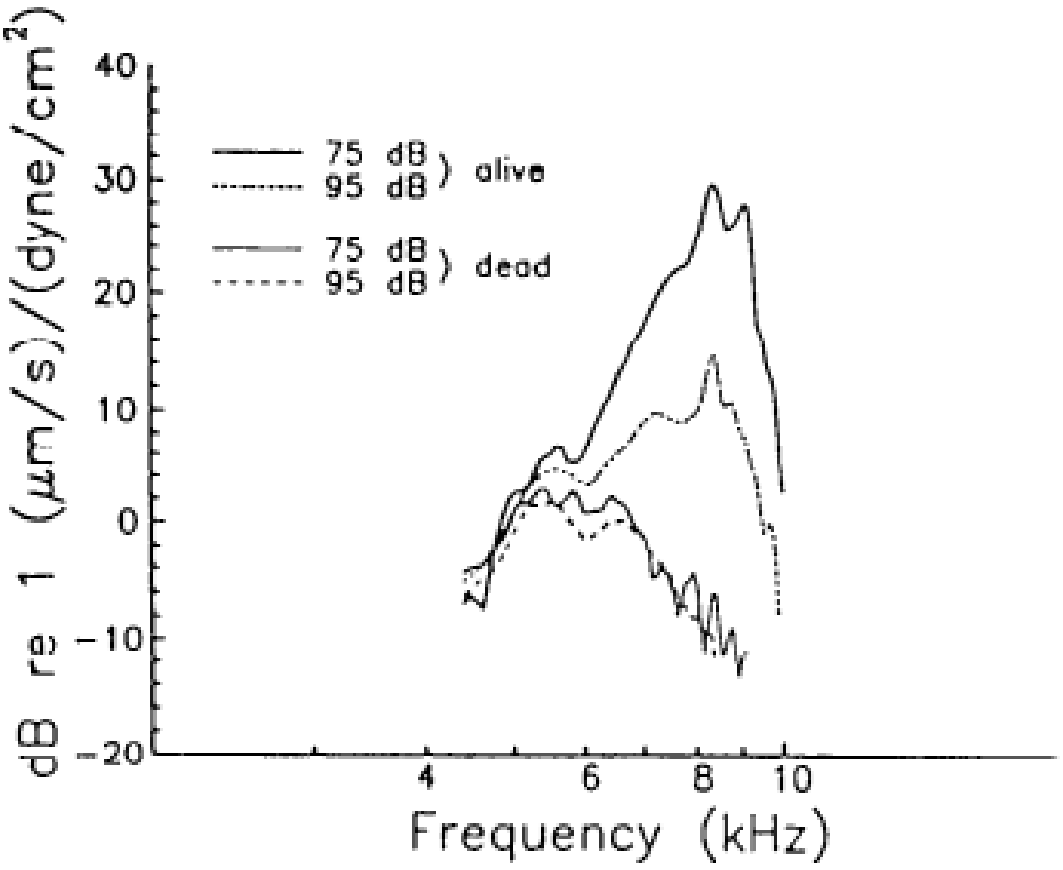

Figure 1.8. Graphical representation of the cochlear amplifier gain. A comparison of alive and dead ears demonstrating the effects of the active cochlear gain functions of basilar membrane displacement in the basal turn of the chinchilla cochlea using laser Doppler velocimetry. Measurements shown at 75 dB and 95 dB sound levels. Hearing sensitivity is reduced significantly in dead ears when compared to alive. (From Ruggero and Rich, 1991).

The tuning of dead ears becomes independent of the stimulus level, i.e., linear, providing evidence of a nonlinear active process under normal physiological conditions. The processes demonstrated were later termed “the cochlear amplifier” by Davis (1983) and it has become the accepted theory to explain the observed frequency selectivity of the auditory nerve fibre responses and the pattern of the BM responses to low sound pressure levels (SPL). At this current date, the primary hypothesised mechanism which supplies energy to the cochlear amplifier is from OHC somatic electromotility (Brownell *et al*., 1985; Ashmore, 1987; Santos-Sacchi and Dilger, 1988), concluding that OHCs amplify BM motion (Ashmore, 1987).

OHCs are capable of rapidly changing their shape in response to electrical stimulation (Brownell *et al*., 1985; Kachar *et* al., 1986; Ashmore, 1987; Santos-Sacchi and Dilger, 1988); transmembrane potential stimuli lengthen or contract cells by 3-5 % (Santos-Sacchi, 1989). The receptor potentials produced by the OHCs in response to acoustic stimulation are believed to control the OHCs voltage-dependent mechanical response, the reverse transduction. Due to this, OHCs may change their length in synchrony with the receptor potential, pumping energy into the vibration of the cochlear partition. Depolarisation of OHCs causes shortening and hyperpolarisation induces elongation (Ashmore, 1987) in a nonlinear manner (Santos-Sacchi, 1989). The local release of energy, for a tone of a specific frequency, is the main theory which supports the cochlear amplifier mechanism.

The OHC electromotility is observed, when a transmembrane voltage is applied, due to a motor protein, prestin, located in the plasma membrane, acting similar to that of a piezoelectric actuator. Prestin belongs to the SLC26A family of membrane antiporters transferring anionic molecules across the cell membrane and is abundantly expressed within the OHC (Muallem and Ashmore, 2006). Interestingly, prestin is not expressed in other hair cells and likely acts in conjunction with proteins and lipids of the OHC lateral wall to form motor complexes. Intracellular voltage changes induce prestin motor complexes generating force by changing its surface area. It has been seen that intracellular anions modulate prestin function but can also inhibit electromotility and decrease longitudinal stiffness of OHCs (Oliver *et al*, 2001; He *et al*., 2003; Rybalchenko and Santos-Sacchi, 2003). Further evidence demonstrating the importance of prestin to OHC electromotility and thus, the cochlear amplifier, is observed in prestin knockout mice. Liberman *et al* (2002) directly deleted prestin in mice and found a loss in OHC electromotility and SNHL (40-60 dB). This evidence demonstrates the importance of prestin to normal hearing function.

1.2 Electrical and Acoustic Responses of the Cochlea

Electrical and acoustic measurements can be made from the cochlea to further understand the mechanisms of hearing. Improving our understanding of the hearing organ will, in time, enable further advancements in hearing rehabilitation. Cochlea generated electrical potentials can be measured to explore cochlea physiology under specific experimental parameters. Acoustic responses have outlined the complex sharp frequency selectivity and tuning of the cochlea with a key emphasis on OHC mechanics and functionality.

1.2.1 The gross evoked electrical potentials

Placing electrodes within or in the vicinity of the cochlea enables the possibility to record gross stimulus-evoked potentials, which are derived from the massed activity of large numbers of individual receptor and nerve cells. The gross evoked potential recorded at the RWM of the cochlea is a complex summation of electrical signals from various sources. The sources can be split into three groups:

1. Cochlear Microphonic (CM)
2. Summating Potential (SP)
3. Compound Action Potential (CAP)

The CM is an alternating-current (AC) potential created predominantly by the mass receptor currents of OHCs, and partially IHCs, following BM movement (Dallos and Cheatham, 1976). A major component of the recorded RWM potential is CM, see figure 1.9 of a gross electrical potential. The current that flows through the hair cells must also flow through the scala media and ST which produces a voltage drop across resistances of the scalae. In order for the currents flowing through the hair cells to 'ground', via the vascular system, the current must flow through the same two resistances, therefore totalling the sum of the current of the individual hair cells. Thus, the voltages produced in the scalae are composed of contributions from many hair cells. The CM follows the acoustic stimulation waveform and provides information regarding the overall state of the OHCs within specific regions of the cochlea but cannot provide information of individual hair cells.

The summating potential (SP) is a change of the electrical potential produced in the cochlea in response to a sound and is visible as a baseline shift in the recorded signal (Johnstone and Johnstone, 1966). SP is the evoked direct current (DC) and is an extracellular correlate of the DC component of the current flowing through the hair cells. The SP can be recorded as either a positive or negative shift of the potential in the scala media (Johnstone and Johnstone, 1966). The SP is likely to receive contributions from both IHCs and OHCs, but maybe other sources.

During auditory stimulation there is a series of deflections at the beginning, and sometimes at the end of the stimulus, called the N1 and N2 neural potentials of the CAP. The CAP is generated by the summed activity of the auditory nerve fibres which produces synchronised

action potentials at the start of the stimulus. N1, the first dominant wave, arrives 1 ms after the onset of the CM and N2, the second dominant wave, approximately 1ms after that. As the intensity increases from low levels, N1 is the first to appear, followed at higher intensities by N2 (figure 1.9).

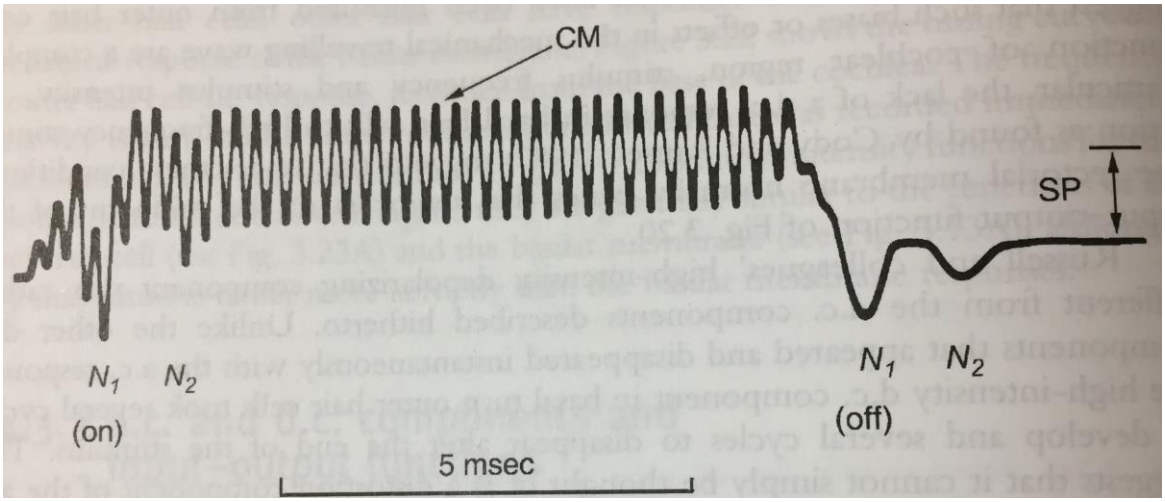

Figure 1.9. The response to a tone burst, recorded with gross electrodes, displaying the cochlear microphonic (CM), N1 and N2 neural potentials of the compound action potential (CAP) and the DC shift of the microphonic from the baseline, the summating potential (SP). (Taken from Pickles, 2008)

1.2.2 Otoacoustic emissions

In 1948, Thomas Gold theorised that the sharp frequency selectivity displayed by the cochlea resulted from a feedback system consisting of a mechanical-to-electrical transduction process coupled to an electrical-to-mechanical transduction process (Gold, 1948). Gold's suggestion of a reverse-transduction process, in the form of an electromechanical conversion mechanism, suggested the possibility of detecting this process in the form of sound in the ear canal. It was not until the late 1970's that Gold's hypothesis was experimentally demonstrated. In 1978, Kemp confirmed the idea of otoacoustic emissions (OAEs), defined as the release of sound energy produced within the cochlea and propagated to the middle ear and external auditory meatus (Kemp, 1978). It was further understood that energy emitted by the cochlea can be recorded as acoustic vibrations in the ear canal using specialised methods and apparatus. Kemp hypothesised that the OHCs of the cochlea produced OAEs as a result of active and nonlinear

mechanical feedback processes, which can be spontaneous or evoked by low and medium sound intensities (Kemp, 1978).

There are two general categories of OAEs which differ by mechanism of excitation: spontaneous and evoked. Spontaneous OAEs are stationary narrow-band signals occurring without external acoustic stimulation and can be detected in ~50 % of individuals with normal hearing. These emissions comprise of energy at one or more frequencies produced by the normal ear and recorded in the ear canal with a highly sensitive microphone. The latter for evoked excitation are divided into three types of OAEs, transient-evoked (TEOAEs), stimulus-frequency (SFOAEs) and distortion-product (DPOAEs) OAEs.

TEOAEs are low-intensity sound waves produced and emitted by the cochlea upon short acoustic stimulus, such as clicks or tone bursts. Click stimulation includes a broad band of frequencies and activates the cochlea from basal to apical regions of the BM. TEOAEs can be detected in individuals with normal OHC function at the frequency analysed, or in individuals with auditory thresholds below 30-dB hearing loss (HL) (Serra *et al*., 2015). Impaired hearing can be screened using TEOAE, however, the test is unable to detect the type or degree of impairment. SFOAEs are evoked with a constant low intensity pure-tone stimulus and are generally swept or changed slowly across a region of frequencies. Experimentally and clinically, SFOAEs are explored the least, when compared to TEOAEs and DPOAEs.

DPOAEs are sounds generated by the OHCs in response to stimulation with two pure tones, with frequencies f_1 and f_2 ($f_1 < f_2$), known as primaries. The frequencies of the pure tones are closely similar, usually $f_2/f_1 = 1.22$, evoking a robust DPOAE. When two pure tones are presented to the ear simultaneously, the most common distortion product occurs at $2f_1 - f_1$, termed the cubic difference tone.

1.3 Hearing loss

Loss of the auditory sense is incredibly hindering because of both loss of hearing and also the difficulty of communication, learning and assessing environmental stimuli. There are many causes of damage to the mammalian ear that can cause partial or profound deafness depending on cause and severity.

1.3.1 Conductive hearing loss

Conductive hearing loss arises when there are complications with the outer or middle ear preventing sufficient sound transmission to the inner ear. Sound wave transmission from the outer ear to the inner ear relies on mechanical vibration conduction. Sound vibrations are collected at the pinna and propagated through the auditory canal to the tympanic membrane. Displacement of the tympanic membrane transmits the mechanical vibration through the ossicular chain, of the middle ear, and to the OW, transferring the vibrations into the perilymph and endolymph of the cochlea, exciting the BM. In conductive hearing loss, the mechanism of sound conduction to the inner ear is compromised, resulting in partial or profound deafness. Conductive hearing loss can be due simply to a blockage of the auditory canal by an occluding cerumen (ear wax) plug or by canal atresia. If severe, a bone conduction hearing device should be provided to allow hearing to develop, in the case of neonates, or to rehabilitate auditory sense. Refer to section 1.4 for current treatments.

Tympanic membrane perforations or damage is common, resulting in partial or profound deafness. Trauma, otitis media and sudden exposure to very loud sound (>140 dB) can cause severe damage to one or both ears resulting in a compromised tympanic membrane. Head injuries can damage the eardrum perforating the tympanic membrane, causing periodic or constant deafness, bleeding and vertigo. Very loud sounds induce a large pressure in the ear over a small-time range (<1.5 ms) causing the eardrum to ‘burst’ which ruptures the tympanic membrane. An example would be a blast trauma, such as an explosion, rapidly altering the pressure within the ear.

Otosclerosis is a disease which affects the ossicular chain preventing efficient vibration transmission to the cochlea. Bone remodelling processes of the bony cochlea wall result in a fixated stapes preventing displacement of the ossicular chain and thus the OW. There are many linked causes of otosclerosis, such as genetic, inflammation (autoimmune responses – viral), metabolic and hormonal factors. Fixation of the ossicular chain can cause up to 40 dB hearing loss in the lower frequencies, resulting in the requirement of a hearing aid device. In some cases, depending on the severity of bone remodelling, the ossicular chain can be surgically altered re-establishing displacement. An ossicular prosthesis can be implanted which provides auditory rehabilitation.

1.3.2 Sensorineural hearing loss

SNHL occurs within the inner ear, usually because of non-functioning sensory hair cells, causing partial or profound deafness. The cause of SNHL can be a viral infection, such as Cytomegalovirus, which is the most common type of progressive SNHL in children. SNHL can be genetically inherited with over forty genes having been recognised to cause hearing loss (Angeli *et al*., 2012). Many environmental factors can cause SNHL such as trauma, aging, ototoxic drugs, infections and noise exposure. Noise exposure has been acknowledged as one of the main environmental factors causing hearing loss (Lalwani and Gürtler, 2008).

Sudden sensorineural hearing loss (SSNHL) can be a result of overpowering vibrations, such as an explosion, or can be caused by viral infections. Drugs can also damage hair cells or other vital structures of the inner ear. SSNHL often causes deafness in a single ear thus not compromising the auditory sense entirely.

1.4 Auditory rehabilitation

Aural rehabilitation begins firstly by identifying and diagnosing the type of hearing loss, whether that be conductive, sensorineural or mixed, and then causation. For example, a patient with conductive hearing loss, caused by ossicular chain immobilisation, would unlikely benefit from a conventional hearing aid. This patient would require ossicular chain remodelling. Once the diagnosis is made, methods of auditory rehabilitation can be offered to the patient

1.4.1 Auditory prostheses

There is a plethora of different auditory rehabilitation methods proposed in current literature which attempt to excite the cochlea through either the OW, RWM or bone conduction. The most common treatment for SNHL, or in some cases mixed hearing loss, is a CI which bypasses the auditory periphery to electrically stimulate the auditory nerve (Macherey and Carlyon, 2014). The fundamental function of the CI is to transduce incoming sound from the environment into electrical stimulation patterns and deliver this to the auditory nerve fibres

(figure 1.10). This device is clinical offered to partial or profound deaf patients. However, alternative devices are showing significant improvements in auditory rehabilitation.

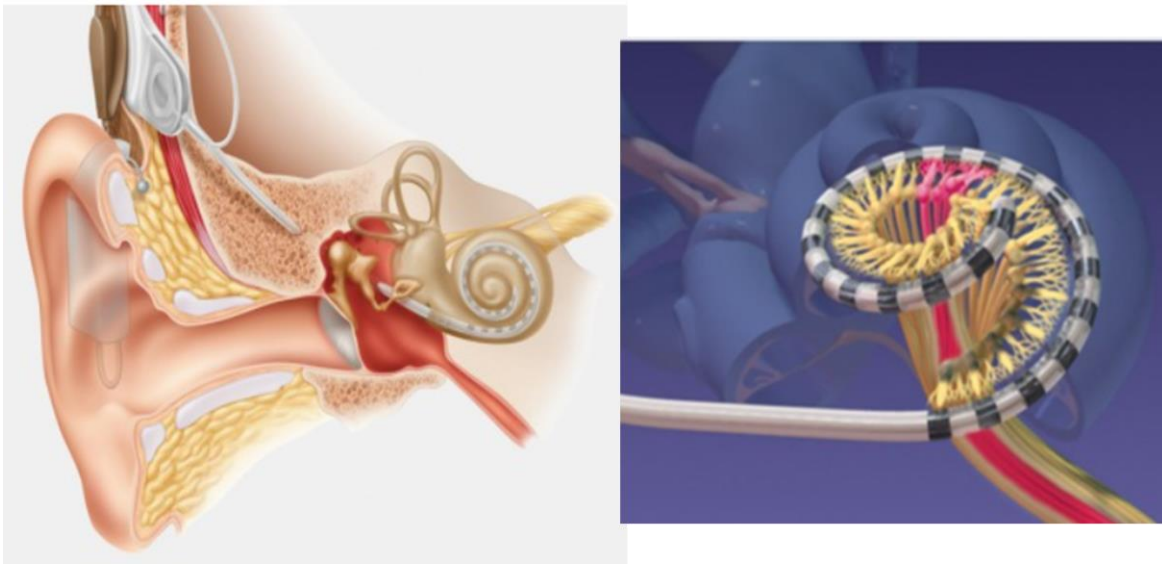

Figure 1.10. Cochlear implant. Diagrams illustrating the placement of a CI onto a patient's skull and within the middle and inner ear. Incoming sounds are detected by the microphone, processed into electrical signals and transmitted to the receiver. The electrical signals are passed down an endocochlear electrode and stimulate the auditory nerve directly. (From Lenarz, 2018).

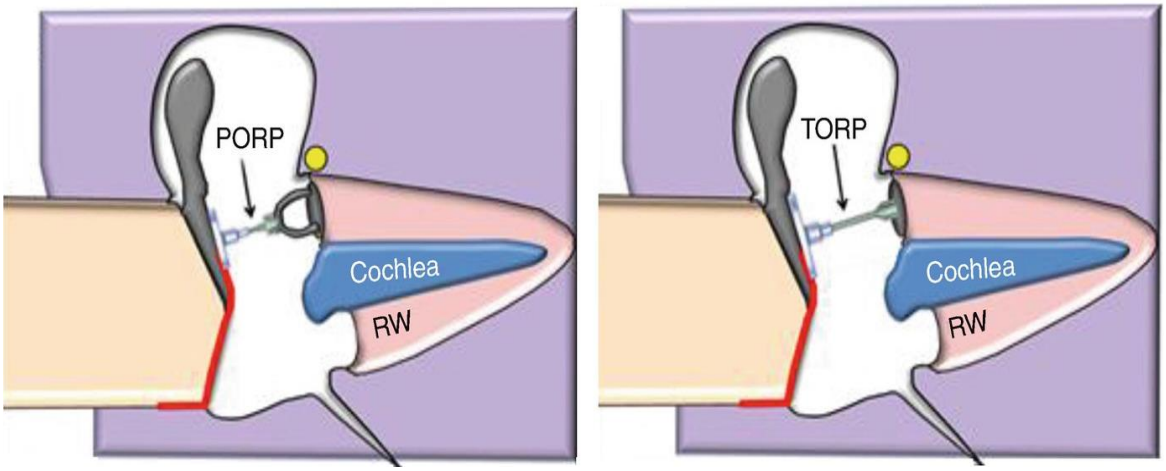

Figure 1.11. Ossicular chain reconstruction. A diagrammatical representation of both a partial ossicular replacement prosthesis (PORP) and a total ossicular replacement prosthesis (TORP). The red lines, below the protheses, illustrates a tympanic membrane skin graft commonly required during ossicular chain reconstruction surgery. (Adapted from Mansour *et al*., 2018).

A partial ossicular replacement prosthesis (PORP) or total ossicular replacement prostheses (TORP) can be surgically implanted in the middle ear to rehabilitate conductive hearing loss via ossicular chain reconstruction (figure 1.11). These devices can also be coupled to a floating mass transducer (FMT) which displaces the ossicular chain and subsequently the OW to further improve cochlea excitation. Work by Shimuzi and Turia (2011) demonstrated the coupling of a FMT with a PORP or TORP, and implanting into human temporal bone, increased frequency performance when compared to the ossicular prostheses alone (Shimiza and Turia, 2011). Tos and Saloman (1994) also used an ossicular prosthesis but coupled with a magnetic head which was energised by a coil deep in the ear canal connected to a post-auricular hearing aid (Tos and Saloman, 1994). There was a functional gain of 40 to 70 dB HL across the 125 to 8 kHz frequency range.

Cochlear excitation utilising non-conventional routes has been explored, with an emphasis on the RWM route. The RWM has available space behind it, the middle ear cavity, whereas the OW is obstructed by the ossicular chain. A magnetic device has been postulated, to vibrate the RWM, and carried out by Spindel *et al* (1991) and Weddell *et al* (2014) displaying auditory nerve threshold CAP measurements. Much work has focused on cochlear excitation via the RWM however minimal work has explored intracochlear pressure relief through the RWM (Spindel *et al*., 1991; Spindel *et al*., 1995; Weddell *et al*., 2014). Spindel *et al* (1995) demonstrated and engineered a suitable electromagnetic device that could drive the cochlea, displacing the BM, and produce auditory brainstem responses similar to acoustic stimulation. Intracochlear pressure was not considered in this paper, however an electromagnetic device still used today was postulated and tested. Weddell *et al* (2014) demonstrated the use of an electromagnetic prosthesis, that partially occludes the RW, generates near-field pressure, producing a fluid-jet flow, that excites the cochlea. Conventional hearing characterises far-field pressure between the scalae of the cochlea to stimulate the BM, whereas Weddell *et al* exploit near-field pressure i.e., pressure generated within the vicinity of the RWM. In this paper a proposed model was shown to calculate the area of RWM occlusion to allow suitable BM excitation and pressure release which will be utilised in our research.

In a similar work, a floating mass transducer (FMT) is placed on the RWM, which is a commercially available implantable hearing device, to excite the cochlea. An FMT is a small piston-like mass that can be coupled to a vibrating ossicular chain or connected to an audio processor, that transduces sound energy into electrical energy driving a piezo actuator, to

vibrate the OW or RWM. Kiefer *et al* (2006) implanted a FMT to the RWM of a patient with a malformed ossicular chain and demonstrated aided hearing thresholds of 15 and 30 dB in the 20 – 20,000 Hz (2,000 – 5,000 Hz most sensitive) frequency range (Kiefer *et al*., 2006). Colletti *et al* reported the hearing rehabilitation of a FMT placed on the RWM in seven patients with hearing impairment due to ossicular chain malformation and middle ear reconstruction was not suitable (Colletti *et al*., 2006). Their results demonstrated aided thresholds of 20 – 30 dB HL for all patients. A paper later published by Colletti *et al* (2009) reported similar results in 19 patients (Colletti *et al*., 2009).

A bone conduction device (BCD) may be used to stimulate the inner ear by means of vibration transfer through the skull. In cases of single or bilateral conductive hearing loss, and in rarer cases mixed hearing loss, where a conventional hearing aid would not be ideal or tolerated, patients can be fitted with a BCD. BCDs can be wearable, where a pair of glasses, for example, is fitted with a microphone and sound processor, which coverts sound into mechanical vibrations (Mudry and Tjellström, 2011). BCDs can also be surgically implanted under the scalp. In the 1970s, the bone anchored hearing aid (BAHA) was first introduced into clinical practice (Lusting *et al*., 2001). The BAHA consists of an external sound processor which captures incoming sounds in the air, converts the sound into vibrations, and then transfers the vibrations through a magnet to a small implant within the skull bone (figure 1.12). The implant then transmits the vibrations through the conductive skull bone directly to the inner ear. The vibrations displace the BM exciting the cochlea. In cases of outer and middle ear malformations resulting in conductive hearing loss, where current middle ear prostheses would not be a viable option, a BAHA can assist in improving hearing. BAHAs are advised for patients under the age of 5 years old who suffer conductive hearing loss in an attempt to develop speech (David's *et al*., 2007).

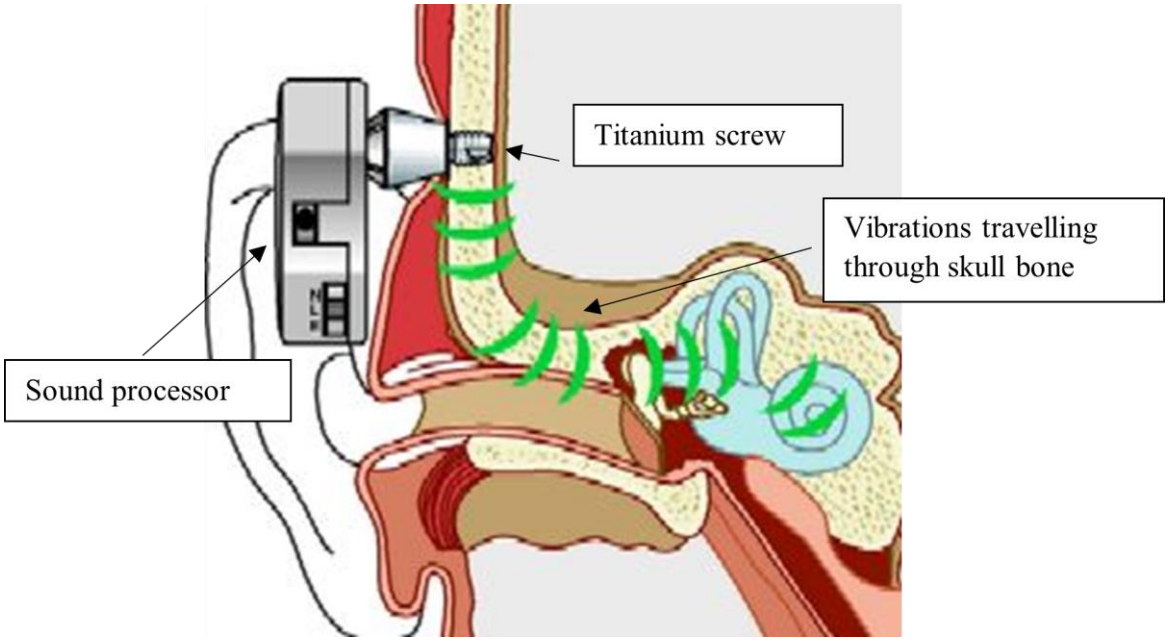

Figure 1.12 Bone anchored hearing aid (BAHA). A schematic of a BAHA illustrating the positioning and surgical implications required to fit the device. An external sound processor is connected to a titanium screw that is embedded into the skull bone. Vibrations are transferred into the screw, via the sound processor, and through the bone directly exciting the cochlea. Adapted from Medical Advisory Secretariat, 2002.

If a patient with conductive hearing loss is too young to undergo BAHA surgery, an external bone conductive device is recommended. Lusting *et al* (2001) demonstrated a 42 dB gain using a BAHA in patients with osteosclerosis. In patients with chronic Otitis Media, a 33 dB gain was observed, and patients with external auditory canal stenosis/ atresia, presented an average gain of 22 dB. See (Bento *et al*., 2012) for further clinical studies. Complications can arise with a BAHA due to local infection, allergies, lack of osteointegration, sound processor damage and inflammation (Asma *et al*., 2013; Bento *et al*., 2012; Gluth *et al*., 2010).

1.4.2 Auditory prostheses limitations

The complications with conventional hearing aids, when treating conductive hearing loss, are sound quality, background noise and high amplitude acoustic feedback. The use of an electromagnetic or floating mass device is a ‘non-acoustic’ method of auditory rehabilitation

and will help eliminate the issues with conventional hearing aids. Acoustic feedback will be reduced or eliminated as the transmission is magnetic, or electrical, and not acoustic energy. The use of a 'non-acoustic' method will improve sound quality as there is lower signal degradation due to direct inner ear transmission. An implantable device also bypasses the ear canal reducing risks of infection or blockage.

1.4.3 Drug delivery to the inner ear

The inner ear is a unique niche for drug delivery with considerable challenges to overcome before effective drug distribution along the entire cochlear spiral is possible. Access to the inner ear is limited, physically, due to its position within the temporal bone of the skull. Surgical treatments are highly invasive, requiring the removal of very hard bone (temporal bone), to gain access to the inner ear. Due to the inaccessibility of the inner ear and small size of the cochlea, methods of drug delivery have been further explored in an attempt to demonstrate less invasive techniques but more importantly, the ability to deliver drugs to the desired location within the inner ear.

A systemic approach to deliver drugs to the inner ear is challenging due to the presence of the blood-labyrinth barrier (BLB). Located in the stria vascularis, the BLB is a highly specialised capillary network that regulates exchanges between the blood and the intrastitial space within the cochlea. The BLB significantly reduces the concentration of blood-born toxic substances entering the inner ear and selectively facilitates ion, fluid and nutrient diffusion into the cochlea, maintaining cochlear homeostasis. The BLB is comprised of endothelial cells in the strial microvasculature, elaborated tight and adherent junctions, pericytes, basement membrane and perivascular resident macrophage-like melanocytes, which form a complex cochlear-vascular unit. The presence of the BLB is essential for normal hearing function, maintaining cochlear homeostasis, however, complicates matters when treatment is required to rehabilitate auditory function.

Drugs can be delivered to the inner ear via the systemic route, but only a select few can reach the desired site of action at therapeutic concentrations, in the inner ear, due to the BLB. High systemic drug doses are necessary in order to achieve therapeutic levels in the inner ear however are often associated with complications (McCall *et al*., 2010). Steroids as a treatment

for SNHL has been explored since the 1980's as a method of otologic management, displaying varying results. Glucocorticoids, for example, have been shown to recover hearing loss in patients with SNHL and autoimmune inner ear disease (AIED) (Wilson *et al*., 1980; Mockowitz *et al.,* 1984; McCabe, 1989; Veldmann *et al*., 1993). Clinical usefulness was limited by undesirable complications arising from the high systemic doses required to achieve therapeutic concentration in the cochlea (Parnes *et al*., 1999). Horie *et* al (2010) utilised encapsulation technology, using polyethylene glycol-coated polylactic acid (PLA), to demonstrate improved supply and longevity of steroids in the inner ear after systemic administration. The use of PLA encapsulated steroids, and other potential drug delivery systems, displays increased efficacy in the treatment of SNHL. Encapsulated drugs demonstrate an ability to cross the BLB more readily than free administration of drugs. The steroid mechanism of action within the inner ear is not fully understood, although known to have anti-inflammatory properties and to promote vasodilation, with increased microvascular blood flow, in the cochlea.

The RWM behaves like a semipermeable membrane allowing the diffusion of low molecular weight molecules such as corticosteroids and aminoglycoside antibiotics. The permeability of the RWM can be affected by other factors such as substance charge, liposolubility, concentration and configuration but also the thickness of the RWM (Goycoolea *et al., 1988).* The fundamental advantage of the increasing interest in RWM drug delivery is the ability to bypass the BLB and directly administer the drug to the inner ear. This results in higher inner ear drug concentrations but without the systemic approach complications as overall doses administered are lower. This method also avoids damaging the unaffected ear as could be seen with systemic administered drugs. Various techniques have been explored using biomaterials, such as nanoparticles, biodegradable materials, CI or the drug alone with no carrier, to explore the RWM as point of drug delivery into the inner ear. Chapter 1.4.5 looks at how drugs can be locally administered to the RWM.

1.4.4 Inner ear drug distribution and clearance

To achieve effective transfer of therapeutic substances through the RWM and into the inner ear, specific drug clearance mechanisms must be described. Firstly, the Eustachian tube, located in the middle ear cavity connected to the nasopharynx, plays a large part in clearance

of substances injected into the middle ear. If the viscosity of the substance is low, it will be rapidly excreted through the Eustachian tube and into the nasopharynx. Therefore, the substance must have a high enough viscosity, or a drug-delivery device is necessary, to prevent rapid excretion from the middle ear cavity.

Secondly, the continuous delivery of drugs onto the RWM is essential for local drug delivery into the inner ear. Bioactive molecules, especially those that are encapsulated, require specific periods of time to complete their pharmacological actions. It is difficult to predict the exact drug volumes that have diffused into the inner ear and the volumes that have been cleared into the middle ear cavity, thus a prolonged drug supply or a slow-release drug delivery system is favoured.

The last condition to note is ‘clearance’ within the inner ear. However, before discussing clearance, it would be beneficial to discuss the general principles of drug distribution within the inner ear. The inner ear is a complex structure comprising of scalae, large fluid-filled extracellular spaces, which interact with each other, surrounding systemic blood circulation and the middle ear cavity. The inner ear fluids, endolymph and perilymph, do not flow, are not ‘stirred’ and are poorly compressible. Locally delivered pharmacological agents are spread through the cochlear fluids by passive diffusion. The diffusion coefficient of a substance depends highly on its molecular characteristics, with weight being a key contributor.

Drug distribution within the inner ear has been divided into two processes, ‘radial’ and ‘longitudinal’ (Ohyama *et al*., 1988; Salt and Plontke, 2005). Radial distribution is between parallel scalae, of the same cochlear turn, and the vascular system. The lateral wall is an area of particularly fast diffusion due to its contribution to the maintenance of cochlear fluid homeostasis (Salt *et al*., 1991). Systemic blood interaction occurs at the lateral wall, through endothelial cells of capillary beds, providing a tight blood-labyrinth barrier. Longitudinal distribution is the diffusion and flow along the scalae, with the flow of endolymph and perilymph noted to be very low (Ohyama *et al*., 1988). The helicotrema connecting the ST and SV at the cochlear apex, the basal region of the SV and the vestibulum are other areas of longitudinal distribution. Figure 1.13 illustrates the diffusion of a substance from the round window to the scalae and surrounding compartments through radial and longitudinal distribution.

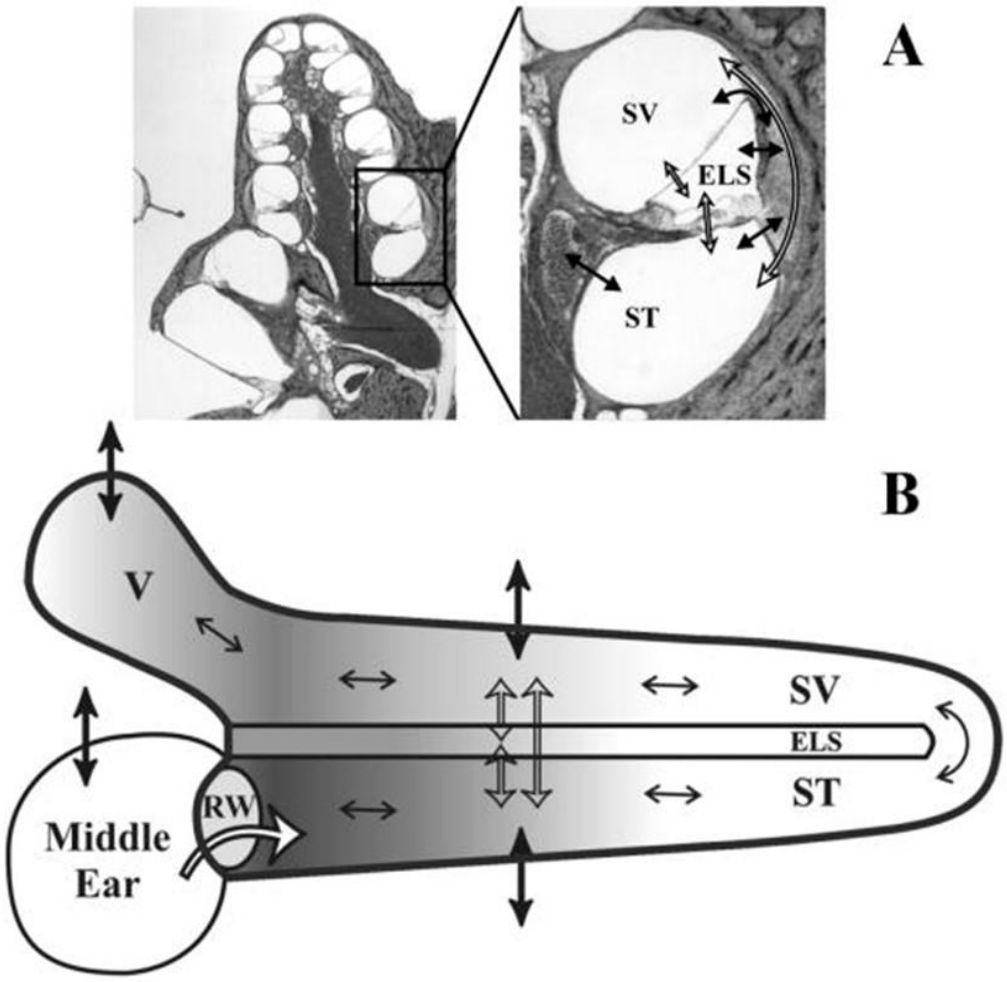

Figure 1.13. (A) Substance distribution through the guinea pig cochlea via radial distribution. Open arrows show the distribution between scalae and solid arrows the clearance from the scalae to the blood circulation. SV: scala vestibuli, ST: scala tympani, ELS: endolymphatic space. (B) Schematic of longitudinal distribution of a substance in an unrolled cochlea. Scalae dimensions, diffusion and flow along the scalae, and the helicotrema/ vestibulum are factors effecting distribution. Substance concentration is illustrated by shading. (Adapted from Salt and Plontke, 2005).

Clearance is the loss of a substance, in the cochlear fluid, to the surrounding blood and tissues. The diffusion of a substance will not strictly follow the path through the cochlea as seen with the mechanism of auditory stimulation. The substance will diffuse into all surrounding cells, fluids, and compartments reducing therapeutic concentrations and subsequently substance

diffusion rate. The capillary beds in the lateral wall and modiolus facilitate much of the clearance. The collective processes which contribute to the clearance of a substance include loss to the blood through endothelial cells in capillary beds, drug accumulation by surrounding tissues (receptor binding and metabolism) and uptake into intracellular spaces (Salt and Plontke, 2005). Removal of the substance from the RWM or the application of a fluid, such as buffer solution, can increase the rate of clearance. Clearance reduces the concentration of a substance within the inner ear and, in time, will reach a steady state concentration. Steady state refers to the point at which diffusion is balanced by clearance preventing the substance reaching the apical regions of the cochlea at therapeutic concentrations. The rate at which a substance is cleared depends on that specific substance, known as clearance rate. The magnitude of longitudinal drug concentration gradients is dependent on the substance diffusion and clearance rate. A concentration gradient within the inner ear is characterised by a very large concentration at the application site, commonly the round window, and a very low concentration at the apex of the cochlea. When the steady state concentration is met, it is clear a concentration gradient forms, which is a challenge that needs further work to overcome (Salt, 2005).

1.4.5 Methods of inner ear drug delivery

There are four main methods of drug delivery that utilise the RWM, an intratympanic injection, osmotic pumping, direct round window injection and a drug loaded CI. Intratympanic drug delivery is performed by inserting a fine needle into the ear canal, through the tympanum and then depositing the drug into the middle ear, above the RWM, see figure 1.14.

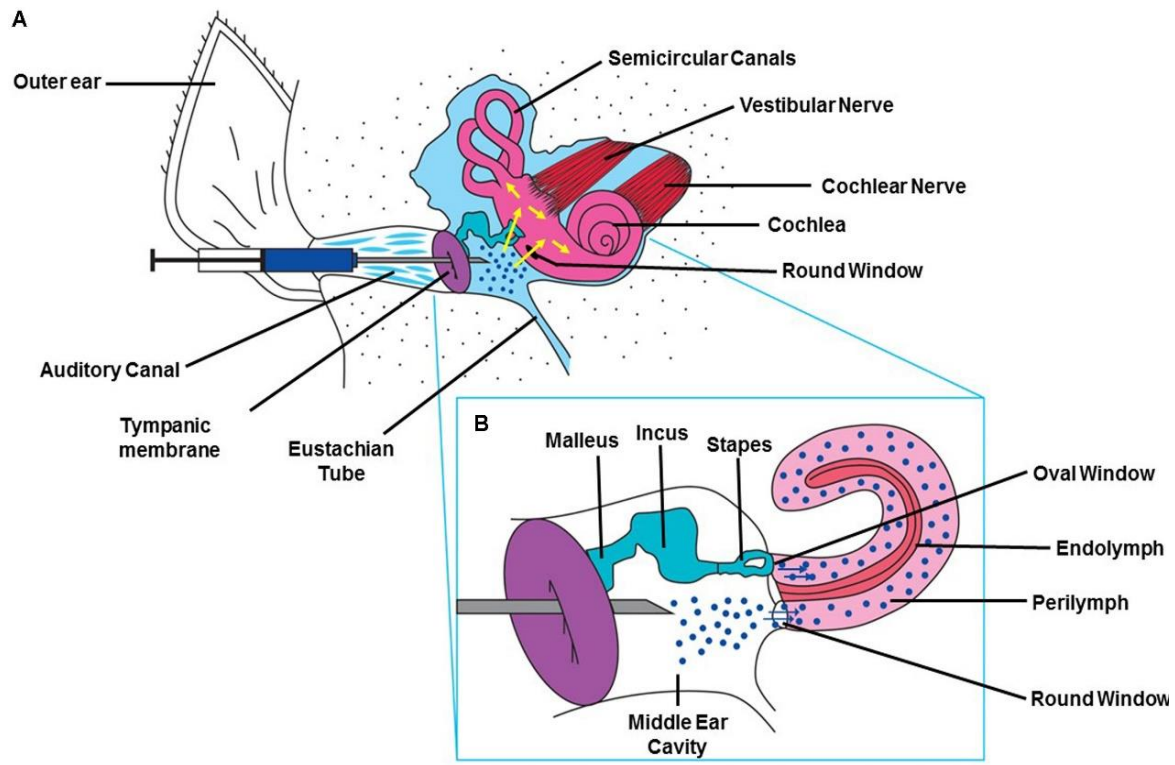

Figure 1.14. (A) A schematic to illustrate the method of intratympanic drug delivery targeting the middle ear. The fine needle is inserted into the ear canal and through the tympanum. The drug is deposited into the middle ear and in abundance to fill the middle ear cavity. (B) A zoomed in schematic of intratympanic drug delivery displaying the diffusion of the drug into the cochlea. (Adapted from Rybak *et al*., 2019).

Intratympanic drug delivery was first described by Liel (1879) for the treatment of eustachian tube dysfunction and then decades later by Ersner *et al* (1951) for the treatment of Meniere's disease. Today, intratympanic injections are administered to patients who suffer with tinnitus, SSNHL, vertigo, and Meniere's disease (Liu *et* al., 2016; Yener *et al*., 2020; Leng *et al*., 2017). Typically, corticosteroids, such as dexamethasone, are used for this method of delivery and patients would require multiple injections within a four-week period. Complications such as increasing tinnitus, transient dizziness and post-injection vertigo have been documented (Liu *et al*., 2016).

The use of osmotic pumps *in vivo* is a relatively new strategy to overcome the challenges of inner ear drug delivery. A small volume pump is implanted subcutaneously and a cannula directed to the round window niche or through the round window into the cochlea. Osmotic

pressure generated in the outer section of the pump forces the drug, loaded into an impermeable inner chamber, out through the cannula and into the target tissue. Reservoir volumes of 0.1 to 2 ml and flow rates from 0.1 to 10 μl/hr are typically used in pumping models. Drug infusion is continuous and can last 1 day to 6 weeks (Pararas *et al*., 2012). Infusion rates are slow allowing drug-perilymph total fluid volume equilibrium to be maintained by clearance mechanisms. Osmotic pumps have been utilised to determine its effectiveness in treating noise induced hearing loss (dexamethasone and methylprednisone), electrode insertion trauma-induced hearing loss (dexamethasone), hair cell death prevention (dexamethasone) and Meniere's disease (aminoglycosides) (Himeno *et al*., 2002; Takemura *et al*., 2004; Sendowski *et al*., 2006; Eshragi *et al*., 2006; McCall *et al*., 2010). The use of pumps to deliver drugs to the inner ear is very exciting work and should hopefully be moved to clinical trials soon.

After CI surgery, a process that entails inserting an electrode deep into the cochlea, it is common for the remaining hair cells to be damaged affecting residual hearing. Electrode implantation trauma triggers the inflammatory response which results in further inner ear complications. An interesting method of reducing the trauma and preserving residual hearing caused by electrode insertion is by loading the CI with pharmacological agents. Different options are available to those attempting to achieve CI drug delivery. The electrode carrier may be coated with the drug (typically in combination with a hydrogel), the drug may be integrated within the electrode carrier or the electrode carrier can be modified to equip a drug delivery channel which is connected to a drug reservoir or pump (Krenzlin *et al.*, 2012; Plontke *et al*., 2017). A dexamethasone eluting CI has shown to reduce inner ear inflammatory response, loss of sensory cells, deterioration of hearing thresholds, increased impedance and fibrosis around the electrode array (Bas *et al*., 2016; Douchement *et al*., 2015; Farhadi *et al*., 2013; Wilk *et al*., 2016). As a method of improving CI integration into patients, drug loaded electrodes are very promising. See Plontke *et al* (2017) review for further insight.

For the testing of new pharmacological agents, a direct injection into the cochlea via the RWM is often performed *in vivo*. It has been reported that injections through the guinea pig RWM does not damage hearing (Kho *et al*., 2000). The challenge associated with RWM injections is the efflux of fluid at the perforation site resulting in lower therapeutic concentrations of the drug in the inner ear. Methods of reducing fluid efflux is using glass pipettes or micro-needles and applying a gel to the round window, such as hyaluronate gel, to close the perforation (Hahn *et al*., 2012).

The challenge that remains is the formation of a base-apex concentration gradient due to the clearance of drugs from the inner ear. Drug concentrations at the apex are predicted to be significantly lower than that in the base because of drug clearance and cochlea geometry (i.e., the reducing volume from base to apex). The apex of the cochlea corresponds to approximately 45-55 % of the cochlea and reduced drug concentrations at this region will complicate treatments.

1.5 Guinea Pigs in Otologic Research

Otological research frequently requires the use of animal models, utilising mice, guinea pigs and rats, which closely resemble the anatomy of the human ear. Anatomical knowledge of the select animal ear is essential to ensure the techniques used to acquire data are both accurate and reliable, but above all, to avoid animal stress. Using techniques that are not appropriate to certain animals, due to bone fragility, for example, can result in unnecessary morbidity and mortality to a large number of animals. Here, guinea pig models are used to complete the research, due to their resemblance to the human ear and desirable behaviour traits. Albuquergue *et al* (2009) distinguished the similarities between guinea pig and human ears concluding that guinea pigs are the most desirable in otological research.

The guinea pig cochlea has three and a half turns, rat cochlea has two and a half turns and the human cochlea has two and half turns. It has been demonstrated that guinea pigs are best for handling because of their size and docile nature. The strength of the guinea pig temporal bone allows for better opening of the tympanic bulla without damaging the middle ear cavity. Rats, for example, are smaller and more difficult to perform middle ear surgical techniques on as their tympanic bulla is likely to break at the time of opening. Furthermore, opening of the auditory bulla can damage the ossicles. During surgical preparations, it is easier to sedate guinea pigs due to their docile nature, but also due to their larger size. More importantly for this research, the RWM is more accessible in guinea pigs, when compared to rats, and the guinea pig RWM has a similar structure to humans (Bledsoe, *et al*., 1988). Although the cochlea is smaller in guinea pigs, clinical translation into human studies would be possible by ‘scaling up’ the proposed methods to fit the human cochlea geometry. Diffusion and clearance mechanisms are comparatively similar between humans and guinea pigs.

1.6 The Aims

The main objective of this thesis is to determine the efficiency of cochlear excitation and drug delivery through the RWM. In chapter three, we investigate the feasibility of utilising the RWM as a location for drug delivery into the inner ear. We use a pharmacological agent of known physiological effect, which blocks the cochlear amplifier, to determine the distance the drug diffuses throughout the cochlear spiral via passive diffusion. Elevation of hearing CAP thresholds of the auditory nerve, at target frequencies, will confirm the drug has reached that region of the cochlea. Elevations at the apex of the cochlea, at frequencies 1 – 5 kHz, are of most interest, as this region is the furthest away from the RWM.

In chapter four, we explore the RWM as a means of hearing rehabilitation for patients with conductive hearing loss, with specific interest on ossicular chain fixation, as a result of middle ear diseases. It is known that displacing the RWM, at frequencies similar to that of incoming sound, excites the cochlea. This work looks to measure the efficiency of RWM stimulation utilising probes that partially occlude the RWM. By not completely occluding the RWM, the exposed area that is not covered by the probe footplate, is able to effectively relieve intracochlear pressure.

By applying the findings collected from chapters three and four, in chapter five we investigate whether a probe, that partially occludes and vibrates the RWM, can be utilised to enhance drug delivery to the inner ear. Inaudible, low frequency micro vibrations of the RWM are studied to determine the effect on drug mixing and distribution within the guinea pig cochlea. From this, we can develop a proof of concept that supports a novel method of drug distribution along the cochlear spiral. Furthermore, we argue that cochlear drug distribution utilising RWM micro vibrations does not require ossicular chain functionality.

Chapter Two

Materials and Methods

The materials and methods chapter aims to describe the experimental techniques and animal preparations necessary to gather acoustic, mechanical and electrophysiological measurements on guinea pigs. All work was undertaken within sound attenuated booths (IAC Audiometric booth) and on gas inflated tables (LINOS, technical Manufacturing Corporation). Experimental control, data acquisition and data analysis were performed using a PC with programs written in MATLAB (The MathWorks). All procedures involving animals were performed in accordance with UK Home Office regulations with approval from the local ethics committee.

In this work, two types of RWM vibrations were utilised to achieve a desired response within the cochlea. For the round window stimulation method, see section 2.5, low amplitude, high frequency vibrations were used to stimulate the cochlea. High frequency vibrations enable the device to mimic the effect of incoming sound vibrations. In the RWM micro vibrations method, see section 2.6, large amplitude, low frequency vibrations were used to displace the cochlear fluids without causing damage to inner ear components. In order to achieve this, two different devices were designed that provided the parameters required.

2.1 In Vivo Drug Administration

Before an experiment can be undertaken *in vivo*, the animal must be anaesthetised correctly and in a manner that minimises stress. To achieve this, the route of drug administration is

Table 2.1 An overview of the five typical routes for *in vivo* drug administration and the drugs administered in our experiments.

Route of Administration	Injection Site	Administered Drug	Reasoning
Intraperitoneal	Lower left quadrant of abdomen	Pentobarbital	Minimise stress to animal and ease of administration
Intramuscular	Quadricep muscle	Fentanyl & Medetomidine Hypnorm	Ease of administration and fast absorption
Subcutaneous	Under the skin around neck/ back area	Hanks' Balanced Salt Solution 1X Atropine Sulphate	Slow absorption over a period of time

essential to ensure the animal is in a controlled anaesthetised state. There are five main routes of drug administration *in vivo*: intraperitoneal (IP), intramuscular (IM), subcutaneous (SC), intravenous (IV) and oral. Table 2.1 outlines the injection site along with the drugs used in our experiments and the reasoning for that injection method.

Pentobarbital is administered via the IP route to sedate the animal whilst minimising stress. Once the animal is sedated, fentanyl and medetomidine are administered into the quadricep muscle to anaesthetise. Before any experimental work is conducted on the animal, a pain receptive test is conducted. This entails carefully but firmly squeezing the paws/ feet with tweezers to determine the animal's reflective state. If the experiment is due to last longer than 2 hours, a subcutaneous injection of Hanks' Balanced Salt Solution 1X (Gibco) is administered to maintain blood pH and prevent dehydration.

2.2 Animal Preparation

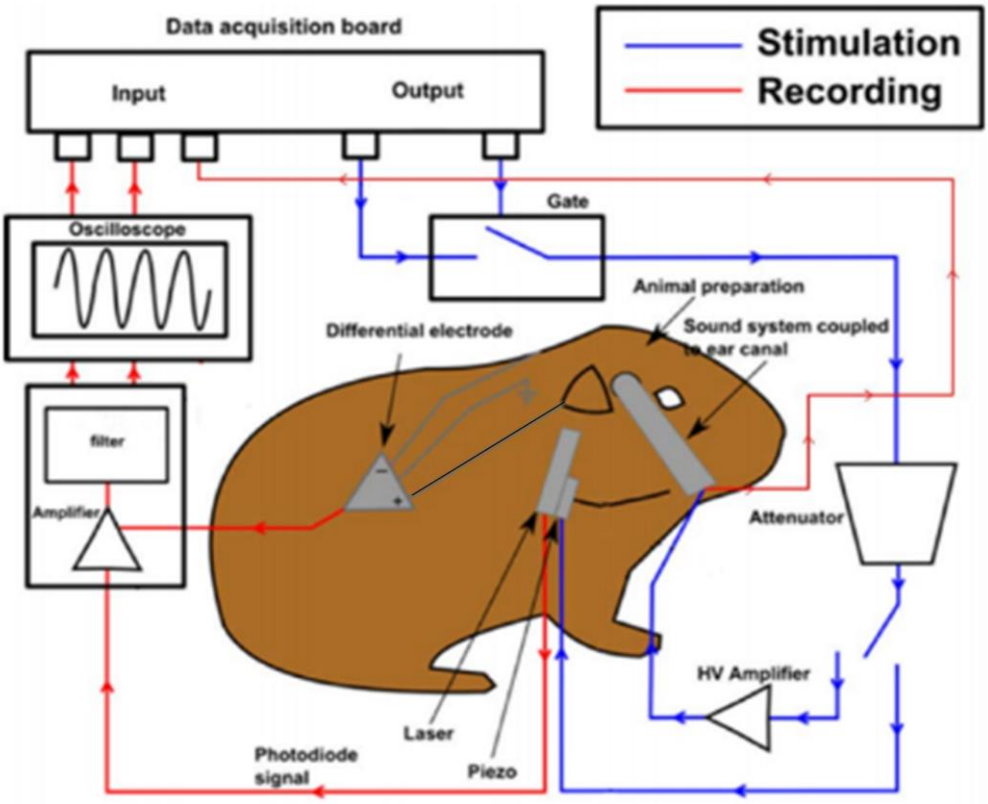

Figure 2.1. Experimental setup. An overview of the electrical set up for sound stimulation and recording of acoustic, electrical, and mechanical responses from the guinea pig cochlea. For two tone stimulation, two outputs with attenuators are required however are not illustrated here for simplicity. (Adapted from Weddell, 2013).

Pigmented guinea pigs of varying weight (200-400 g) and gender were anaesthetised with the neuroleptic anaesthetic technique (atropine sulphate 0.06 mg/kg subcutaneous, pentobarbital 30mg/kg intraperitoneal, fentanyl/ fluanisone (Hypnorm) 500 µl/kg intramuscular). Additional Hypnorm injections were administered every 40 minutes. Further doses of Pentobarbital were given as necessary to maintain a non-reflexive state. During periods of Hypnorm unavailability, fentanyl (50 µg/ml) and medetomidine (200 µl/kg) were used. When administering fentanyl and medetomidine, atropine sulphate was excluded. Hanks' Balanced Salt Solution 1X (Gibco) (6 ml/kg) was administered during experiments of large duration. An electrocardiogram was recorded utilising a pair of sharp electrodes placed at either side of the thorax, subcutaneously.

The animal was then placed on a heated blanket and in a heated head holder at 38 ºc, followed by a tracheostomy allowing artificial respiration with a mixture of 95% oxygen and 5% carbon dioxide. See figure 2.1 for an overview of the experimental setup

To access the RWM, the auditory bulla was opened. The pinna was removed and tissue cleared away revealing the temporal bone. The auditory bulla is then visible (prominence in the bone) to which a small incision is made forming a 5 mm in diameter hole using a scalpel blade. The head of the animal was then fixed to the head stage using dental cement and a steel bar immobilising the head without applying pressure. A Teflon coated Ag-AgCl wire was placed onto the cochlear bony ridge in the proximity of the RWM as well as two reference Ag-AgCl electrodes placed either side of the cranium. A laboratory standard signal amplifier was used to amplify electrical recordings (Hartley, Brighton, UK). Electrocochleography was measured through differential signalling of this electrode. Thresholds of the N1 peak of the CAP were estimated visually using 10 ms tone stimuli at a repetition rate of 10 Hz.

In order to fix the stapes, Superglue ^{TM} (ethyl 2-cyanoacrylate) was applied onto the tympanum, from the ear canal, and left to dry for approximately 30 minutes. Probes were not replaced during the gluing process. To prevent excessive fluid build-up in the round window niche, released into the middle ear cavity by surrounding tissue during the surgery, fine absorbent paper wicks were used to remove fluid when required.

2.3 Acoustic Stimulation

Hearing sensitivity thresholds were measured before experimental measurements were made to ensure the animal did not suffer from hearing loss. For acoustic stimulation, sound was delivered to the tympanic membrane by a closed acoustic system comprising two Bruel and Kjaer 4134 1/2-inch microphones for delivering tones and a single Bruel and Kjaer 4133 1/2-inch microphone for monitoring sound pressure at the tympanum. The microphones were coupled to the ear canal via 10 mm long, 4 mm diameter tubes to a conical speculum, the 1 mm diameter opening of which was placed approximately 1 mm from the tympanum. The closed sound system was calibrated *in situ* for frequencies between 1 and 30 kHz.

2.4 In Vivo Electrophysiology

Electrophysiology recordings were achieved by differential electrodes that recorded local field potentials of the auditory nerve. The CAP electrode, a Teflon coated Ag-AgCl wire, was placed on the bony ledge of the round window niche, see figure 2.1 and 2.3. The ground and reference electrodes were placed on the skull, under the skin. Measurements of the amplitude of gross electrical potentials generated by the auditory nerve require amplification. A laboratory standard signal amplifier was used to amplify electrical recordings (Hartley, Brighton, UK). The amplified recording is then displayed on an oscilloscope, as an N1 peak of the CAP, see figure 2.2. The first trace on the oscilloscope has a Y axis of voltage, in millivolts (mV), the second trace is in volts (V) and the X axis is time, in ms, for both traces.

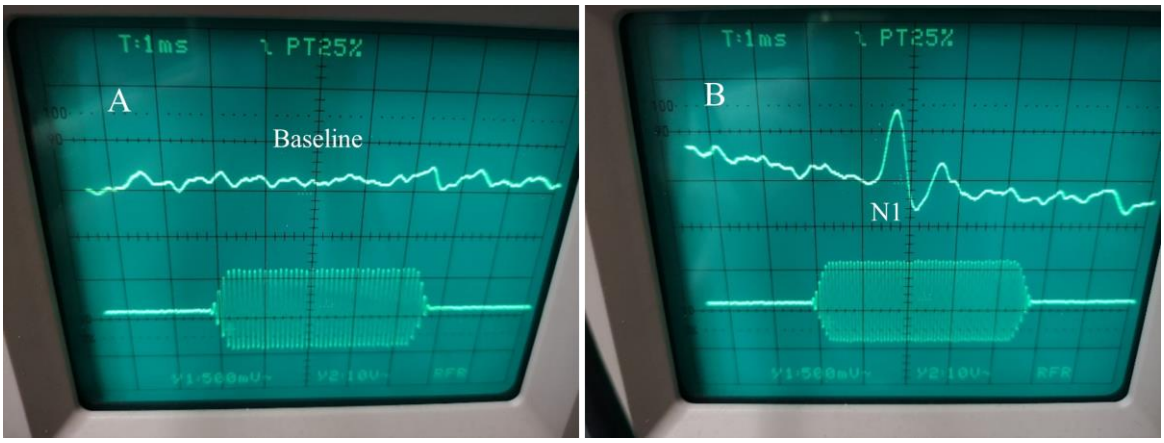

Figure 2.2. Photographs of **A**. The oscilloscope baseline **B**. A compound action potential (CAP) as a negative 1 (N1) peak in response to an auditory stimulus of 45 dB SPL at 9 kHz in a guinea pig. Trace Y1 is at 500 mV and trace Y2 is at 10 V with the X axis displaying time at 1 ms. Y1 is recorded potential from the RW bony ledge. Trace Y2 is a sinusoidal wave at 9 kHz representing the frequency of the auditory stimulus used to elicit a CAP.

In our experiments, sound pressure level (SPL) and probe displacements were utilised to induce a CAP determining sensitivity thresholds visually. Manual control is achieved by carefully increasing the stimuli (SPL or probe displacement) until the N1 neural potential is observed on

the oscilloscope (see figure 2.2), then the stimuli is slowly decreased until N1 is no longer visible. This threshold level of stimulation was recorded.

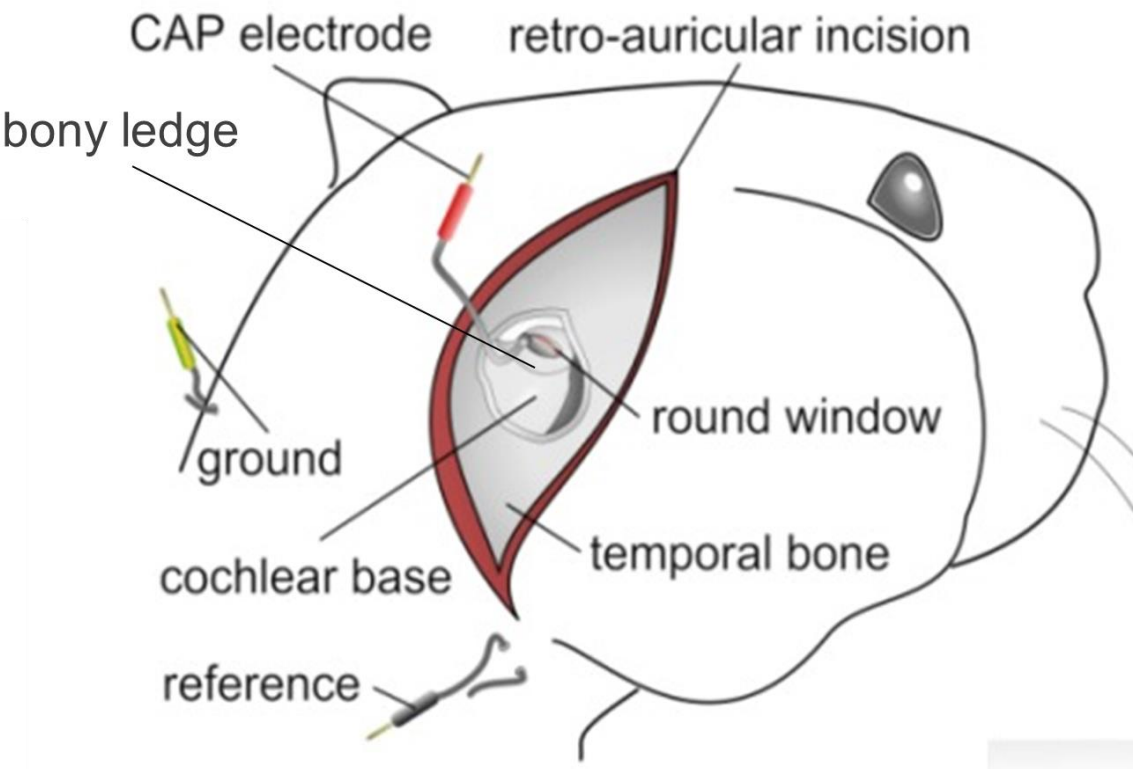

Figure 2.3. A schematic of the round window niche displaying placement of compound action potential (CAP), ground and reference electrodes. The CAP electrode rests on the bony ledge and to the left of the round window membrane. The CAP electrode does not make contact with the round window membrane but is placed in close proximity on the bone which lies directly below. (Adapted from Schultz *et al*., 2012)

2.5 Round Window Stimulation

To perform RWM stimulation, two end plated piezoelectric stacks, consisting of multiple chips bonded via epoxy and glass beads (Thorlabs, PK4CMP2), were modified with tungsten wire (Advent Research Materials), see figure 2.4 for a drawing. Three probes were used in this study, with footplate diameters of 0.3 mm (0.07 mm^2), 0.5 mm (0.2 mm^2) and 0.75 mm (0.44 mm^2). Each probe was a 20 mm long section of tungsten wire (with an equal diameter to that of the footplate) which had been shaped to a right angle at the tip, grinded and polished to a flat circular footplate.

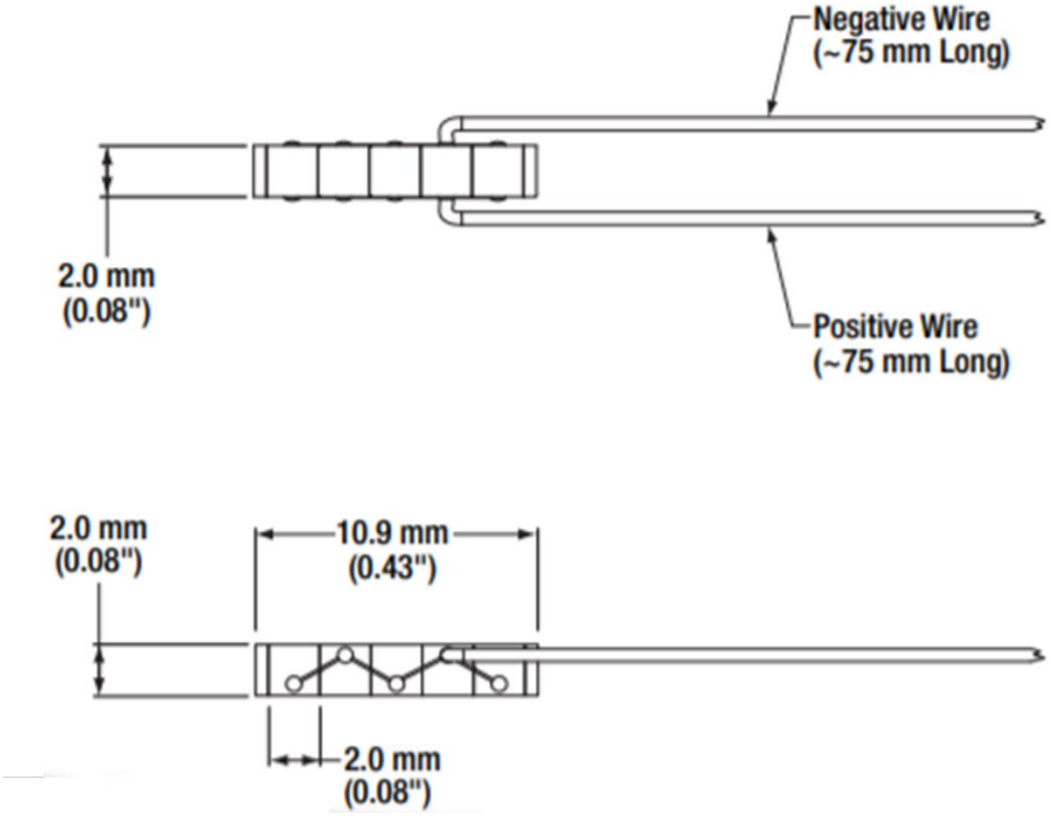

Figure 2.4 A drawing representing the dimensions of the piezoelectric actuators used in this work. The Piezo wires were soldered to RG-59/U coaxial cables (75 Ohm) which were connected to a bespoke piezo driver (Hartley, Brighton, UK). (Taken from Thorlabs. CTN003603-S01, Rev B data sheet, 2020).

Each probe was bonded to a separate piezo using super glue (ethyl 2-cyanoacrylate). The piezo was bonded to a thin steel rod, using Araldite ™, which was then inserted into a micro manipulator. The piezo was wired to RG-59/U coaxial cables (75 Ohm) and plugged into a laboratory standard piezo driver (Hartley, Brighton, UK) during an experiment.

Utilising the micro manipulator, the probe footplate was placed perpendicularly on the centre of the RWM, using the tympanic bulla opening and the space available in the round window niche as an entry point. Each piezo had a maximum displacement of 9.5 µm ± 15 % and a voltage range of 0-150 V. Stimulating current through the piezo was generated by a Data Translation 3010 board. Maximum voltage applied to the piezo was 10 V which corresponds to 0 dB attenuation. A voltage divider was utilised for measurements too sensitive for the above set-up, removing 9 V, thus reducing the buffer voltage to 1 V, with 1 V corresponding to 20

dB attenuation. High-frequency cut-off of the system for electrical stimulation *in situ* was above 100 kHz.

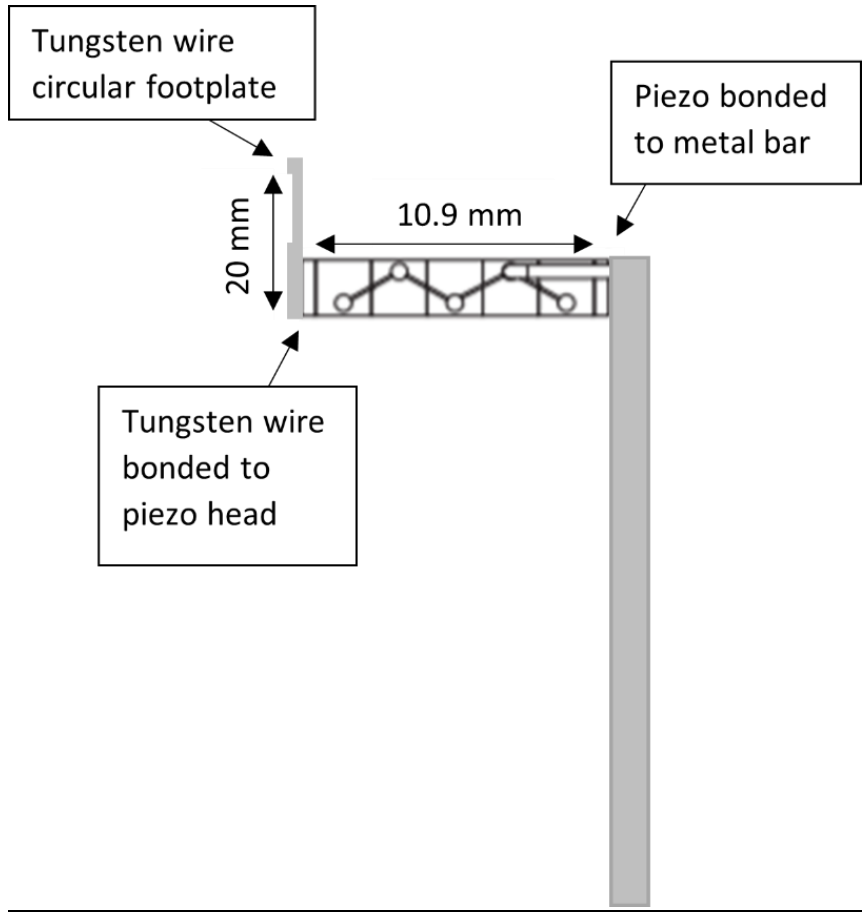

Figure 2.5. A simple schematic illustrating the tungsten wire probe and piezoelectric actuator set up. Each probe was a 20 mm section of tungsten wire (with an equal diameter to that of the footplate) which had been shaped to a right angle at the tip, grinded and polished to a flat circular footplate. The probe was bonded to the piezo head using Superglue ™ and the piezo was bonded to a metal bar with Araldite ™. The Piezo wires were fixed to the metal bar using cable ties – see figure 2.6 for a photograph. (Modified from Thorlabs. CTN003603-S01, Rev B data sheet, 2020).

The probe footplate was placed perpendicular to the RWM (Figure 2.6). A perpendicular approach enabled maximum cochlear excitation for each probe diameter demonstrating a clear and repeatable difference between RWM coverage.

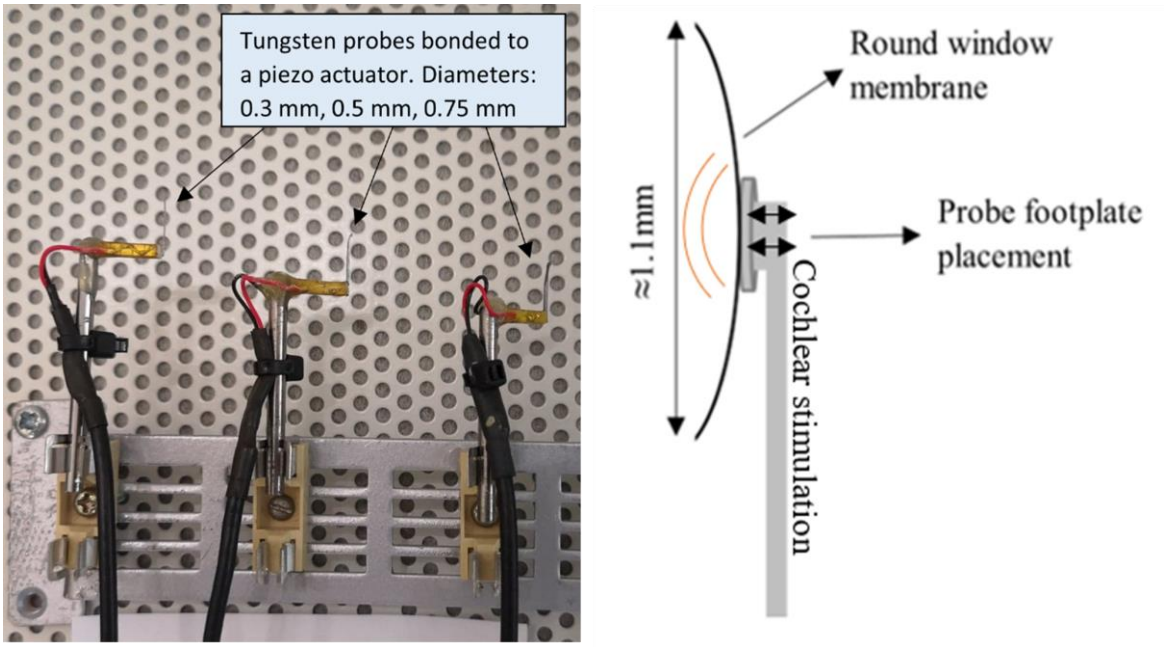

Figure 2.6. A photograph of the probe setups and a diagrammatic visualisation of the probe placement on the round window membrane. The tungsten probes (diameters 0.3 mm, 0.5 mm and 0.75 mm) were bonded onto a piezo actuator which were fixed to steel bars. The steel bar was then inserted into a micro manipulator allowing fine probe placement onto the round window.

2.6 Round Window Micro Vibrations

A miniature loudspeaker (Visaton K16), modified with a carbon probe, was used to vibrate the RWM in drug delivery experiments, see figures 2.7 and 2.8 for an overview of the loudspeaker. The miniature loudspeaker was 16 mm in diameter, with 50 ohms coil resistance and 0.5 W power rating. A carbon probe, 50 mm in length and 0.5 mm in diameter, was fixed centrally on the loudspeaker coil with a fine amount of superglue. The probe was perpendicular to the speaker face and remained absolutely straight during experiments to ensure no sideward deviation. The loudspeaker was fixed to a steel rod, using araldite, and the rod held in a micro manipulator for precise probe placement. The loudspeaker was wired to RG-59/U coaxial cables (75 Ohm). A programmable synthesiser/ signal generator 0.1 mHz – 50 MHz (PHILIPS PM9153) was used to drive the loudspeaker in the experiments. To achieve 20 μm peak-to-peak probe displacement, at a frequency of 4 Hz and 2 Hz, 1 V and 0.5 V was provided to the loudspeaker, respectively, table 2.2 provides an overview. A laser vibrometer (Polytec CLV-

2534 Laser Vibrometer) and oscilloscope (HAMEG Instruments) were used to calibrate probe displacements before the experiment.

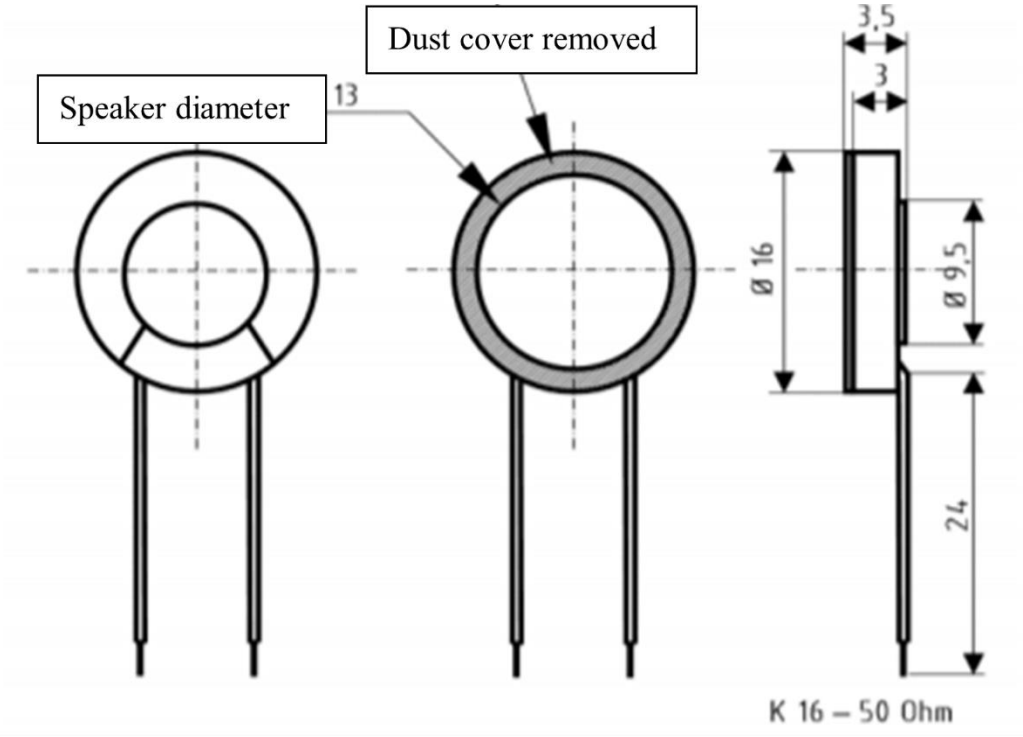

Figure 2.7. A drawing representing the dimensions of the miniature loudspeaker used to vibrate the round window membrane. The dust cover was removed allowing for direct fixing of the carbon probe to the speaker coil providing maximum transfer of vibrations. All measurements are in mm. (Modified from Visaton Art. No. 2815 data sheet, 2015).

The probe was placed at a 45-degree angle to the RWM (figure 2.9). After placement, animal hearing sensitivity was measured, between 1-30 kHz, by recording auditory nerve CAP thresholds. Upon confirmation the animal had adequate hearing, 5 µl of 100 mM salicylate, in Hanks' Balanced Salt Solution 1X (Gibco) (pH: 7.84 – HANNA instruments pH 209 Meter), was placed into the round window niche using a thin cannula tube and syringe set up. Immediately after salicylate placement, the probe was vibrated. In the first 20 minutes period, acoustic CAP threshold recordings were taken after every 3-5 minutes to record the fast action of salicylate at the basal region of the cochlear. Due to the very low frequency used to vibrate the RWM, there is no auditory nerve CAP during probe displacement due to the probe vibrations, allowing acoustic CAP threshold recordings at acoustic frequencies to be taken during RWM vibrations. After the first 20-minute period, further CAP recordings were made every 10 minutes until a total of 60 minutes of RWM micro vibrations (i.e., 4 further recordings

after the initial 20 minutes). To washout, the probe was removed and the salicylate was cleared using fine paper wicks. The acoustic CAP threshold recovery was recorded.

Figure 2.8. A photograph of the miniature loudspeaker prior to modification. A steel bar was fixed to the rear of the speaker using araldite. The steel bar was then inserted into a micro manipulator allowing for precise probe placement onto the round window membrane. The loudspeaker wires were soldered to RG-59/U coaxial cables (75 Ohm) which were connected to a programmable synthesiser/ signal generator 0.1 mHz – 50 MHz (PHILIPS PM9153) used to drive the loudspeaker. The dust cover was removed and the carbon probe, 50 mm in length and 0.5 mm in diameter, was fixed centrally on the speaker coil using a fine amount of superglue. The probe tip was positioned perpendicular to the speaker face. This improved coupling between the probe tip and round window membrane. (Modified from Visaton Art. No. 2815 data sheet, 2015).

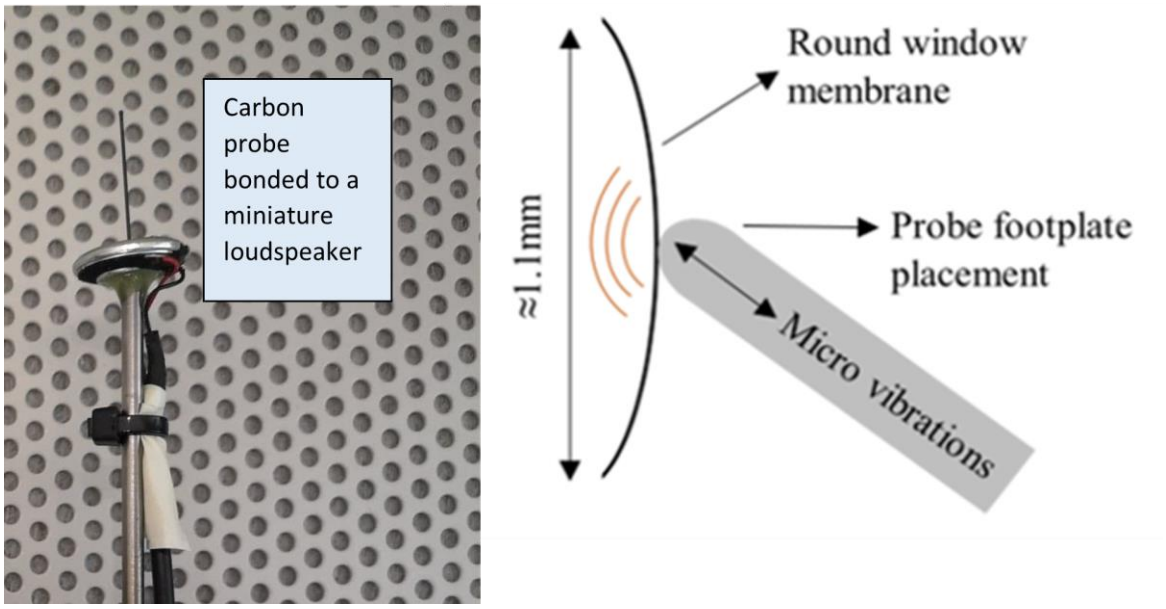

Figure 2.9. A photograph of the 50 mm in length, 0.5 mm diameter carbon probe and loudspeaker setup with a diagrammatic visualisation of the carbon probe placement on the round window membrane. The probe tip was curved using a very thin layer of super glue preventing fragmentation and RWM damage.

Table 2.2 An overview of the settings used for round window membrane micro vibrations. A programmable synthesiser/ signal generator 0.1 mHz – 50 MHz provided a voltage (1 V and 0.5 V) to the loudspeaker at a frequency (4 Hz and 2Hz) which displaced the probe tip. Using a laser vibrometer (sensitivity 0.002m/s/V), the probe tip velocity, measured in mV, was used to quantify the probe displacement.

Frequency of loudspeaker vibration (Hz)	Voltage applied to the loudspeaker (V)	Laser vibrometer velocity measurement of probe (mV)	Equivalent displacement amplitude (μm)	Peak-to-peak probe displacement (μm)
4	1	250	10	20
2	0.5	125	10	20

Note the slightly off centred position of the loudspeaker and subsequent carbon probe in figure 2.9. This is to allow a preferred angle of approach when placing the probe onto the round

window membrane. Prior to this adjustment, placement of the probe was much more challenging.

A probe of 0.75 mm in diameter was not possible, when attached to a miniature sound speaker, and therefore a 0.5 mm probe was used. Due to the increased size of the miniature sound speaker and its design, when compared to a piezo actuator, probe displacement was along its length, in a forward motion, rather than in a lateral motion. The tip of the carbon probe was slightly curved allowing maximum contact between the probe tip and the RWM. A perpendicular approach was tested, along with repositioning of the animal head. However, the miniature loudspeaker blocked line of sight of the probe tip, down the microscope, and thus could not be achieved.

2.7 Acoustic System and Round Window Probe Calibrations

Before measuring guinea pig hearing sensitivity thresholds, the acoustic system was calibrated *in situ*. Sound was delivered to the tympanum via a closed acoustic system comprised of two Bruel & Kjaer 4133 1/2-inch microphones, used to deliver tones, and a single Bruel & Kjaer 1/2-inch microphone for monitoring sound pressure at the tympanum. The microphones were

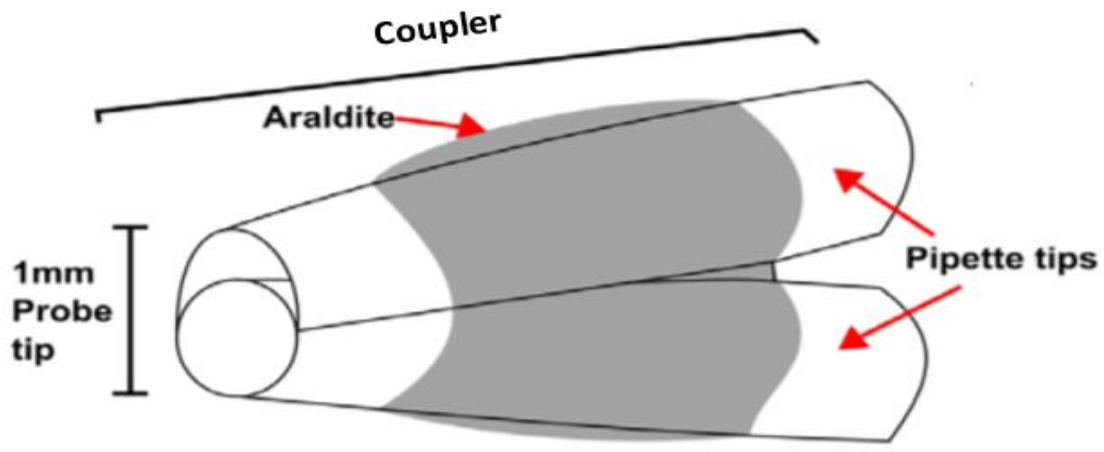

Figure 2.10. A bespoke coupler constructed from two yellow plastic pipette tips (Plastibrand, Sigma – Aldrich) and shaped to form a probe of similar diameter to that of the guinea pig auditory canal. A microphone (bottom tip) and speaker (top tip) closed acoustic system was coupled using a bespoke coupler set up used to deliver sound to the tympanum. The two tips are held together with a single strand of nylon thread and araldite (Huntsman Advanced Materials). The probe was tested to ensure minimal sound reflection, resonances, and anti-resonances inside the probe chamber. (Modified from Weddell, 2013).

fed into a bespoke coupler see figure 2.10, positioned into the ear canal, and the coupler's tip was placed approximately 1 mm from the tympanum.

To calibrate the closed acoustic system, a frequency stimulus of quasi-white noise (0.1 – 200 kHz) was delivered to the tympanum via speaker one and monitored by the recording microphone, *in situ*. The recorded frequency response, in volts (V), is then obtained and used to convert its output to dB SPL re 2 x 10^{-5} Pa. A 1 kHz sound level calibrator of 94 dB SPL (Sound Level Calibrator Type 4230, Bruel & Kjaer) was utilised to calibrate the recording microphone prior to placement within the closed acoustic system. Speaker one was then stimulated to play a test-tone of 1 kHz and the frequency response recorded in volts. The test-tone is used to calculate the voltage response of the microphone per dB SPL of the 1 kHz test-tone frequency.

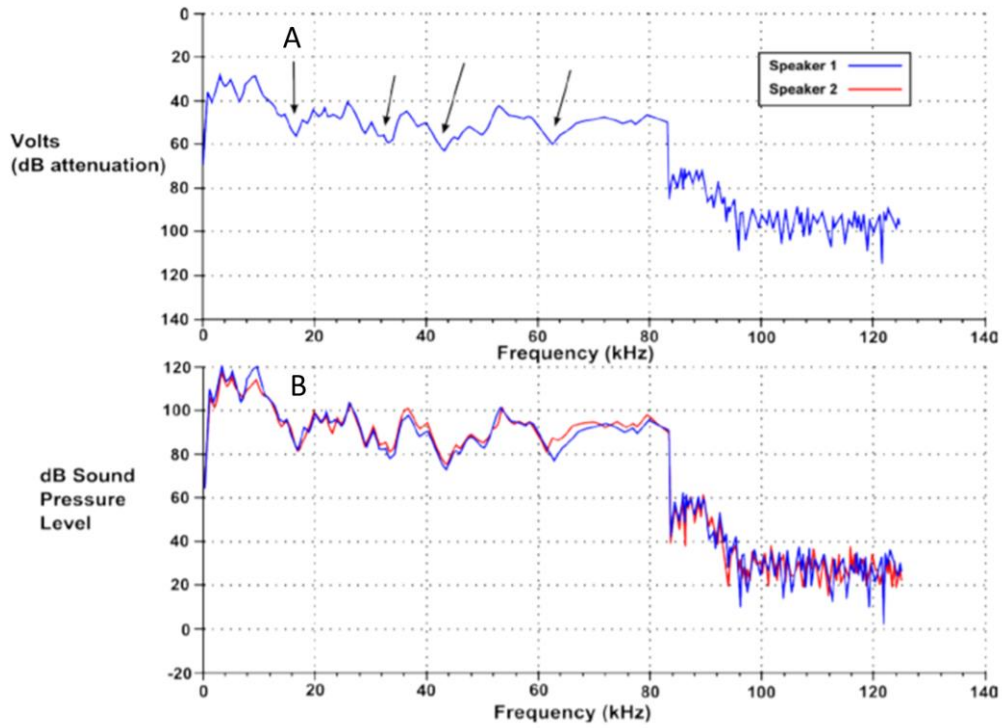

Figure 2.11. Sound calibration curve of frequency response of speakers one and two. Curve A is the frequency response of speaker one in volts (V) and curve B is the frequency response in dB SPL, of speakers one and two, at dB SPL re 2 x 10^{-5} Pa. The black arrows represent the internal reflections, resonances, and anti-resonances. (Adapted from Weddell, 2013).

With this conversion factor, a calibration curve can be made for all frequencies (0.1 – 100 kHz) required due to the known frequency response linearity property of the recording microphone (Figure 2.11). The frequency response recorded from the test-tone can be utilised to calculate the voltage response per dB SPL across all frequencies of interest deriving a calibration curve in dB SPL re 2 x 10^{-5} Pa. Speaker two was calibrated using the same conversion factor after playing a burst of quasi-white noise (0.1 – 100 kHz). A programme written in MATLAB (The Mathworks, Inc) automated this calibration process for guinea pig experiments.

The calibration curve would characterise numerous notches. The displayed notches (Figure 2.11 A, black arrows) were representations of internal reflections, resonances and anti-resonances within the acoustic system – more specifically, the coupler. The coupler-canal complex was the main contributor to these notches therefore alterations to coupler placement were made to reduce the notches. After adjustments were made, a new calibration curve would be made.

The probes used to displace the RWM required calibration allowing exact displacements, at a desired frequency, to be known. A laser vibrometer (Polytec CLV-2534) was used to measure the velocity at which the probe displaced. The laser was placed at least 300 mm away from the probe and the laser beam was focused centrally on probe footplate. Measurements were taken at all frequency (1 – 30 kHz) and dB attenuation ranges re 10 V (0 – 120 dB attenuation) used in the experiments. The velocity data was then converted into corresponding voltages, in other words, the voltage applied to the piezo/ loudspeaker to displace the probe at a specific velocity. The sensitivity of the laser vibrometer used was 0.002 m/s/V, therefore:

$$Sensitivity = \frac{Velocity}{Voltage}$$

From this equation, the velocity amplitude of the probe can be calculated. The oscillatory motion of the probe follows that of a sine wave, which is associated with two factors, amplitude and frequency. Utilising this relationship of simple harmonic motion, displacement can be derived. The general equation that that describes motion which follows a sine wave is:

$$x(t) = A\ sin(2\pi ft)$$

Where A is the amplitude of displacement, f is the frequency, and $x(t)$ is the displacement of x at time t. $2\pi f$ is angular velocity ω, therefore $x(t)$ can be deduced to:

$$x(t) = A\ sin(\omega t)$$

If $x(t)$ is the displacement of the system, then the velocity is:

$$v = \frac{dx}{dt}$$

Adding this relationship to the sinusoidal equation:

$$v(t) = \frac{dx}{dt} = A\ \omega\ cos(\omega t) = B\ cos(\omega t)$$

Where B is the velocity amplitude. Therefore, the displacement amplitude could be calculated as:

$$A = \frac{B}{\omega}$$

And, recalling the first step, ω is equal to $2\pi f$. When calculating displacement for probe calibrations, velocity was in metres per second, π was rounded to 3.14 and frequency was in Hertz, providing a displacement in metres. The displacement was then converted to nanometres. When calibrating the probes, oscillations of the probe at all frequency and attenuation ranges, used in our experiments, were measured to determine displacement. Each probe 0.3 mm, 0.5 mm and 0.75 mm was calibrated this way. Once the probe displacements were known from the measured velocity, graphs were plotted displaying the linear relationship

between displacement and dB attenuation for the voltage applied to the piezo re 10 V, as seen in figure 2.12. Each probe was calibrated 3 times to form an averaged plot and standard deviation was not plotted to allow ease of displacement extrapolation.

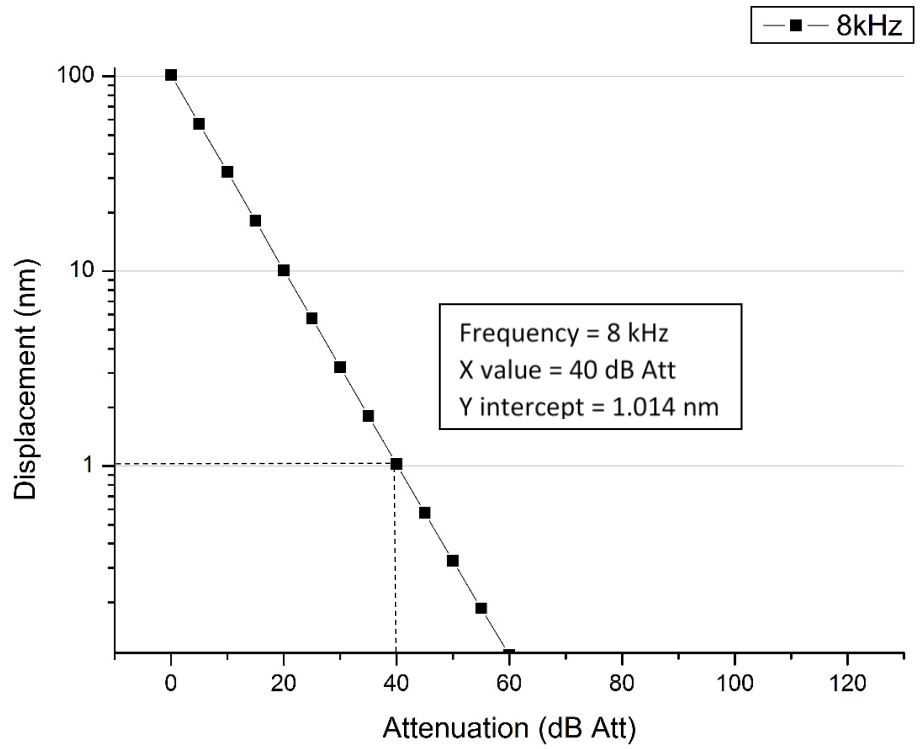

Figure 2.12. An example of a displacement graph used to determine the displacement at the dB of attenuation for voltages applied to the piezo re 10 V of an oscillating probe. This displacement is for the 0.75 mm probe oscillating at 8 kHz. When the 0.75 mm probe oscillated at 8 kHz, with a dB attenuation of 40 dB Att, displacement was extrapolated and determined to be 1.014 nm. The maximum voltage of attenuation to the 0.3 mm and 0.5 mm probes was 10 V and to the 0.75 mm probe, 1 V. A lower voltage was required to decrease probe displacement.

In the RWM stimulation experiments, attenuation is recorded to determine the required level of stimulation to elicit a CAP at a particular frequency. The frequency range 1 – 30 kHz was used in all experiments therefore thirty calibration curves for each probe were made. The raw data gathered were a series of dB attenuations which were later used in data analysis to determine the probe displacement required to generate a threshold CAP at a specific frequency.

2.8 Salicylate Application

Five microliters of sodium salicylate mixed with Hanks' Balanced Salt Solution 1X (Gibco) (pH: 7.84 – HANNA instruments pH 209 Meter), at a concentration of either 100 mM in experiments on salicylate diffusion in the ST or 1 M in experiments with complete block of the cochlear amplifier, was applied on the RWM using a thin cannula tube and syringe set up. The solution was removed from the RWM using paper wicks to observe the wash out effect. Sodium salicylate is a weak acid, pKa 2.79, that is unionised at a low pH and ionised at a higher pH, therefore does not readily cross membranes.

2.9 Signal Generation

Voltage signals to the piezo were sinusoidal stimuli of 40 ms in duration (with 110 ms between stimuli) shaped with raised cosines of 0.5 ms duration at the beginning and at the end of each sinusoidal pip. All acoustic stimuli in this work were shaped with raised cosines of 0.5 ms duration at the beginning and at the end of stimulation. White noise for acoustical calibration and tone sequences for auditory and mechanical stimulation were synthesized by a Data Translation 3010 board at 250 kHz and delivered to the microphones or to the piezo through low-pass filters (100 kHz cut-off frequency). Signals from the acoustic measuring amplifier were digitized at 250 kHz using the same board and averaged in the time domain.

2.10 Mathematical Modelling (Chapter Three)

Pooled data from 5 animals were used to find an optimized set of the model parameters via fitting the entire set of experimental data using the Genetic Algorithm (GA) tool in MATLAB (The MathWorks. Inc, 2018a) (Figure 3.3). The combined best fit to the entire set of experimental data for the optimized set of parameters is illustrated in Figure 3.5. Figure 3.3 shows the same plots for each of the frequencies along the corresponding experimental data. It is worth noting, that the optimisation procedure was performed over the entire experimental set up in order to fit the data for all the experimental frequencies simultaneously (Figure 3.3). The optimized set of model parameters (Table 1) found due to the general optimization procedure was used to predict cochlear responses and concentrations of salicylate (Figure 3.6) along the entire cochlear length and over arbitrary time duration.

2.11 Statistical Analysis

An unpaired, parametric t-test was the statistical test employed throughout this thesis. Chapter four looks to compare the sensitivity of cochlear excitation, by recording CAP threshold

recordings in response to 3 varied size probes (0.3 mm, 0.5 mm and 0.75 mm) displacing the RWM. The statistical analysis here was used to compare the probes to each other i.e., 0.3 mm vs 0.5 mm, or 0.3 mm vs 0.75 mm, therefore an analysis of variance (ANOVA) test was not used. All statistical analysis was performed in Origin (Origin Lab).

In line with the 3R's, a power analysis was conducted prior to all experimentation including animals, using the free power analysis tool on the NC3Rs website. N numbers used in experiments, to provide statistically significant data, were in line with the power analysis prediction preventing an unnecessary use of an excess number of animals. The statistical test of choice, an unpaired t-test, the predicted mean values from pilot experiments and the number of experimental groups were factors considered when conducting the power analysis. Peer reviewed publications, with a similar hypothesis, also aided the decision for suitable N numbers in this work. Experimental data was collected and a statistical test carried out, after each experiment, including standard deviation calculations, until the data was statistically significantly different, without breaching the N number the power analysis predicted.

2.12 Fluorescent dye experiments

Lucifer yellow CH, lithium salt (Thermo Fisher Scientific) was used to visualize diffusion in straight water filled pipes (Figure 2.13). The pipes with an approximate length of 40 mm were constructed using Tygon™ LMT-55 tubing (1.14 mm ID, 0.80 mm wall, Fisher Scientific).

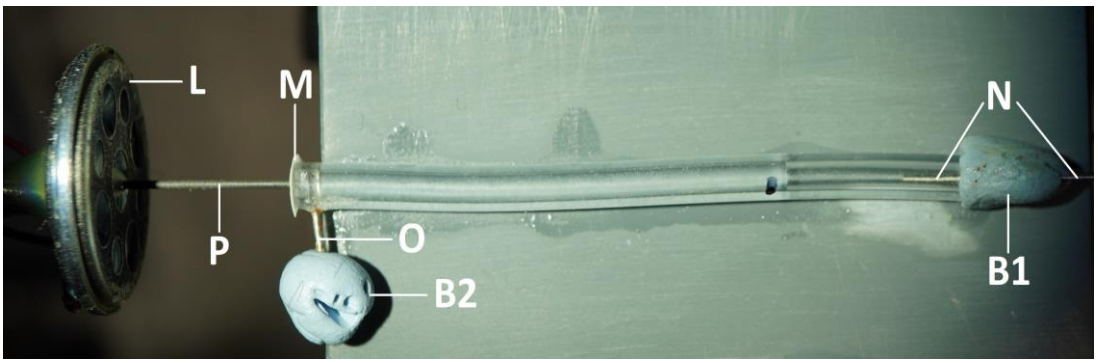

Figure 2.13 Experimental arrangement for dye diffusion experiments. L – miniature loudspeaker; P – carbon probe; M – latex membrane; O – filling outlet; B1 and B2 – Blu Tack plugs; N – pressure relief needle.

An outlet (O, Figure 2.13) was made with a 25G needle and inserted through the pipe's wall close to one end and fixed in place with superglue. A membrane (M, Figure 2.13), cut from a laboratory latex glove (typical thickness of 0.1 mm), was glued with Superglue™ at the same pipe end making sure that the glue does not cover the open surface of the membrane. The other

pipe end was closed with a Blu Tack (Blue-tack.co.uk) plug (B1, Figure 2.13) to prevent water evaporation and a 25G needle (N, Figure 2.13) was inserted through the plug into the pipe to provide pressure relief. The outlet was used to fill the pipe with deionized water to a distance of about 30 mm from the latex membrane and to inject 0.2 µl of 5% Lucifer yellow water solution into the pipe using a pipette. The outlet was closed with a Blu Tack plug (B2, Figure 2.13) after the Lucifer yellow injection. Lucifer yellow fluorescence was excited using a 470 nm laser source (Dragon Lasers, Changchun Jilin, China) and still images were taken (Sony α6100 camera, Sony Macro E 30mm F/3.5 lens) through an optical band pass filter (FB540-10, Thorlabs Inc.) to assess dye diffusion over time. The same miniature loudspeaker K16-50 Ohm (Visaton GmbH, Haan, Germany) with the carbon probe attached as used for the RWM micro vibration experiments was employed to vibrate the latex membrane in assisted diffusion experiments. The carbon probe touching the membrane was pushed slightly toward inside of the pipes at rest to ensure membrane tension and its relaxation during backward phase of probe strokes. Fluorescence intensity profiles were measured along the pipe axis using Fiji open-source image processing package.

Chapter Three

Drug Diffusion along an Intact Mammalian Cochlea

3.1 Abstract

Intratympanic drug administration depends on the ability of drugs to pass through the round window membrane (RWM) at the base of the cochlea and diffuse from this location to the apex. While the RWM permeability for many different drugs can be promoted, passive diffusion along the narrowing spiral of the cochlea is limited. Earlier measurements of the distribution of marker ions, corticosteroids and antibiotics demonstrated that the concentration of substances applied to the RWM was two to three orders of magnitude higher in the base compared to the apex. The measurements, however, involved perforating the cochlear bony wall and, in some cases, sampling perilymph. These manipulations can change the flow rate of perilymph and lead to intake of perilymph through the cochlear aqueduct, thereby disguising concentration gradients of the delivered substances. In this study, the suppressive effect of salicylate on cochlear amplification via block of the outer hair cell (OHC) somatic motility was utilized to assess salicylate diffusion along intact guinea pig cochlea in vivo. Salicylate solution was applied to the RWM and threshold elevation of auditory nerve responses was measured at different times and frequencies after application. Resultant concentrations of salicylate along the cochlea were calculated by fitting the experimental data using a mathematical model of the diffusion and clearing of salicylate in a tube of variable diameter combined with a model describing salicylate action on cochlear amplification. Concentrations reach a steady-state at different times for different cochlear locations and it takes longer to reach the steady-state at more apical locations. Even at the steady state, the predicted concentration at the apex is negligible. Model predictions for the geometry of the longer human cochlea show even higher differences in the steady-state concentrations of the drugs between cochlear base and apex. Our findings confirm conclusions that achieving therapeutic drug concentrations throughout the entire cochlear duct is hardly possible when the drugs are applied to the RWM and are distributed via passive diffusion. Assisted methods of drug delivery are needed to reach a more uniform distribution of drugs along the cochlea.

3.2 Introduction

The mammalian cochlea is one of the least accessible organs for drug delivery (Salt and Plontke, 2009; Rivera *et al*., 2012; El Kechai *et al*., 2015; Hao and Li, 2019). Systemic administration of many drugs, notably the most frequently used corticosteroids and aminoglycoside antibiotics, is severely limited by the blood-labyrinth barrier (BLB) (Salt and Hirose, 2018). The drugs noted are able to cross the BLB, however not at therapeutic concentrations, therefore a local approach is desirable. Local intratympanic administration (Schuknecht, 1956; Bowe and Jacob, 2010) would be a preferable option for these drugs and local delivery is the only option for many old and newly emerging classes of drugs and therapies including local anaesthetics, antioxidants, apoptosis inhibitors, neurotransmitters and their antagonists, monoclonal antibodies, growth factors, signalling pathway regulators and genetic material (see Devare *et al*., 2018; Hao and Li, 2019 for the latest reviews). Intratympanic administration of drugs relies on their remaining in contact with the RWM long enough to allow their diffusion into the perilymph of the ST. The ability of drugs to pass through the RWM does not, however, guarantee their sufficient distribution along the cochlear spiral. Drug distribution in the ST is limited by the low flow rate of perilymph within the cochlea and by cochlear geometry. The longitudinal flow of perilymph in the cochlea has been shown to be relatively slow, if present at all, (Ohyama *et al*., 1988) and drug distribution in the perilymph is dominated by passive diffusion. Passive diffusion along the ST is, however, constrained because the cochlea is a relatively long and narrow tube with a cochlear cross-section that decreases gradually from the RWM at the base to the apex. It is in the cochlear apex where human speech processing is initiated (e.g. Nuttall *et al*., 2018) and where drug delivery to the cochlea has greatest potential therapeutic and socioeconomic impact.

However, direct measurements of the distribution of marker ions and contrasting agents (Salt and Ma., 2001; Haghpanahi *et al*., 2013), corticosteroids (Plontke *et al*., 2008; Creber *et al*., 2018) and antibiotics (Mynatt *et al*., 2006; Plontke *et al*., 2007a) or measurements of the physiological effects of drugs (Chen *et al*., 2005; Borkholder *et al*., 2010) demonstrated that the concentration of substances applied to the RWM was much higher in the cochlear base than in the apex. These measurements, however, involved perforating the cochlear bony wall and, in some cases, sampling perilymph. These manipulations can change the flow rate of perilymph (Ohyama *et al*., 1988; Salt and Ma., 2001) and lead to the intake of cerebrospinal fluid through

the cochlear aqueduct (Salt *et al*., 2003), thereby disguising concentration gradients of the delivered substances.

A few studies investigated the distribution of substances applied to the RWM in the intact cochlea without breaking cochlear boundaries. This was done mainly in morphological studies investigating the distribution of dexamethasone and other substances along the cochlea after their intratympanic administration (Saijo and Kimura, 1984; Imamura and Adams, 2003; Hargunani *et al*., 2006; Grewal *et al*., 2013). While these studies confirmed the existence of base-to-apex gradients, the actual concentrations of substances along the cochlea were not measured. Borkholder *et al* (2014) measured the threshold elevation of distortion product otoacoustic emission (DPOAE) produced by primary tones of different frequencies after intratympanic application of salicylate. Salicylate affects cochlear amplification in a concentration-dependent manner but the DPOAE is a nonlinear phenomenon and the dependence of DPOAE thresholds on the primary tone level and cochlear amplification is complex (Lukashkin *et al*., 2002). As a result, salicylate concentrations along the cochlear spiral cannot be easily derived from the DPOAE threshold elevations.

The purpose of the current study is to quantify drug diffusion from the RWM along an intact guinea pig cochlea, to identify the factors that limit passive drug diffusion along the cochlea, and to analyse possible solutions to overcome these limitations. Salicylate was used as a model drug with well-characterized physiological effects. A mathematical model, which includes a diffusion component and a biophysical component describing the action of salicylate on the cochlear amplifier was validated using experimental data and used to assess the distribution of substances along the human cochlea.

3.3 Model Overview

Diffusion and Clearing Equation

The mathematical modelling stated below was a collaborative effort by Samuel M. Flaherty, Ildar I Sadreev and Andrei N Lukashkin. The biology, literature overview and experimental measurements were completed by Samuel and Andrei. The mathematical models were generated by Ildar.

For the purpose of modelling, the ST is approximated by a tube with a decreasing diameter similar to that described in previous models, for example by Plontke et al., (2007b) (Figure

3.1A). The radii of the tube, $r(0)$ and $r(l)$, are equal to a and b at $x = 0$ and $x = l$, respectively, where l is the ST length. All the dimensions are known (Thorne *et al*., 1999) and symmetry along y and z axes is assumed. Zero longitudinal perilymph flow in the compartment is assumed (Ohyama *et al*., 1988) and only the passive diffusion of a drug (salicylate) with diffusion coefficient kd is considered. In addition to diffusion, there is also clearing of the drug characterized by the clearing coefficient kc. This clearing can be represented simply as a leak through the scalae boundary (e.g., loss to the vasculature and tissues, and to other cochlear compartments). The diffusion and clearing processes are assumed to be completely independent. Because the tube radius is much smaller than its length, i.e., $r(x) \ll l$ for all x in $[0, l]$, only diffusion along x axis is considered and the concentration $c(x, t)$ within each cross-section for a fixed instance t is assumed to be constant, i.e., it does not change along the y axis. If the area of the cross-section is $S(x)$ then the diffusion can be described by the following partial differential equation (see Appendix for detailed derivation):

$$\frac{dc(x,t)}{dt} = \frac{1}{S(x)} \cdot \frac{d}{dx}\left(S(x) \cdot k_d \cdot \frac{dc(x,t)}{dx}\right) - c(x,t) \cdot \frac{2k_c}{r(x)}, \quad (1)$$

with the boundary conditions

$$c(0,t) = c_{rw}, \quad (2)$$

$$k_d \frac{dc(l,t)}{dx} = 0 \quad (3)$$

and initial conditions

$$c(0,0) = c_{rw}; x = 0, \quad (4)$$

$$c(x,0) = 0; x > 0. \quad (5)$$

The diffusion coefficient kd is known (Lide, 2002) but the clearing coefficient kc is unknown. The ratio of the diffusion and clearing coefficients can, however, be found via fitting the experimental data. The physical meaning of kd/kc can be described as the ratio between the amount of substance that diffuses through a unit surface normal to the direction of diffusion for a unit concentration gradient and the amount of drug that is cleared through a unit surface normal to the direction of substance exit for a unit substance concentration, both for unit time duration. The diffusion/clearing equation was validated using experimental data on the physiological effect of salicylate on the CAP thresholds. Because the salicylate concentrations

could not be directly inferred from the physiological effect of salicylate, a biophysical element of the model was developed allowing calculations of the salicylate concentrations along the cochlea.

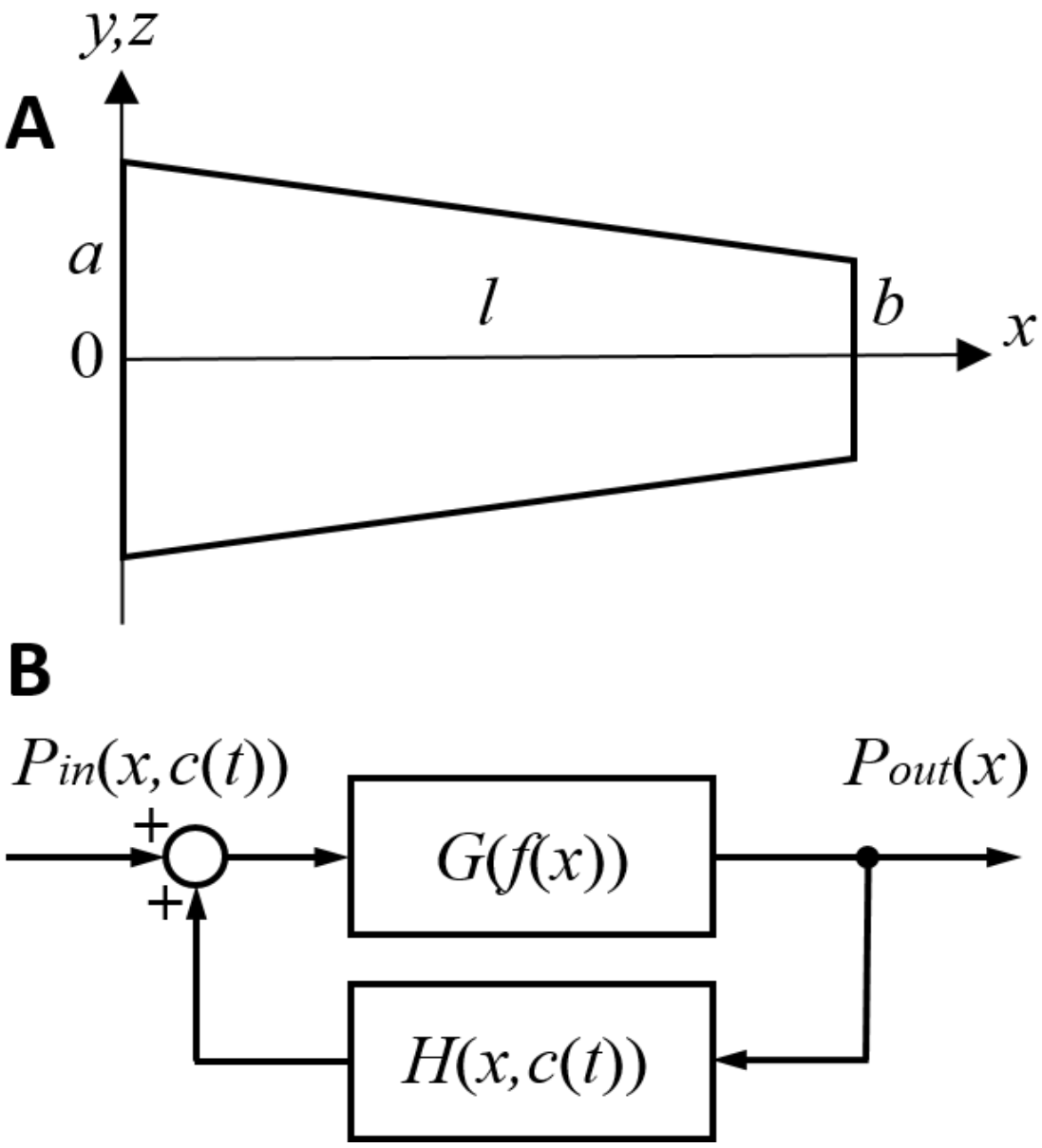

Figure 3.1. A Schematic presentation of (A) the scala tympani (ST) approximated by a tube of decreasing diameter and (B) the cochlear amplifier modelled as a system with positive feedback provided by the outer hair cells (OHCs).

The dependence between frequency of stimulation f and frequency position along the length x of the basilar membrane for the guinea pig cochlea is defined by the Greenwood equation (Greenwood, 1990)

$$f(\tilde{x}) = A \cdot \left(10^{\alpha\tilde{x}} - \beta\right), \quad (6)$$

Where $A = 0.35$, $\alpha = 2.1/18.5$, $\beta = 0.85$ and $\tilde{x} = l - x$ meaning that the starting point for $\tilde{x}$ in Greenwood (1990) is at the apex and not the base of the cochlea, as in this study.

The cochlear amplifier is represented by a positive feedback system (Figure 3.1B) with feedback gain $H(x, c(t))$ due to force generation by the OHCs (Mountain *et al*., 1983; Yates, 1990; Lukashkin and Russell, 1999). The following assumptions are made for a small signal, linear regime:

1. The CAP threshold is observed for different sound pressure $Pin(x, c(t))$ at the tympanum but for the same BM displacements, i.e., for the same constant pressure $Pout(x)$ at the BM for any given frequency/place x during manipulations with the cochlear amplifier. The assumption is based on good correspondence between neural and BM thresholds at the characteristic frequency (Ruggero *et al*., 2000; Temchin *et al*., 2008).
2. Feedback gain $H(x, c(t))$ is proportional to the OHC force $F(x, c(t))$ for any given frequency/place in the cochlea

$$H(x, c(t)) = \alpha \cdot F(x, c(t)), \quad (7)$$

   where α is the gain constant. The initial feedback gain $H(x, 0)$ for any frequency/place before application of salicylate can be found empirically (see below).
3. Salicylate changes only feedback gain $H(x, c(t))$ through changes in $F(x, c(t))$.
4. In line with other modelling studies (e.g., Meaud and Grosh, 2014; Ni *et al*., 2016) it is assumed that pressure/displacement at the BM is a linear combination of the passive BM response due to acoustic stimulation and active response due to the OHC forces.

The link between local salicylate concentration $c(x, t)$ and reduction in force $FR(x, c(t))$ generated by the OHCs can be described by the Hill function (Hallworth, 1997)

$$FR(x, c(t)) = V \frac{c(x,t)^n}{k^n + c(x,t)^n}_{max}, \quad (8)$$

where V_{max}, $k = 0.101$ and $n = 0.983$.

The reduction in force is linked to the force before $F(x,0)$ and after $F(x,c(t))$ salicylate application as

$$FR(x,c(t)) = \frac{F(x,0)-F(x,c(t))}{F(x,0)} = 1 - \frac{F(x,c(t))}{F(x,0)} \quad (9)$$

or,

$$F(x,c(t)) = F(x,0) \cdot (1 - FR(x,c(t))). \quad (10)$$

It can be written for any given frequency/place before salicylate application at $t = 0$ (Figure 3.1 B)

$$\frac{P_{out}(x)}{P_{in}(x,0)} = \frac{G}{1-G\cdot H(x,0)}, \quad (11)$$

where G is the open loop gain. Similarly, at time t after salicylate application

$$\frac{P_{out}(x)}{P_{in}(x,c(t))} = \frac{G}{1-G\cdot H(x,c(t))}. \quad (12)$$

Dividing (11) by (12) and taking into account (7), it could be written

$$\frac{P_{in}(x,c(t))}{P_{in}(x,0)} = \frac{1-G\cdot\alpha\cdot F(x,c(t))}{1-G\cdot\alpha\cdot F(x,0)}. \quad (13)$$

Substituting $F(x,c(t))$ from (10) into (13) and using (7), one can obtain

$$\frac{P_{in}(x,c(t))}{P_{in}(x,0)} = \frac{1-G\cdot H(x,0)\cdot(1-FR(x,c(t)))}{1-G\cdot H(x,0)}. \quad (14)$$

The left part of (14) is measured in the experiment. $FR(x,c(t))$ is calculated using the Hill function (8) with $c(x,t)$ in this equation being calculated using the diffusion/clearing equation (1).

An analytical form of empirical dependence $H(x,0)$, i.e., feedback gain before salicylate application for different frequencies/locations, can be obtained as follows. Feedback from the OHCs can be completely blocked in experiments using a high concentration of salicylate. In this case $H(x,c(t)) = 0$ in (12) and the transfer function of the feedback system (Figure 3.1 B) is equal to the open loop gain G. Then similar to (11) and (12)

$$\frac{P_{out}(x)}{P_{inBlock}(x)} = G, \quad (15)$$

where $P_{inBlock}(x)$ is the sound pressure required to produce a response from the auditory nerve in preparations where the cochlear amplifier is completely blocked, and it does not depend on time. Dividing (11) by (15) and rearranging gives the following equation

$$H(x,0) = \frac{1}{G} \cdot \left(1 - \frac{P_{in}(x,0)}{P_{inBlock}(x)}\right), \tag{16}$$

where $P_{inBlock}(x)/P_{in}(x,0)$ is measured in separate experiments.

G has frequently been assumed to be constant along the cochlea (e.g. Mountain *et al*., 1983; Yates, 1990; Lukashkin and Russell, 1999). In spite of the special design of the cochlea, which minimised energy losses when the BM travelling wave moves from the base to apex (Jones *et al*., 2013), some energy dissipation is still expected during wave propagation in a viscous environment. To account for energy losses, a simple linear dependence of the open loop gain $G(f(x))$ on frequency was assumed:

$$G(f(x)) = s \cdot f(x) + i, \tag{17}$$

where s is the slope and i is the intercept defined as $i = 1 - s \cdot f_l$, with $f_l = 49.9165$ kHz specifying the upper frequency limit of linear dependence for $G(f(x))$. Hence, $G(f(x))$ effectively depends only on a single parameter s, which could be found by fitting the experimental data.

Initial model parameters

Ratio $P_{inBlock}(x)/P_{in}(x,0)$ was measured as a function of frequency f. Equation (6) shows how this frequency can be converted to a coordinate. An arbitrary Hill type function

$$\frac{P_{inBlock}}{P_{in}}(f) = m_1 \frac{f^{m_2}}{m_3^{m_2} + f^{m_2}} + m_4 \tag{18}$$

was fitted to the experimental data with $20\,log_{10}$ transformation for dB using the Genetic Algorithm (GA) tool in MATLAB (The MathWorks. Inc. 2018a) (initial local fit). The obtained m_1, m_2, m_3 and m_4 (Table 1) were then used for the later optimisation procedures described below (final global fit). The feedback gain before application of salicylate $H(x,0) = H(f(x),0)$ was obtained according to (16) and (18) as

$$H(f,0) = \frac{1}{G} \cdot \left(1 - 1/\left(m_1 \frac{f^{m_2}}{m_3^{m_2} + f^{m_2}} + m_4\right)\right) \tag{19}$$

Initial values for all parameters used in the model before the optimisation procedure are shown in table 3.1

Optimized model parameters

Equation (14) with $20\log_{10}$ transformation for dB was solved in MATLAB (The MathWorks. Inc. 2018a) using pdepe solver for partial differential equations and fitted to the entire set of experimental data for all frequencies and salicylate concentrations using Genetic Algorithm (GA) tool in MATLAB (The MathWorks. Inc, 2018a). The squared error

$$SE = \sum_{i=1}^{n}(M_i - E_i)^2$$

was used as a cost function for minimisation, where M are the model predictions and E are the experimental data for points $i = 1 \ldots n$. It is worth noting that only three model parameters were fitted during the global fit/optimisation. These parameters are the cochlear length l, k_d/k_cratio and slope s of the open loop gain $G(f(x))$.

Table 3.1. Model parameter values

Parameter	Unit	Initial value	Optimized value	Source of the initial value
a	mm	0.56	Fixed	Thorne *et al*., 1999
b	mm	0.18	Fixed	*Thorne et al.*, 1999
l	mm	18-19	19	*Thorne et al.*, 1999
k_d	mm^2/s	$0.\ 959e^{-3}$	fixed	Lide, 2002
$ratio = k_d / k_c$	mm	1-10	1.6968	Initial guess
c_{rw}	mM	100	Fixed	experiment
A	kHz	0.35	Fixed	Greenwood, 1990
α	1/mm	2.1/18.5	Fixed	Greenwood, 1990
β	-	0.85	Fixed	Greenwood, 1990
k	mM	0.101	Fixed	Hallworth, 1997
n	-	0.983	Fixed	Hallworth, 1997
V_{max}	-	0.71629	Fixed	Hallworth, 1997
m_1	-	1011.2	Fixed	Experiment
m_2	-	8.1406	Fixed	Experiment
m_3	kHz	3.4816	Fixed	Experiment
m_4	-	31.686	fixed	Experiment
s	1/kHz	0 - 0.0261	0.00014742	Initial guess

3.4 Results

Gain of the cochlear amplifier and corresponding feedback gain of the model, $H(x,0) = H(f(x),0)$ (equation (16)) was determined empirically from elevation of the CAP thresholds after application of 1 M salicylate solution to the RWM which caused a consistent and steady increase in threshold over the entire frequency range (Figure 3.2, black circles). Values for m_1, m_2, m_3 and m_4 (Table 3.1) were determined through fit of the experimental data points by equation (18) (Figure 3.2, red curve) using the Genetic Algorithm (GA) tool in MATLAB (The

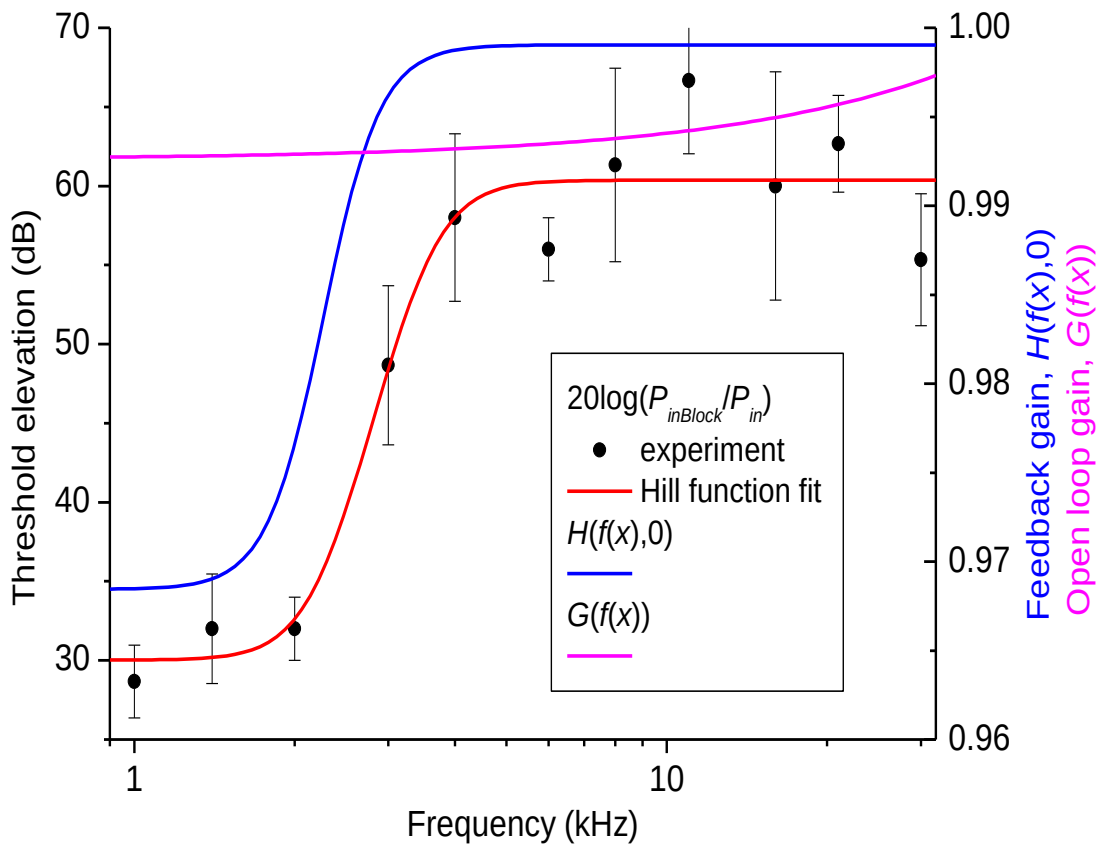

Figure 3.2. Elevation of CAP thresholds after complete block of the cochlear amplifier (left Y-axis) using 1 M salicylate solution and corresponding value of the open loop and feedback gain (right Y-axis). Black circles show the experimental values of threshold elevation (mean ± SD, n = 3). Red curve indicates fit of the experimental data points by equation (18). Related values of the parameters m_1, m_2, m_3 and m_4 are given in table 3.1. Value of the open loop (magenta curve) and feedback (blue curve) gains after the final global optimization procedure were calculated using equations (17) and (19), respectively, with the optimized value of parameter s (Table 3.1).

MathWorks. Inc, 2018a). These values were used for the general optimisation procedure performed at later stages.

100 mM solution of salicylate applied to the RWM caused a rapid increase followed by saturation of CAP thresholds for high frequency tones (Figure 3.4). CAP thresholds increase for tones of lower frequencies was observed after an initial delay and did not reach saturation during the time of observation. Any changes in CAP threshold due to application of salicylate were below the noise floor of measurements for tone frequencies lower than 5 kHz, which corresponds to approximately the apical 55% of cochlear length (Greenwood, 1990; equation (6)). A partial recovery of the CAP threshold, across all frequencies that demonstrated threshold elevations, was observed after salicylate solution was washed out from the RWM (80 minutes post application). This was confirmation that threshold elevation, during the application of salicylate, was due to the specific action of salicylate and not because of general deterioration of preparations.

The absence of CAP threshold changes at frequencies below 5 kHz was presumably due to poor diffusion of salicylate from the RWM into the cochlear apex. It required increasingly longer times for the salicylate concentration to reach steady-state in the more apical regions of the cochlea, making an exact concentration gradient difficult to determine, but at 90% of cochlear length (10 % from the apex), salicylate concentration was about 12 orders of magnitude smaller than at the base even at steady-state (Figure 3.6). The model suggests that this steep concentration gradient is due mainly to the fast clearing of salicylate from the ST which is reflected in the small kd/kc ratio found in the optimization (Table 1). Because the flux J is proportional to the concentration gradient (equation (A20)), changes in salicylate concentration at the RWM will not lead to changes in the concentration gradient between the cochlear base and apex. In this case all steady-state curves for different concentrations of salicylate at the RWM are scaled versions of each other (data not shown). Hence, for a specific substance (i.e., for specific diffusion (kd) and clearing (kc) coefficients) and for a given cochlear geometry, the ratio of steady-state concentrations at the base and apex of the cochlea is a constant and does not depend on substance concentration at the RW. This was further assessed for the human cochlea.

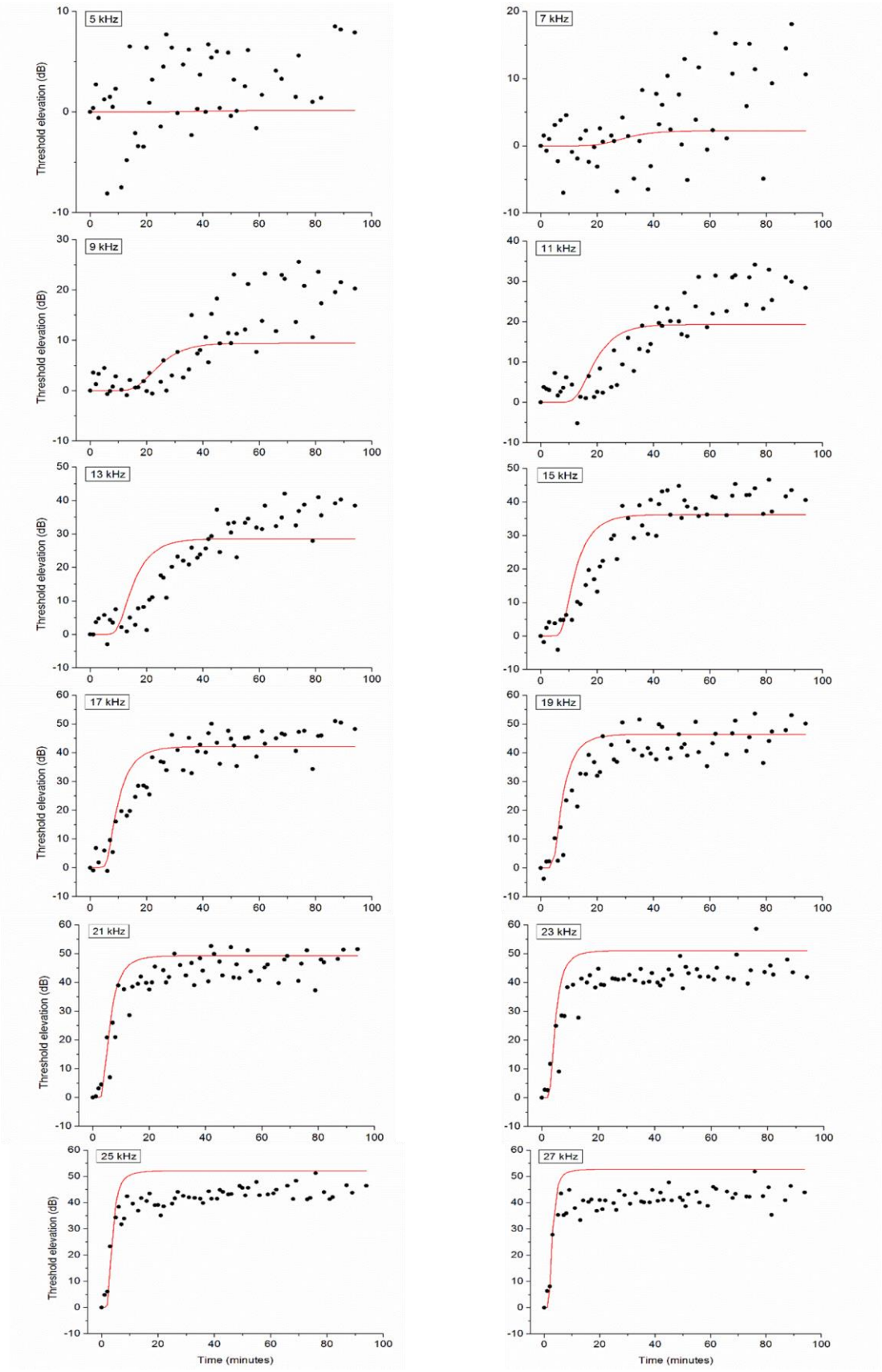

Figure 3.3. Pooled data for 5 animals (black circles) showing the CAP threshold elevation after application of 100 mM solution of salicylate to the RWM at time = 0. Red curves were fitted to the entire set experimental data using general optimization procedure.

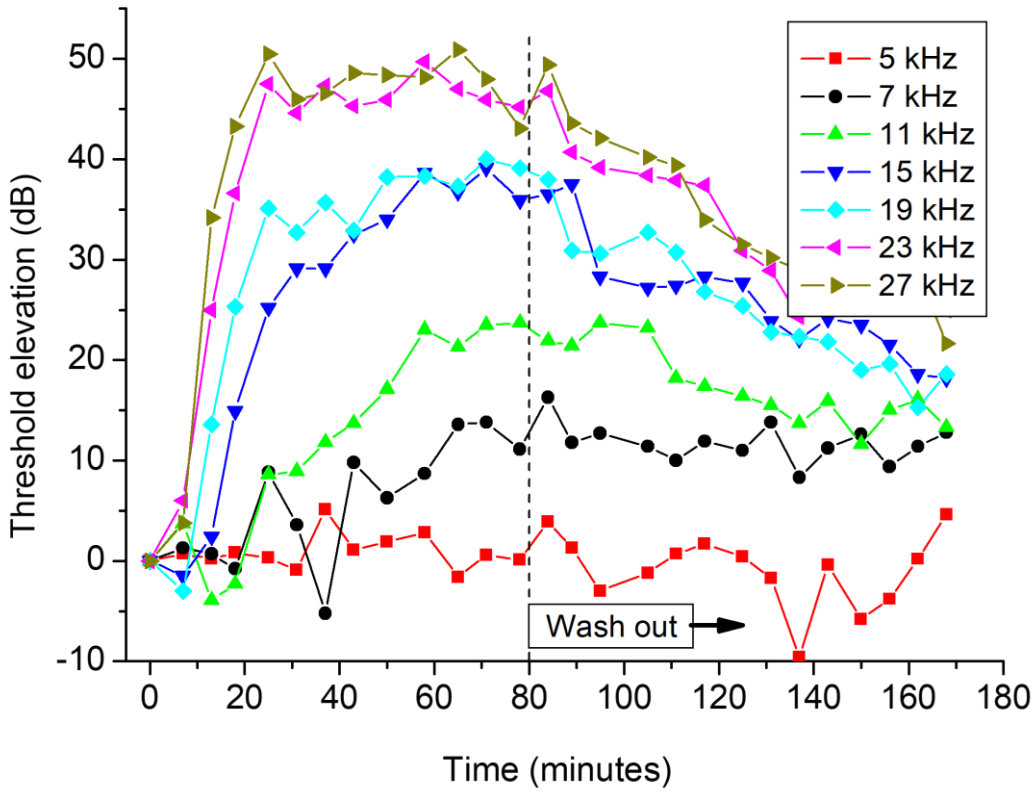

Figure 3.4 Hearing CAP threshold elevation in the guinea pig cochlea after application of 100 mM of salicylate solution to the RWM at time = 0. Salicylate was washed out after 80 minutes of application. Representative example of the CAP threshold elevation in a single preparation.

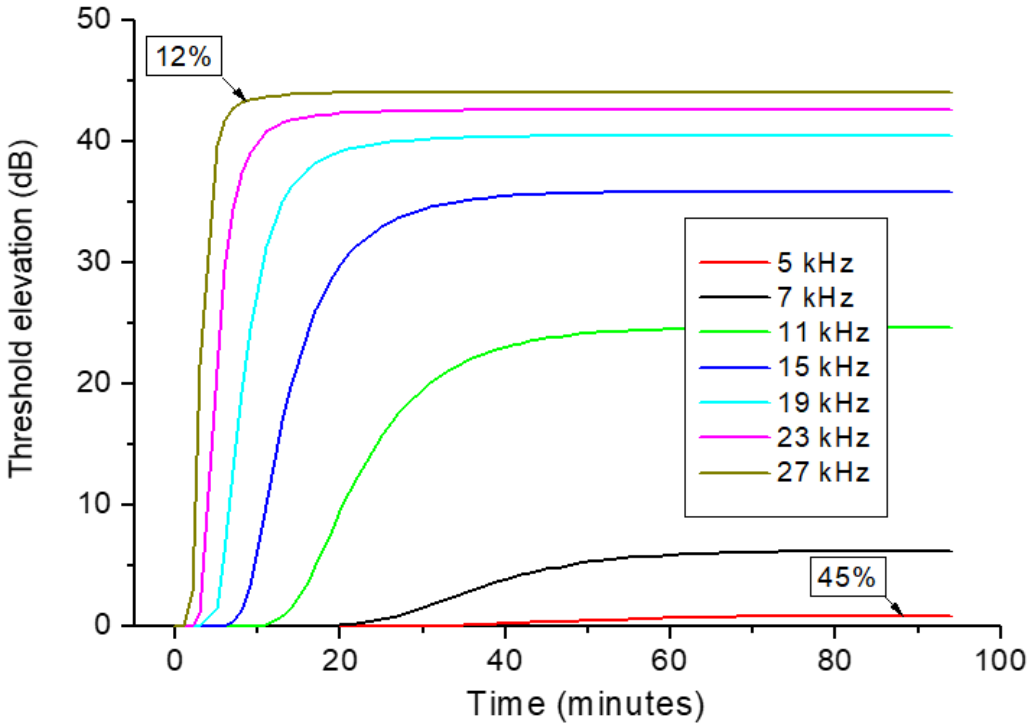

Figure 3.5. Hearing CAP threshold elevation in the guinea pig cochlea after application of 100 mM of salicylate solution to the RWM at time = 0. Combined best fit of the entire set of experimental data on CAP threshold elevation for five preparations using the parameter optimization procedure. Labels indicate percentage of the total cochlear length from the base.

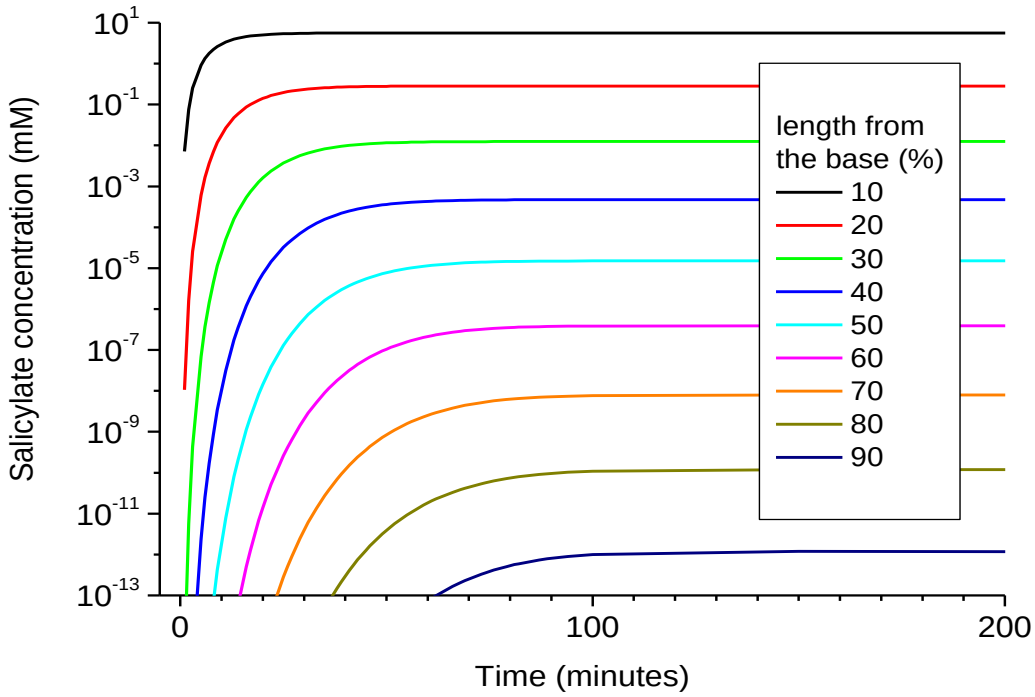

Figure 3.6. The salicylate distribution in the guinea pig cochlea after application of 100 mM of salicylate solution to the RWM at time = 0. Salicylate concentration along the cochlear length calculated using the optimized values of the model parameters (Table 3.1). Figure legend indicates the percentage of the total cochlear length from the base.

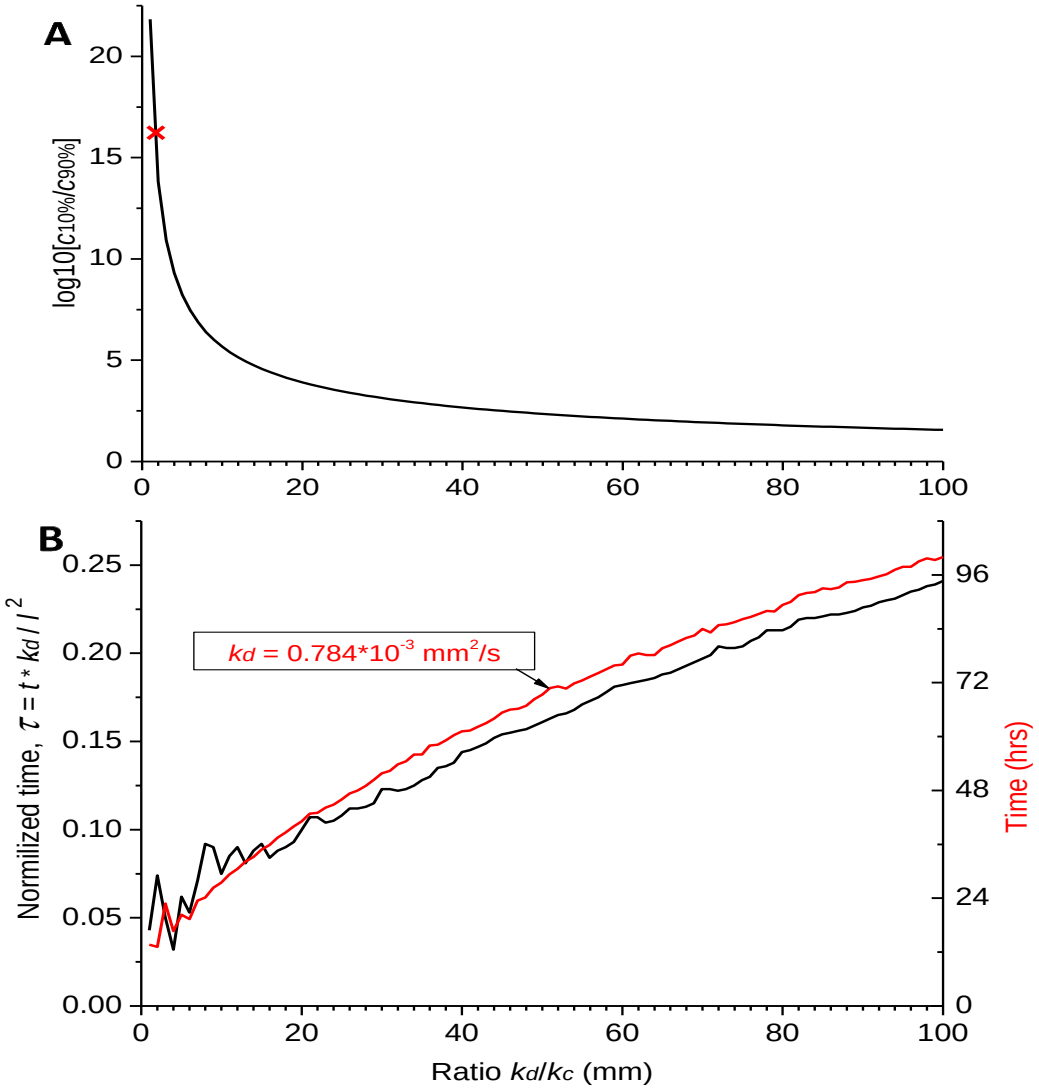

Figure 3.7. Theoretical distribution of an arbitrary substance in the human cochlea. (A) Dependence of the ratio of basal ($c_{10\%}$) and apical ($c_{90\%}$) steady-state concentrations on the ratio of diffusion (k_d) and clearing (k_c) coefficients. Red cross indicates the point for salicylate ($k_d / k_c = 1.7$). (B) Normalized time (black curve, left ordinate) required to reach steady-state concentration at the cochlear apex for substances with different ratio of the diffusion (k_d) and clearing (k_c) coefficients. Red curve shows a specific example of the absolute time (right ordinate) for a substance with the diffusion coefficient (k_d) similar to that of dexamethasone. The steady state was defined as the normalized difference between consecutive numerical values of concentration less than 10^{-4}. Jitter in the curves for small k_d / k_c ratios is due to very low apical concentrations. The following geometrical parameters for human cochlea were used for calculations using the non-dimensional form of the diffusion equation **Error! Reference source not found.**) $a = 0.7981$ mm, $b = 0.3990$ mm and $l = 28.46$ mm (Thorne et al., 1999).

Hence, the validity of the diffusion/clearing equation has been confirmed using the experimental data on salicylate block of the cochlear amplifier, the equation can be used to make conclusions about the distribution of arbitrary substances along the human cochlea (Figure 3.7). Decrease in the relative contribution of clearing into the distribution of a substance along the ST, i.e. increase of kd/kc ratio, leads to a dramatic reduction in the steady-state, base-to-apex gradient of the substance concentration (Figure 3.7A) calculated using the non-dimensional form of the diffusion equation (A33). This result is expected because a larger amount of the substance is available for diffusion into the cochlear apex in this case. For salicylate, however, the difference between the basal and apical concentrations is even larger in the human cochlea (red cross in Figure 3.7A) compared to guinea pigs and reaches 16 orders of magnitude because of the increased length of the human cochlea.

Figure 3.7A provides theoretical estimates of the minimal gradients which can be reached along the ST due to passive diffusion, when substances are in contact with the RWM long enough to establish a concentration equilibrium distribution. Reduction in the base-to-apex gradient for substances with higher kd/kc ratios, which are better retained in the ST, comes at the expense of the much longer substance exposure times required to reach steady-state concentration gradients (Figure 3.7B). For example, for a drug with the diffusion coefficient kd similar to dexamethasone, for which the clearing coefficient is unknown, it takes days of retention at the RWM when realistic kd/kc ratios are assumed (red curve in Figure 3.7B). The problem is that, while it is theoretically possible to achieve smaller base-to apex concentration gradients for a drug with high kd/kc ratios, in practice, it will be cleared from the ST into the cochlear tissue, hence kc cannot be arbitrarily small. In this case, the minimal theoretical difference in the base-to-apex concentrations of the drug is still a few orders of magnitude.

3.5 Discussion

The existence of a base-to-apex drug concentration gradient, when drugs are applied to the RWM, has been well established. From this point of view, this study quantifies these gradients for the intact cochlea when the flow of perilymph in the ST is very small (Ohyama *et al*., 1988). This study does not investigate the problem of the RWM permeability which is a separate challenge and requires specific considerations for particular drugs and formulations (Salt and Plontke, 2018). Instead, sodium salicylate which easily passes through the RWM was used to ensure high concentrations at the cochlear base. Though, passive proton-mediated diffusion of salicylate across biomembranes is observed at micromolar concentrations (Takagi *et al*., 1998),

the RWM diffusional barrier could, presumably, be overcome by the drug at the much higher, submolar concentrations used in this study. While the RWM membrane is highly permeable to salicylate and the CAP threshold elevation at high frequencies started within seconds after salicylate application, the model assumption that salicylate concentrations on both RWM sides were the same might introduce some error in the calculated absolute concentrations. It should be noted, however, that an error in calculation of the absolute concentrations (note that the absolute concentrations were calculated using Hallworth's (1997) empirical dependence between salicylate concentration and the OHC force reduction) does not lead to an error in calculation of the concentration gradient which is the basis for the conclusions in this study. This is true because the flux J is proportional to the concentration gradient (equation (A20)) and gradient curves calculated for different salicylate concentrations at the RWM are scaled versions of each other with the same gradients. It is worth noting that, from discoveries made in preliminary experiments, salicylate concentrations higher than 100 mM used to study diffusion in this work caused elevation of CAP thresholds throughout the entire frequency range. This flooding of the whole cochlea with salicylate was due apparently to overloading of the cochlear clearing and other possible mechanisms involved. In this case, the dynamic equilibrium between diffusion and clearing and steady-state salicylate concentrations cannot be reached and our model cannot be applied. From an experimental standpoint, the use of higher concentrations of salicylate also made time-dependent estimates of diffusion impossible for high frequencies because the clearing mechanism in the basal turn became almost immediately saturated following salicylate application. As a result of the clearing overload and other unidentified processes, salicylate is accumulated throughout the cochlea affecting all the frequencies as it was observed in experiments where 1 M salicylate was applied to the RWM. Of course, therapeutic use of concentrated drug formulations in order to overcome the issues raised by this study could be problematic due to likely side effects and/or restricted aqueous solubility and thus is not a practical solution.

While the steady-state distribution of concentrations, which is the basis for conclusions in this study, is fitted well by the simple diffusion model, the responses for the lower frequencies became gradually slower compared to the model predictions (figure 3.3). This may happen because salicylate action on the cochlear amplifier is not limited by its block of the OHC motility (e.g. Russell and Schauz, 1995; Wu *et al*., 2010) as it is assumed in the model. A compensatory effect from a hypothetical mechanism maintaining cochlear homeostasis and OHC sensitivity and responsible for the 'bounce' phenomenon after exposure to loud sounds

(Kirk *et al*., 1997; Drexl *et al*., 2014) may also explain delayed threshold elevation at subtle salicylate concentrations in the low-frequency cochlear region. Finally, salicylate concentration at the cochlear base may be diluted by the cerebrospinal fluid coming through the cochlear aqueduct into the perilymph which becomes hyperosmotic due to relatively high salicylate concentration at the base. None of these mechanisms should, however, affect our conclusion about the magnitude of the steady-state concentration gradients along the ST.

For a cochlea of given geometry, the concentration gradient along the ST depends only on the relationship between diffusion and clearing and is drug specific. In terms of the current study, it is the value of kd/kc, which defines the ratio between the amount of drug entering through a unit surface of the ST normal to the direction of diffusion and leaving it through a unit area of the side walls within the same time period. Salicylate, which is readily cleared from the ST ($kd/kc = 1.6968$), does not in practice diffuse into the cochlear apex and the resultant theoretical base-to-apex concentration gradient is extremely high (red cross in Figure 3.7A). Drugs which are better retained in the ST (i.e., have higher kd/kc ratio) form smaller concentration gradients, but this is traded for the considerably longer time it takes for these drugs to reach steady-state concentrations in the cochlear apex (Figure 3.7B). Hence, this approach may not be practical when there is only a short time window for the treatment of a specific cochlear disorder. Also, using a drug form which is better retained in the ST will lead to larger concentration differences between the ST and surrounding tissue. This may be a problem for drugs with narrow therapeutic windows, unless an inactive form of the drug is used, for even distribution along the ST through diffusion and it is activated only when the drug is cleared into the surrounding tissue.

Because the retention of a drug at the RWM does not lead to a levelling of its concentration along the cochlear spiral (see also Plontke *et al*., 2007b), different strategies for drug delivery to the cochlear apex should be employed. Stable drug loaded nanocarriers (Zou *et al*., 2014; Li *et al*., 2017; Kamalov *et al*., 2018) which can stay in the ST long enough without being cleared into the surrounding tissue may be a feasible option. When the concentration of nanocarriers along the ST reaches a constant level, the encapsulated drug could be released from the carriers through thermal or light activation (Karimi *et al*., 2016; Yuan *et al*., 2017; Karimi *et al*., 2017) to obtain sufficient drug concentrations along the entire cochlear spiral. A potential problem with this approach is the substantial increase in time required to reach the equilibrium base-to-apex gradient of nanocarrier concentrations, due to the substantially smaller diffusion

coefficients of even the smallest liposomes and micelles, compared to lone drug molecules (Figure 3.6B) (del Amo *et al.*, 2017).

Drug loaded nanoparticles, however, could be used to take advantage of anatomical and cellular feature of the cochlea which enable drug uptake through routes and pathways other than the ST route (Glueckert *et al*., 2018). Disulfiram loaded nanoparticles, for example, were observed in the apical part of the spiral ganglion just one day after their application to the RWM and elevation of auditory brainstem response thresholds, due to disulfiram induced apoptosis of the ganglion neurons, was detected for frequencies corresponding to the cochlear apex within two days after application (Buckiová *et al*., 2012). Nanoparticles can also be effectively driven and distributed along the entire cochlea. Assisted diffusion of magnetically driven, prednisolone-loaded magnetic nanoparticle along the cochlea resulted in a significant increase in the protective effect of the drug against cisplatin-induced ototoxicity compared to intratympanic injections of prednisolone (Ramaswamy *et al*., 2017).

This study investigates passive drug diffusion along the intact cochlea when the drug is applied to the RWM and highlights intrinsic problems with this method of local drug administration into the inner ear. Retaining drugs at the RWM for an arbitrarily long time does not decrease its base-to-apex concentration gradient, which, at steady state, depends solely upon the relationship between drug diffusion along and clearing from the ST. Usage of drug-loaded nanocarriers which utilize the anatomical and cellular properties of the cochlea, and which can be actively distributed along the entire length of the cochlea seems to be a more promising approach.

Chapter Four

A Measure of Round Window Membrane Stimulation Efficiency

4.1 Abstract

Round window membrane (RWM) stimulation is a new method of providing auditory rehabilitation for patients with conductive or mixed hearing loss. Actuators which partially occlude the RWM may improve cochlear excitation efficiency whilst also providing an effective pressure shunt. To determine cochlear excitation efficiency, recordings of compound action potentials (CAP) of the auditory nerve, *in vivo*, in response to displacing probes, were made. Probes of different diameters, which partially occluded the RWM, were tested to determine a change in cochlea excitation efficiency. The results reveal that the largest probe diameter of 0.75 mm, coupled to the RWM, provided the most efficient cochlear excitation. The lowest displacement amplitude required to elicit a CAP was 0.007 nm at 11 kHz using the 0.75 mm probe. The smallest probe diameter of 0.3 mm, used to displace the RWM in this study, was 10 times less efficient when compared to the 0.75 mm probe. Increasing ossicular chain impedance had no effect on cochlear sensitivity utilising this mechanism of RWM stimulation investigated. The outcome of this study is to demonstrate that RWM stimulation can be optimised by using probes which partially occlude the RWM whilst providing an effective pressure shunt through the RWM at the same time. This would enable cochlear excitation by RWM stimulation to be at a maximum efficiency and the most practical. It is argued that this mechanism of cochlear stimulation, through the partially occluded RWM, does not require ossicular chain functionality.

4.2 Introduction

The RWM is one of two openings into the cochlea, the other being the oval window (OW). During normal audition, sound vibrations enter the cochlea via the OW, stimulate the basilar membrane (BM), then exit at the RWM as intracochlear pressure. The RWM acts as a pressure relief valve for the almost incompressible fluids of the cochlea, allowing the movement of the stapes and inner ear components. The physiological importance of the RWM has been highlighted extensively in auditory research. RWM complications, such as immobilization, thickening and congenital malformation will result in impaired hearing (Borrmann and Arnold, 2007; Linder *et al.*, 2003; Martin *et al.*, 2002). Damage to the RWM, such as rupturing, during middle and inner ear surgical interventions, will result in perilymph aspiration and a loss of normal pressure-releasing functionality and thus reduction in auditory sensitivity (Goodhill, 1971).

It is known that displacement of the RWM, at frequencies similar to that of incoming sound, excites the cochlea (Skarzynski *et al.*, 2014; Weddell *et al.*, 2014; Colletti *et al*., 2006; Kiefer *et al*., 2006; Dumon *et al*., 1995). The proposed mechanics of RWM cochlear excitation through the partially occluded RWM is that displacement of the RWM produces near-field pressure (due to fluid mass displacement in the vicinity of the RWM) which in turn generates conventional travelling waves throughout the cochlea partition – in fluid dynamics, this is termed as a fluid-jet flow (Weddell *et al*., 2014). The conventional travelling waves displace the basilar membrane at the frequency regions similar to that of the frequency of the mechanical displacement.

The RWM has been an interesting route for cochlear stimulation with hope to develop middle ear prostheses for patients with conductive and mixed hearing loss. It has been extensively reported that middle ear implants which function at the RWM provide significant recovery of hearing thresholds (Weddell *et al*., 2014; Beltrame *et al*., 2009; Colletti *et* al., 2006; Kiefer *et al*., 2006). A middle ear prosthesis which utilises the RWM route of cochlear stimulation would be required for patients with conductive hearing loss in which, the ossicular chain is compromised and ossicular reconstruction surgery is not an option or the ear canal is malformed. Conditions such as chronic inflammatory middle ear diseases, recurrent cholesteatoma or middle ear distortion interfere with current prosthesis options hindering patient lifestyle (Colletti *et* al., 2006). A prosthesis placed on the RWM could be a viable alternative to current treatments available, such as the conventional hearing aid or a bone

anchored hearing device, providing hearing sensitivities similar to that of conventional acoustic stimulation.

Middle ear prosthesis treatment options for conductive or mixed hearing loss currently available require ossicular chain functionality, where partial or total reconstruction is necessary. In combination with ossicular reconstruction, a floating mass transducer (FMT) can be fitted to improve ossicular chain displacement. A bone conduction device is an alternative method of cochlear excitation that does not require ossicular chain functionality. This device is used in cases of external auditory canal stenosis/ atresia, where the outer and middle ear are non-functional. The bone anchored hearing aid (BAHA) is the clinically used prosthesis with patients benefitting from an average of 25-40dB gain in hearing sensitivity. Complications can arise with a BAHA due to local infection, allergies, lack of osteointegration, sound processor damage and inflammation (Bento *et al.,* 2012). An alternative concept for a middle ear prosthesis is one which partially occludes the RWM but remains capable of exciting the cochlea. Ossicular chain and oval window (OW) functionality would not be necessary with this prosthesis as pressure would be able to escape via the RWM at the regions not occluded by the middle ear prosthesis (Békésy, 1960).

Although, RWM stimulation is a promising route for auditory prostheses, the clinical and experimental reports reveal a high variability regarding the degree of hearing rehabilitation provided (Sprinzl *et al*., 2011). Many groups have looked into optimising the efficiency of cochlear excitation using devices which displace the RWM. Arnold *et al* (2010) demonstrated improved coupling between a floating mass transducer (FMT) and the RWM by underlaying the FMT with connective tissue which completely occluded the RWM. An increase of 45 dB cochlear sensitivity was achieved. Schraven *et al* (2011) revealed that actuator tip size, angle of stimulation and coupling material (connective tissue or a tutopatch), when coupled with the RWM, significantly increased recorded stapes displacements. The RWM in Schraven *et al* study was completely occluded. Finite element models have also been developed to determine an ideal actuator size and coupling condition for RWM stimulation (Tian, *et al*. 2015, Zhang, Gan. 2011). Again, the RWM was completely occluded in these studies. Yang *et al* (2015) demonstrated that increasing ossicular chain impedance, by increasing stapes mass or partially fixing the malleus, decreased cochlear excitation efficiency during RWM stimulation. Liu *et al* (2019) aimed to find whether piezoelectric actuators fitted to the RWM was the most efficient method of cochlear excitation, compared to fitting the actuator to the stapes, incus or umbo, using finite element modelling. They revealed that displacing the RWM was as efficient

as displacing the stapes, especially at higher frequencies, when the RWM was entirely occluded by an actuator. Most, if not all, groups working on RWM stimulation, completely occlude the RWM in their studies. The issue this creates is the inability to effectively relieve intracochlear pressure should the OW be malformed or the ossicular chain be compromised. By partially occluding the RWM with an actuator, the uncovered region can act as an effective pressure shunt removing the requirement for a mobile ossicular chain (Weddell *et al*., 2014).

This work looks to determine the efficiency of cochlear stimulation using mechanically displacing probes which partially occlude the RWM, which has a total area of 1.18 mm^2. Probes of diameters 0.3 mm, 0.5 mm and 0.75 mm are utilised to excite the guinea pig cochlea within a frequency range which will elicit a compound action potential (CAP). By comparing cochlear sensitivity in response to RWM displacement, utilising probes which partially occlude the RWM, it can be determine whether cochlear stimulation can be optimised for maximum excitation efficiency. The optimum efficiency would be the ideal RWM occlusion to uncovered ratio to allow for maximum cochlear excitation and effective pressure relief. The effects of ossicular chain fixation on the sensitivity of the cochlea, during RWM stimulation for each probe size, was recorded. If cochlear sensitivity is unchanged, this mechanism of cochlear stimulation would be suitable for patients with a compromised ossicular chain. Finally, this work strengthens the proposed mechanism of cochlear stimulation through RWM displacements.

4.3 Results

Linearity of probe displacements

The behaviour of the piezoelectric stacks, which had been modified with 20 mm tungsten probes of different diameter (see figure 2.6), followed a linear relationship - the displacement of the probe as a function of voltage was linear. The linearity of the probe displacement was not frequency dependent and remained constant for each device as shown in figure 4.1. Probe displacement frequency graphs, similar to figure 4.1, were used to derive the displacement of the probe to form displacement amplitude CAP threshold curves post experiment. The raw data recorded in the experiments was a series of dB attenuation readings, required to elicit a CAP, which were then used to extrapolate displacement values from probe displacement calibration

curves (figure 4.1). An example of a series of dB attenuation readings for each probe diameter, at frequencies between 1 – 30 kHz, is shown in figure 4.2.

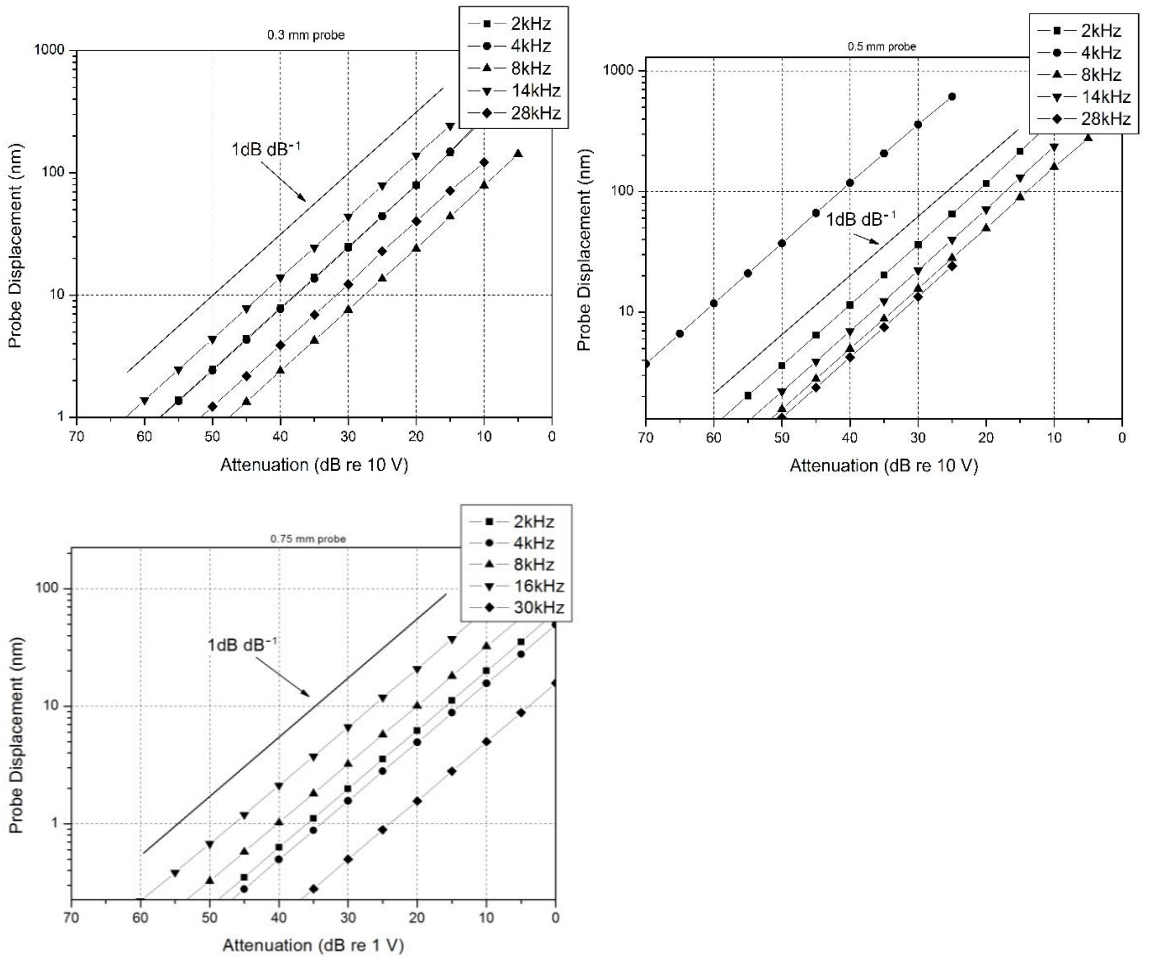

Figure 4.1. The linear displacement of three piezoelectric stack actuators modified with 20 mm long tungsten wire of different diameters: 0.3 mm, 0.5 mm and 0.75 mm. Displacement recordings were averaged from three readings for each frequency measured in the experiments. When calibrating the probes, probe oscillation measurements at all frequency and attenuation ranges used in the experiments were used to determine the probes velocity amplitude, recorded with a laser interferometer. Once the probe velocity amplitude at a specific frequency was known, the displacement amplitude was calculated (see section 2.7). Graphs displaying the linear relationship between probe displacement and dB attenuation for the voltage applied to the piezo re 10 V/ 1 V were generated.

It may have been expected to see this linearity change due to piezo loading i.e., loading the piezo stack with a mass which could affect the action of the piezo. Thin tungsten wire, shaped to form a circular footplate, bonded to a piezo stack, that could be placed perpendicular to the

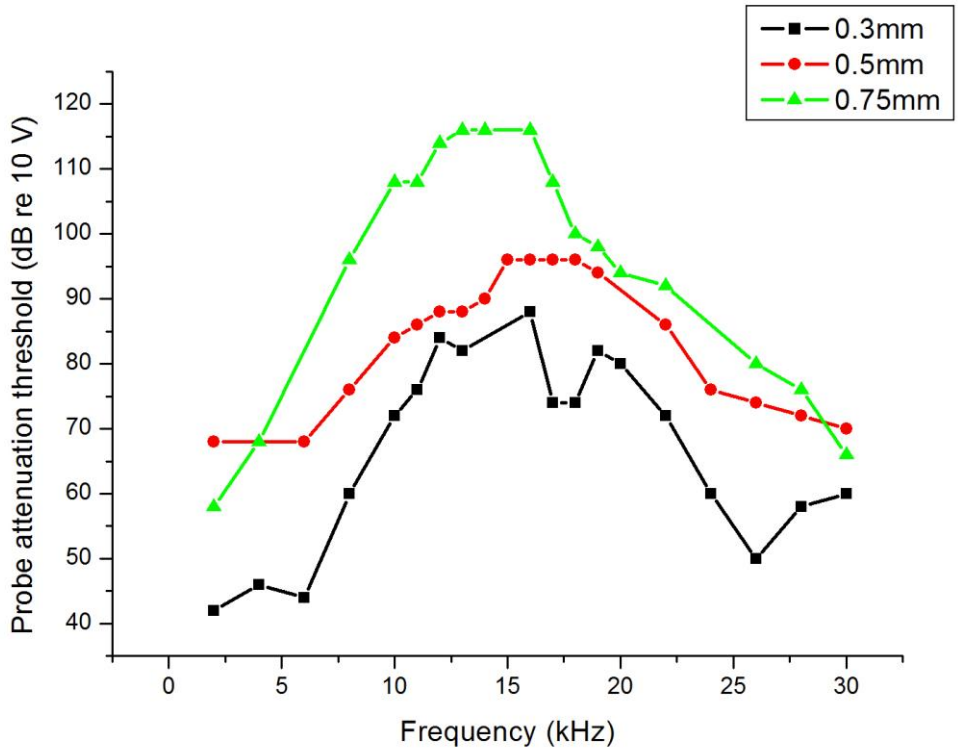

Figure 4.2. An example of the recorded dB attenuation thresholds required to elicit a CAP of the auditory nerve in a single experiment. Post experiment, dB attenuation CAP threshold values were used to derive displacement amplitude CAP threshold curves from probe displacement calibration curves.

RWM, did not alter the displacement-voltage linear relationship. Furthermore, it may have been expected to see probe displacement deviations in which the probe rocked in two planes rather than the sagittal plane. This was not observed when recording the probe displacement motion for the frequencies used in this work, likely due to the relatively short probe size used and as a result of that, a lower mass. Some frequencies were removed from the experiment protocol due to detected probe resonant frequencies which would elicit a much larger and unexpected CAP response and potentially damaging the RWM. To note, the general recorded CAP threshold frequency range was 1-30 kHz however the following frequencies were removed due to resonance: 0.3 mm probe – removed 14 kHz and 15 kHz, 0.5 mm probe – removed 4 kHz and 20 kHz, 0.75 mm probe – removed 6 kHz, 14 kHz, 15 kHz and 24 kHz.

Cochlear excitation was achieved for each probe diameter used in this study, which was confirmed by recording dB attenuation CAP thresholds of the guinea pig auditory nerve used to derive probe displacement amplitude CAP threshold curves (figure 4.3, 4.4, 4.5). Probe diameters of 0.3 mm (0.07 mm^2), 0.5 mm (0.2 mm^2) and 0.75 mm (0.44 mm^2) were utilised to displace the guinea pig RWM (1.18 mm^2). The probes partially covered the RWM allowing pressure to be shunted through the uncovered region of the RWM.

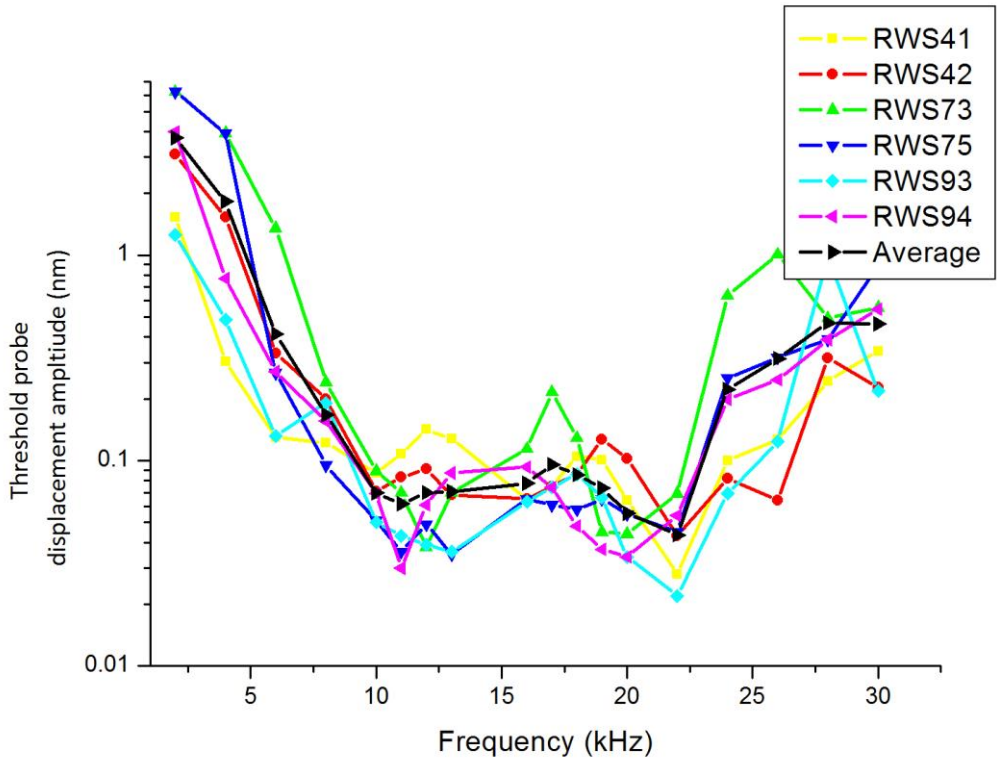

Figure 4.3. Displacement derivation CAP threshold curves in response to a 0.3 mm diameter tungsten probe displacing the RWM at frequencies similar to that of incoming sound (1-30 kHz). The tungsten probe was bonded to a piezo actuator, which was connected to a microphone driver, providing re 10 V. Each point represents the required probe displacement, in nanometres, to elicit a CAP at a specific frequency. Figure key represents a single preparation. Averaged data (N = 6) are shown (black triangles).

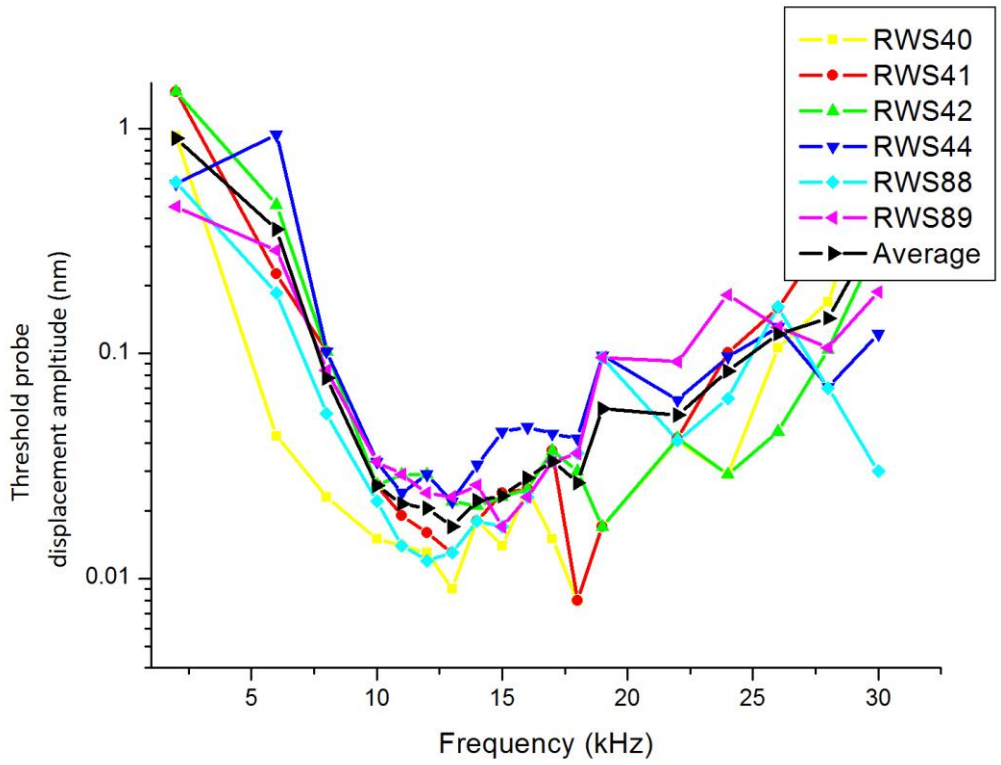

Figure 4.4. Displacement derivation CAP threshold curves in response to a 0.5 mm diameter tungsten probe displacing the RWM at frequencies similar to that of incoming sound (1-30 kHz). The tungsten probe was bonded to a piezo actuator, which was connected to a microphone driver, providing re 10 V. Each point represents the required probe displacement, in nanometres, to elicit a CAP at a specific frequency. Figure key represents a single preparation. Averaged data (N = 6) are shown (black triangles).

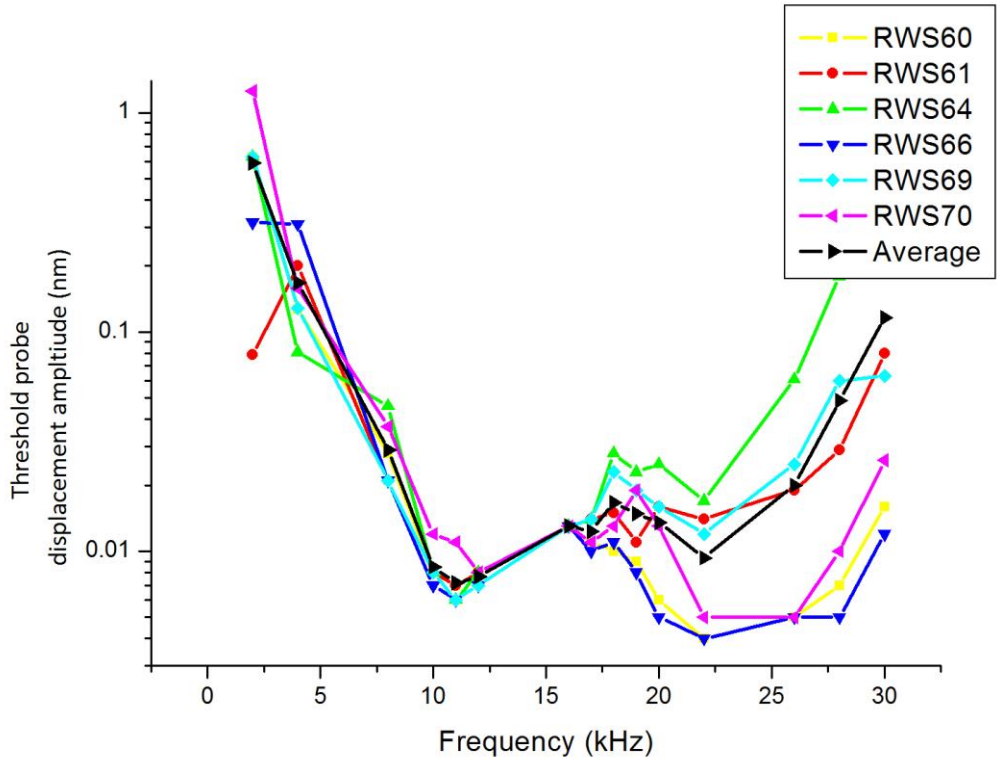

Figure 4.5. Displacement derivation CAP threshold curves in response to a 0.75 mm diameter tungsten probe displacing the RWM at frequencies similar to that of incoming sound (1-30 kHz). The tungsten probe was bonded to a piezo actuator, which was connected to a microphone driver, providing re 1 V. Each point represents the required probe displacement, in nanometres, to elicit a CAP at a specific frequency. Figure key represents a single preparation. Averaged data (N = 6) are shown (black triangles).

When comparing CAP threshold curves for probe diameters 0.3 mm and 0.5 mm, there is no statistically significant difference in the threshold responses at frequencies 6, 19, 22, 24, 26 and 30 kHz and when comparing CAP threshold curves for probe diameters 0.5 mm and 0.75 mm, there is no statistically significant difference in the threshold responses at frequencies 2, 18, 28 and 30 kHz (figure 4.6) ($p>0.05$, unpaired t-test). Threshold responses at the remaining

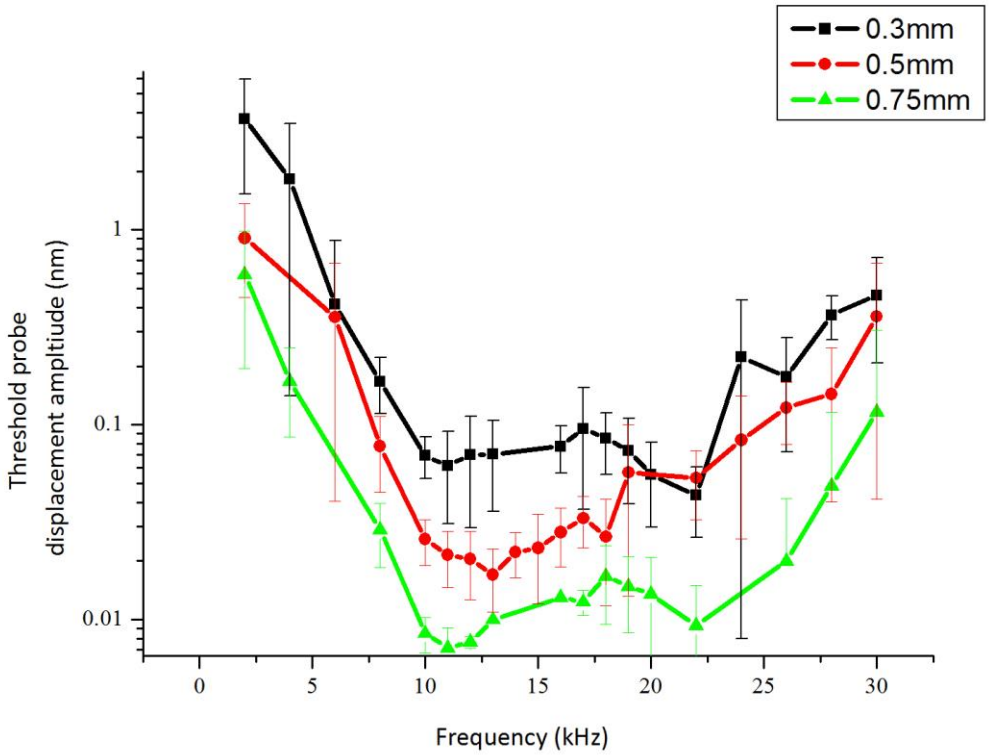

Figure 4.6. Auditory nerve CAP threshold (mean ± SD) curves in response to mechanical RWM stimulation. Three probes of diameters 0.3 mm, 0.5 mm and 0.75 mm, which partially occluded the RWM, were used to displace the RWM at frequencies similar to that of incoming sound (1-30 kHz). The tungsten probes were bonded to piezo actuators, which were connected to a microphone driver, providing 10 V. The 0.75 mm probe required a lower voltage, 1 V, achieving smaller RWM displacements. Each point represents the required probe displacement, in nanometres, to elicit a CAP of the auditory nerve at a specific frequency in the guinea pig. Eighteen preparations, six preparations per probe, were used to determine a statistically significant difference of responses between the three probe diameters used.

frequencies are significantly different. All CAP threshold data when comparing 0.3 mm and 0.75 mm diameter probes is significantly different ($p<0.05$, unpaired t-test).

The most sensitive region of guinea pig hearing in our experiments was between 10-20 kHz, which corresponds to the minimum displacement required to elicit a CAP. This region for each probe diameter (0.3 mm, 0.5 mm, 0.75 mm) shifts along the displacement axis and thus demonstrates the effect of RWM occlusion on cochlear excitation. The 10-20 kHz region, for the 0.3 mm probe curve (figure 4.3, 4.6), lies at 0.1 nm, whereas the curve for 0.75 mm probe lies at 0.01 nm (figure 4.5, 4.6). The lowest average displacement required to elicit a CAP of the auditory nerve during RWM stimulation was 0.007 nm at 11 kHz using the 0.75 mm probe revealing the guinea pig cochlear sensitivity to be subnanometric, in regard to RWM

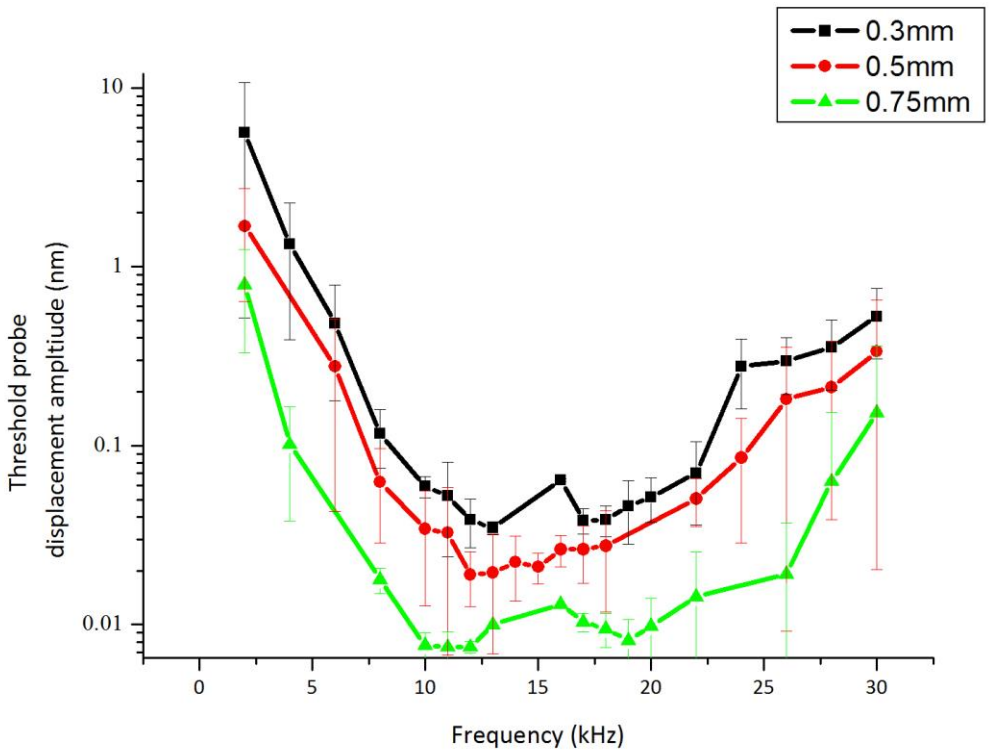

Figure 4.7. Auditory nerve CAP threshold (mean ± SD) curves in response to mechanical RWM stimulation with a fixed ossicular chain. Three probes of diameters 0.3 mm, 0.5 mm and 0.75 mm, which partially occluded the RWM, were used to displace the RWM at frequencies similar to that of incoming sound (1-30 kHz). The tungsten probes were bonded to piezo actuators, which were connected to a microphone driver, providing 10 V. The 0.75 mm probe required a lower voltage, 1 V, achieving smaller RWM displacements. Each point represents the required probe displacement, in nanometres, to elicit a CAP of the auditory nerve at a specific frequency in the guinea pig. Eighteen preparations, six preparations per probe, were used to determine a statistically significant difference of responses between the three probe diameters used.

displacement (figure 4.6). Remaining at the same frequency of 11 kHz, the 0.3 mm probe required an average displacement of 0.07 nm to elicit a CAP (figure 4.3, 4.6). A probe diameter increase of 0.45 mm, and thus an increase in RWM occlusion, has improved cochlear sensitivity by 10 times. The 0.5 mm probe curve is situated approximately between the 0.3 mm and 0.75 mm curves, thus showing an increase in cochlear sensitivity by 5 times, when compared to the 0.3mm curve (figure 4.6). All probe CAP threshold curves follow a similar trend, an inverted bell curve, which resembles that of acoustic threshold curves. The most sensitive frequencies in our experiments were 22 kHz (0.3 mm probe diameter), 13 kHz (0.5 mm probe diameter) and 11 kHz (0.75 mm diameter) (figure 4.6).

The middle ear ossicles have a relatively high acoustic impedance. The probes utilised in this work partially occlude the guinea pig RWM, with a total area of 1.18 mm^2, enabling the low-impedance region of the RWM not covered by the probe to simultaneously relieve intracochlear pressure. This suggests that fixation of the ossicular chain would show no effect on cochlear excitation by probes which partially occlude the RWM. It is demonstrated that fixation of the ossicular chain, by super gluing the tympanum, did not lead to statistically significant changes in the CAP thresholds (figure 4.7). The 10-20 kHz region of the CAP threshold curves for each probe (0.3mm, 0.5mm, 0.75mm) lies in the same formation for both unfixed and fixed ossicular chain preparations (figure 4.6 and 4.7).

The data collected for the CAP threshold curves recorded when the ossicular chain was fixed displayed statistically significant differences at most frequencies (figure 4.7). When comparing CAP threshold curves for probe diameters 0.3 mm to 0.5 mm, there is no statistical significance at frequencies 2, 6, 28 and 30 kHz and when comparing CAP threshold curves for probe diameters 0.5 mm and 0.75 mm, there is no statistical significance at frequencies 13, 28 and 30 kHz. The remaining frequencies are statistically different ($p<0.05$, unpaired t-test). The CAP threshold data when comparing 0.3 mm and 0.75 mm diameter probes is statistically different. To determine whether there was a statistical difference between the unfixed and fixed CAP threshold data for all probe diameters, an unpaired t-test ($p<0.05$) for all data gathered was employed. When comparing probe diameters unfixed 0.3 mm to fixed 0.3 mm CAP threshold data, all frequencies apart from 13, 17 and 18 kHz were not statistically different. When comparing unfixed 0.5 mm to fixed 0.5 mm CAP threshold data, all frequencies were not statistically different. When comparing unfixed 0.75 mm to fixed 0.75 mm, all frequencies apart from 8, 18, and 19 kHz were not statistically different.

The mechanical probes used in this work partially occlude the RWM, allowing the uncovered region to continue to act as a pressure shunt, as seen in 'normal' hearing. If pressure escapes through the RWM, ossicular chain functionality would not be necessary for RWM stimulation to excite the cochlea. The data presented in figure 4.10 demonstrates that fixing the tympanum with Superglue™ increases ossicular chain impedance. To demonstrate the effect of gluing the tympanum, the 0.75 mm probe was used for the ossicular chain displacement recordings. The 0.75 mm probe covered the largest portion of the RWM and thus reduces the uncovered region available for pressure shunting. At the highest probe displacement, equal to 0 dB voltage attenuation, a drop of 10 times ossicular chain displacement is observed when comparing the

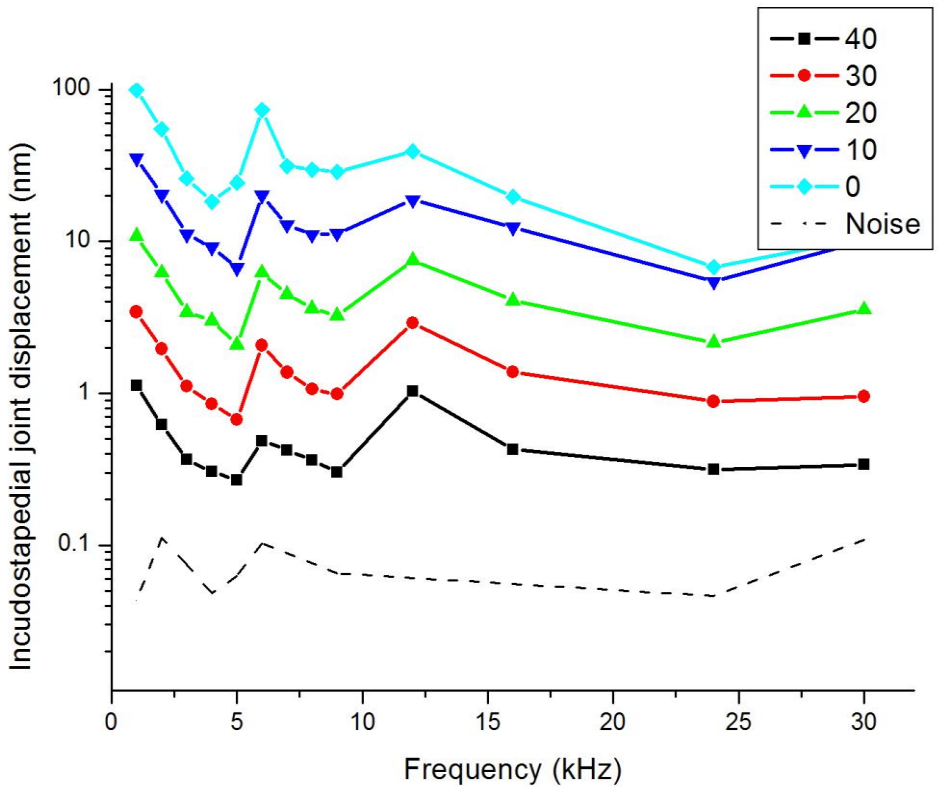

Figure 4.8. The displacement of the guinea pig incudostapedial joint (mean, SD is not shown for clarity, N = 3) during RWM stimulation using a probe that partially occludes the RWM. Incudostapedial joint displacements were derived post experiment using the equation outlined in section 2.7. The 0.75 mm diameter probe was used for these recordings and displaced the RWM at the maximum voltage of 10 volts, which is equal to the highest displacement (0 dB attenuation is equal to 10 volts and the largest probe displacement). The figure legend represents the voltage attenuations in dB applied to the piezo in the experiment. The noise curve represents the noise floor of the laser interferometer.

unfixed and fixed data across all frequencies tested. It should be noted that it was not possible to fix the ossicular chain completely. However, significant 20 dB drop in measured responses of the fixed ossicular chain did not lead to changes in the CAP threshold responses. Thus, mobility of the ossicular chain was not required in our experiments with cochlear excitation using probes which partially occluded the RWM.

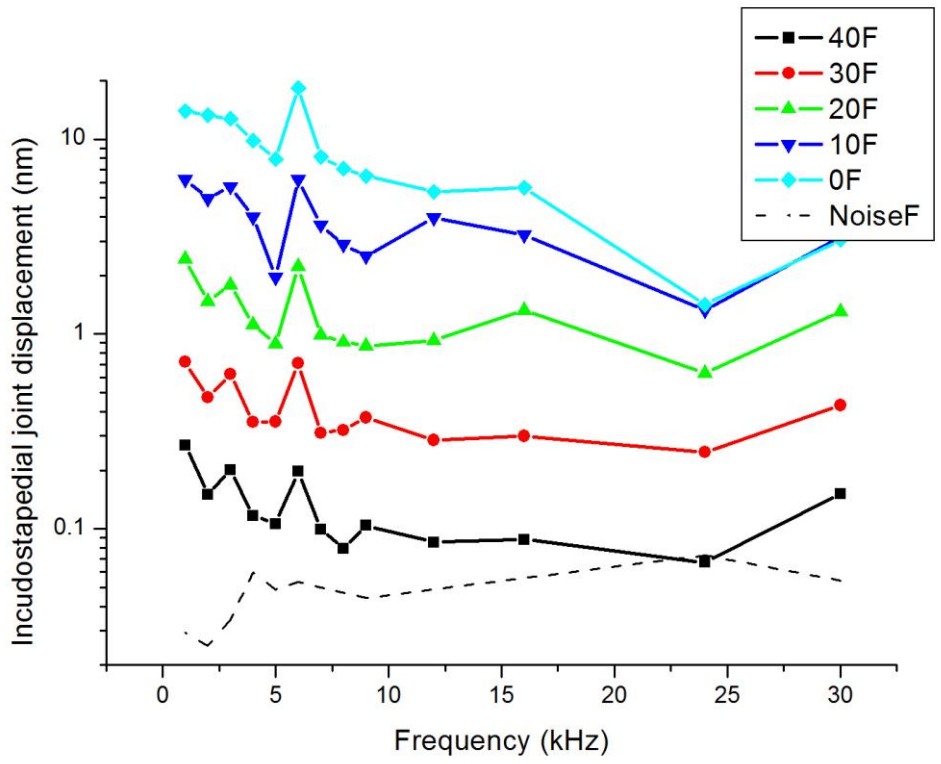

Figure 4.9. The displacement of the guinea pig incudostapedial joint (mean, SD is not shown for clarity, N = 3) during RWM stimulation, using a probe that partially occludes the RWM, when the ossicular chain is immobilised. Incudostapedial joint displacements were derived post experiment using the equation outlined in section 2.7. The 0.75 mm diameter probe was used for these recordings and displaced the RWM at the maximum voltage of 10 volts, which is equal to the highest displacement (0 dB attenuation is equal to 10 volts and the largest probe displacement). The figure legend represents the dB attenuation applied to the piezo in the experiment ('F' is an abbreviation for 'Fixed'). To fix the ossicular chain, super glue was applied to the tympanum down the ear canal. The noise curve represents the noise floor of the laser interferometer.

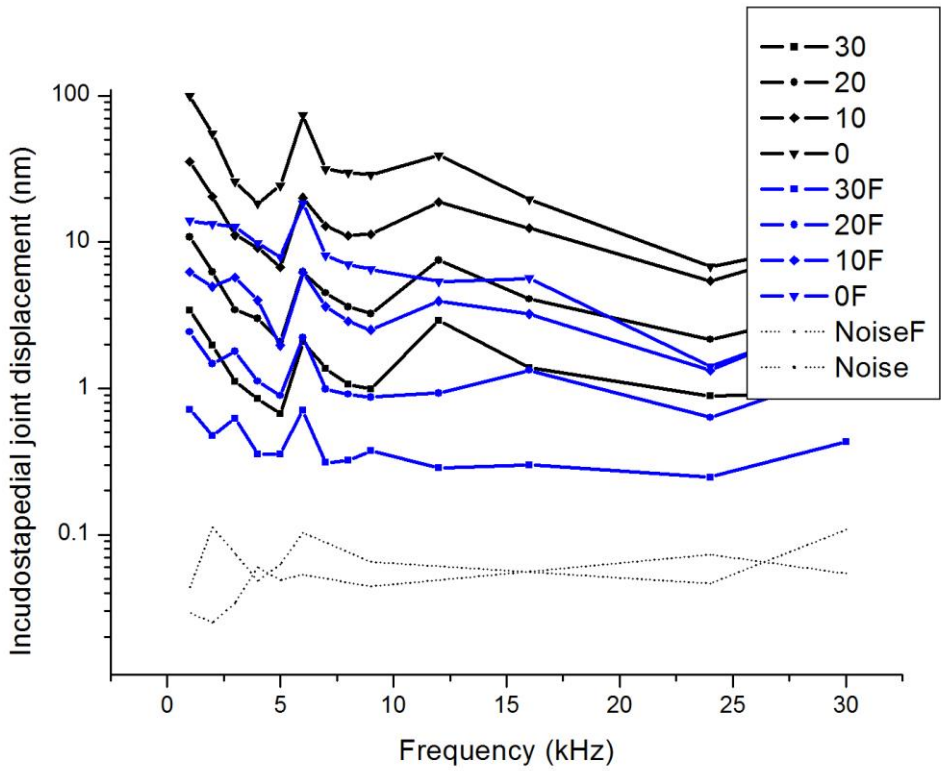

Figure 4.10. The displacement of the incudostapedial joint when super glue was applied to the tympanum (blue curves) and not applied to the tympanum (black curves) during RWM stimulation using a probe that partially occludes the RWM joint (mean, SD is not shown for clarity, N = 3). Incudostapedial joint displacements were derived post experiment using the equation outlined in section 2.7. The 0.75 mm diameter probe was used for these recordings and displaced the RWM at the maximum voltage of 10 volts, which is equal to the highest displacement (0 dB attenuation is equal to 10 volts and the largest probe displacement). The figure legend represents the dB attenuation applied to the piezo in the experiment ('F' is an abbreviation for 'Fixed'). To fix the ossicular chain, super glue was applied to the tympanum down the ear canal. The noise curve represents the noise floor of the laser interferometer.

4.4 Discussion

Mechanical hearing devices, which partially cover the RWM during stimulation and excite the cochlea, is a new application to overcome conductive and mixed hearing loss. Most groups working on the RWM route for hearing rehabilitation using auditory prostheses aim to completely occlude the RWM to optimise energy transfer into the cochlea (Liu *et al.*, 2019; Shin and Cho, 2018; van Drunen *et al*., 2017; Skarzynski *et al*., 2014). Our work confirms the relative sensitivity of the guinea pig cochlea in response to probes which partially occlude the RWM by different areas but allow for effective intracochlear pressure shunting. The change in sensitivity is validated by significant differences in the auditory nerve CAP threshold curve sensitivities recorded during RWM stimulation for each displacing probe (figure 4.2, 4.3, 4.4). The shift in cochlear excitation sensitivity, seen in figure 4.4, reveals that RWM stimulation of the cochlear can be optimised for efficiency when utilising probes which partially occlude the RWM.

The spread of data seen in figure 4.3, 4.4 and 4.5 is likely due to a few factors; variations in probe placements, probe contact with the RWM and preparations differences – such as animal auditory sensitivity. Interestingly at the most sensitive region, between 10-20 kHz for each probe, the spread of data becomes much smaller which suggests the larger data spreads at the low and high frequencies is possibly due to a greater range of hearing thresholds i.e., where the hearing sensitivity is worse. Whereas, at the most sensitive region, the hearing threshold range is much smaller. This is consistent with work by Skarzynski *et al* (2014) in which high frequency hearing in patients with conductive or mixed hearing loss, who had been fitted with a RWM stimulating device, had a much larger data spread than at the most sensitive region (2-5 kHz).

Measures of cochlear excitation efficiency, using auditory prostheses that partially cover the RWM, has been explored previously by measuring stapes displacement. Schraven *et al* (2012) found that larger tip diameters used for RWM stimulation, *in vivo*, resulted in larger stapes displacements when compared to tip diameters which occluded a smaller region of the RWM. Other groups have looked to measure cochlear excitation efficiency when changing further parameters for RWM stimulation. Findings from Yang *et al* (2016) indicate that increasing ossicular chain impedance, by partial malleus fixation or increasing the mass of the stapes, decreases the intracochlear equivalent SPL at low frequencies and high frequencies respectively during RWM stimulation. Comparable work by Liu *et al* (2019) came to a similar

conclusion. It is assumed for both studies that the displacing device completely covered the RWM when coupling in a human temporal bone model. Arnold *et al* (2010) looked to improve the coupling of a floating mass transducer (FMT) to the RWM to optimise vibration transfer into and throughout the cochlear fluids. They found that placing the FMT perpendicular to the RWM, which completely occluded the RWM, and underlying the FMT with connective tissue, improved coupling by 45 dB when compared to tight fixation. A measure of cochlear excitation efficiency utilising displacing probes which partially occlude the RWM and recording the subsequent electrophysiological responses of the auditory nerve is original work.

Our work demonstrates that partial coverage of the RWM does not affect RWM impedance sufficiently to prevent pressure shunting, even at the highest probe diameter. This is validated by increasing the impedance of the ossicular chain, using Superglue^{TM}, and recording no significant change in the CAP threshold curves between a fixed and unfixed ossicular chain (Figure 4.6 and 4.7). The parameter of RWM occlusion should be one that is carefully considered in the design of future auditory prostheses which utilise the RWM route. Patients who suffer from a compromised middle ear may benefit further with a hearing device which partially occludes the RWM allowing effective pressure relief at the uncovered regions.

Increasing the area of the RWM which is occluded by a hearing device changes two main factors regarding cochlear excitation. Firstly, a larger RWM occlusion area increases the contact region between the probe and the RWM. When the probe diameter increases, and thus the area of the RWM which is occluded increases, the generated intracochlear pressure also increases. The region of the RWM not occluded by the probe footplate decreases as the probe diameter increases and so pressure relief efficiency through the RWM is reduced. This would account for the significant change in CAP threshold sensitivity curves recorded for each probe diameter in this work. This work supports the findings from Schraven *et al* (2012) who utilised actuators with varying tip diameters, which partially covered the RWM, to displace the RWM and recorded the stapes displacements in human temporal bones.

However, the second factor that effects RWM stimulation of the cochlea is intracochlear pressure relief. A probe which occludes a larger area of the RWM will result in lower pressure shunting through the uncovered RWM regions and so the pressure must escape through the OW or the theoretical third window (Schraven *et al*., 2012). The postulated third window of the cochlea has been identified as the vasculature of the cochlea to the cochlear aqueduct which may provide effective pressure relief (Koka *et al*., 2010; Lupo *et al*., 2009). However, it has

been demonstrated that the effect of the third window on pressure relief for partial RWM stimulation is negligible due to the relatively low impedance of the partially occluded RWM (Weddell *et al.,* 2014). Therefore, the larger pressure generation within the cochlea must travel along the cochlear partition and dissipate through the OW, resulting in the larger stapes displacement measurements Schraven *et al* (2012) recorded. Our results demonstrate that fixing the stapes did not have an effect on the sensitivity of the cochlea during RWM stimulation using a probe which covered the maximum area of the RWM in this work (D: 0.75 mm A: 0.44 mm^2) (Figure 4.7).

The mode of partial RWM stimulation in our work has previously been described as a fluid-jet flow within the vicinity of the RWM that generates near-field pressure (Weddell, *et al*. 2014). This mechanism generates a conventional travelling wave that originates in the vicinity of the RWM and then travels throughout the cochlear partition displacing the BM exciting auditory hair cells. Our work further confirms this theory and shines light on the sensitivity of the cochlea when the parameters of the fluid-jet flow are altered. By increasing the probe-RWM coupling interface, the generated travelling wave has a greater amplitude due to the increased intracochlear pressure formed by the action of the displacing probe however allowing effective pressure shunting. This is confirmed by the significant differences in the cochlear CAP threshold curves recorded using the three probe diameters in this work (Figure 4.4).

The findings outlined in this study demonstrate the varied cochlear excitation sensitivity in response to displacing probes which partially cover the RWM. The largest probe diameter used in this work, 0.75 mm, was 10 times more sensitive when recording CAP threshold measurements when compared to the lowest probe diameter used, 0.3 mm. This reveals that RWM stimulation can be further optimised to provide both efficient cochlear excitation but also effective intracochlear pressure relief. Ossicular chain functionality is not required for RWM stimulation, when using a displacing probe which partially occludes the RWM, and there is scope to optimise this mechanism of stimulation. Without the requirement of ossicular chain functionality, a hearing device operating at an optimum occlusion to exposure ratio could be the most effective auditory prosthesis design to date.

Chapter Five

Inaudible Round Window Membrane Micro vibrations enhance drug delivery to the inner ear

5.1 Abstract

Inner ear drug delivery systems are essential in order to battle inner ear auditory complications. Due to the cochlea's inaccessibility and complex nature, new drug delivery technologies must be designed to ensure safe, efficient and uniform drug distribution along the entire cochlear spiral. This is a proof-of-concept chapter in which drug distribution along the entire cochlea is enhanced utilising RWM low frequency micro vibrations. A miniature loudspeaker modified with a carbon probe, which partially occludes the RWM, was used to improve perilymph drug mixing. Evidence is provided of cochlear apical drug distribution without breaching cochlear boundaries. It is further suggested that stapes functionality is not required for the effective drug distribution described. The novel method of local drug delivery to the cochlea discussed could be implemented into clinically approved auditory prostheses for patients who suffer with mixed or SNHL.

5.2 Introduction

Inner ear drug delivery systems are essential in order to battle inner ear auditory complications. Due to the cochlea's inaccessibility and complex nature, new drug delivery technologies must be designed to ensure safe, efficient and uniform drug distribution along the entire cochlear spiral. The blood labyrinth barrier hinders the effectiveness of systemic drug administration to the inner ear and so local administration becomes increasingly important. Transtympanic drug delivery and direct cochlear injections share the fundamental challenge of limited passive diffusion within the ST, restricting uniform drug delivery throughout the cochlear spiral.

Therapeutic compounds for treating inner ear complications are in high demand with more than 43 biotechnology companies exploring experimental compounds for inner ear treatment (Schilder *et al*., 2019). Drugs such as local anaesthetics, corticosteroids (namely dexamethasone), monoclonal antibodies, growth factors apoptosis inhibitors, and vectors for gene therapy are under clinical investigation (Hao and Li, 2019; Kanzaki, 2018). See Hao and Li 2019 review. The problem still remains however that without reliable systems for inner ear drug delivery, such investigations are highly restricted.

The main route for drug delivery into the cochlea is the RWM, a semi-permeable membranous opening into the cochlea, located within the tympanic cavity. *In situ*, the RWM acts as a pressure shunt during cochlear excitation. The RWM allows the diffusion of most therapeutic substances into the inner ear. RWM permeability is mainly influenced by membrane thickness, molecule liposolubility, molecule's size and molecule electrical charge (Swan *et al*., 2008). Typically, therapeutic compounds are injected into the middle ear cavity, which serves as a reservoir for the drug, and diffusion into the inner ear occurs at the RWM. Diffusion also occurs at the oval window, which is located within the middle ear, above the RWM. The oval window is covered by the bong stapes footplate therefore causing problems for diffusion quantification and oval window delivery systems (King *et al*., 2013; Mikulec *et al*., 2009).

Following diffusion of a therapeutic substance across the RWM and into the ST, the next challenge is distribution of the drug throughout the cochlear spiral. It is known that passive diffusion of drugs in the cochlea causes a very large cochlear base –apex concentration gradient, where concentrations at the basal region are much larger than at the apical regions. Direct measurements of diffusion rates have been made utilising drugs of known action (such as cochlear amplification inhibition) (Sadreev *et al*., 2019), marker ions and contrasting agents, corticosteroids, and antibiotics. Passive diffusion within the ST is restricted due to cochlea

geometry. The cochlea, if imagined unravelled, is a long and narrow tube with a gradually decreasing cross-section from base to apex. Drug distribution in the ST further hindered by the relatively slow longitudinal flow rate of perilymph (Ohyama *et al*., 1988). Highlighting the issues of passive drug diffusion illustrates the importance of external forces required to drive diffusion of drugs through the cochlear spiral.

Previously proposed methods to address the challenge of uniform drug distribution along the cochlear spiral required the physician to breach cochlear boundaries. Methods such as cochleostomy, canalostomy and intracochlear administration involve the perforation of the semi-circular canals or the cochlea. In doing this, further complications could arise, thus reducing effectiveness of treatment. To date, there are three current methods of drug delivery to the inner ear which do not breach cochlear boundaries and offer relatively improved drug distribution. The first strategy is that of cochlear pumping which introduces pressure oscillations to the ear canal at low frequencies to avoid noise induced hearing loss (Lukashkin, *et al*. 2020). This method has shown promise in improving drug distribution through the cochlear spiral however has been tested on guinea pigs only. Although the guinea pig and human cochlea do share geometric similarities, the human cochlea is longer and the apical decrease in the cross-section of scalae is smaller than in guinea pigs (Thorne *et al*., 1999). This therefore will require alterations to the experimental design, such as longer pumping times, which could result in noise induced hearing damage.

The second strategy is to improve drug retention at the RWM prolonging drug exposure allowing diffusion into cochlear apex. Key examples include hydrogel drug delivery systems, microwicks and osmotic pumps. The challenges seen with this strategy is the establishment of steady-state concentration gradients along the cochlea spiral (Sadreev *et al*., 2019). This gradient is formed due to the relationship between diffusion and clearing of therapeutic compounds in the ST. As a result, the cochlear base-apex gradient can remain large. The third strategy utilises drug loaded nanoparticles which can exploit cochlea anatomical and cellular characteristics, improving drug uptake and diffusion (Glueckert *et al*., 2018; Hao and Li., 2019). The spread of the nanocarriers can be limited and the need of a catheter to improve spread can result in hearing impairment. Interestingly, nanoparticles can be eluted from a CI although adding further risks of trauma. Improving substance spread within the inner ear is the main challenge with this method of drug delivery. A potential solution could be the use of superparamagnetic nanoparticles in an external magnetic field (Nguyen *et al*., 2016). By use of

magnets, the spread and location of the nanoparticles can be controlled externally and then the payload released upon successful positioning.

Middle ear prostheses are frequently used in otology for the treatment of conductive hearing loss. A device is implanted into the middle ear and stimulates the RWM, exciting the cochlea. It is demonstrated here that micro vibrations introduced to the intact cochlea via the RWM enhances drugs distribution along the guinea pig cochlea. Micro vibrations are generated at low frequencies, preventing noise induced hearing loss, and at a sinusoidal displacement of 20 μm peak-to-peak.

5.3 Results

Hearing sensitivity, assessed by measured CAP thresholds, did not change when 20 μm peak-to-peak continuous probe vibrations were applied to the RWM at 2 Hz and 4 Hz for up to 60 minutes (Figure 5.1). No gross electrical responses, which could be associated with the probe stimulation, were recorded. This made it possible to record the CAP thresholds continuously without interruption of the probe vibrations at 2 Hz and 4 Hz. In the experiments, the probe (area 0.22 mm^2) covered only a small part of the RWM. Under these conditions, most of the pressure relief during the probe movement was through the RWM area not occluded by the probe.

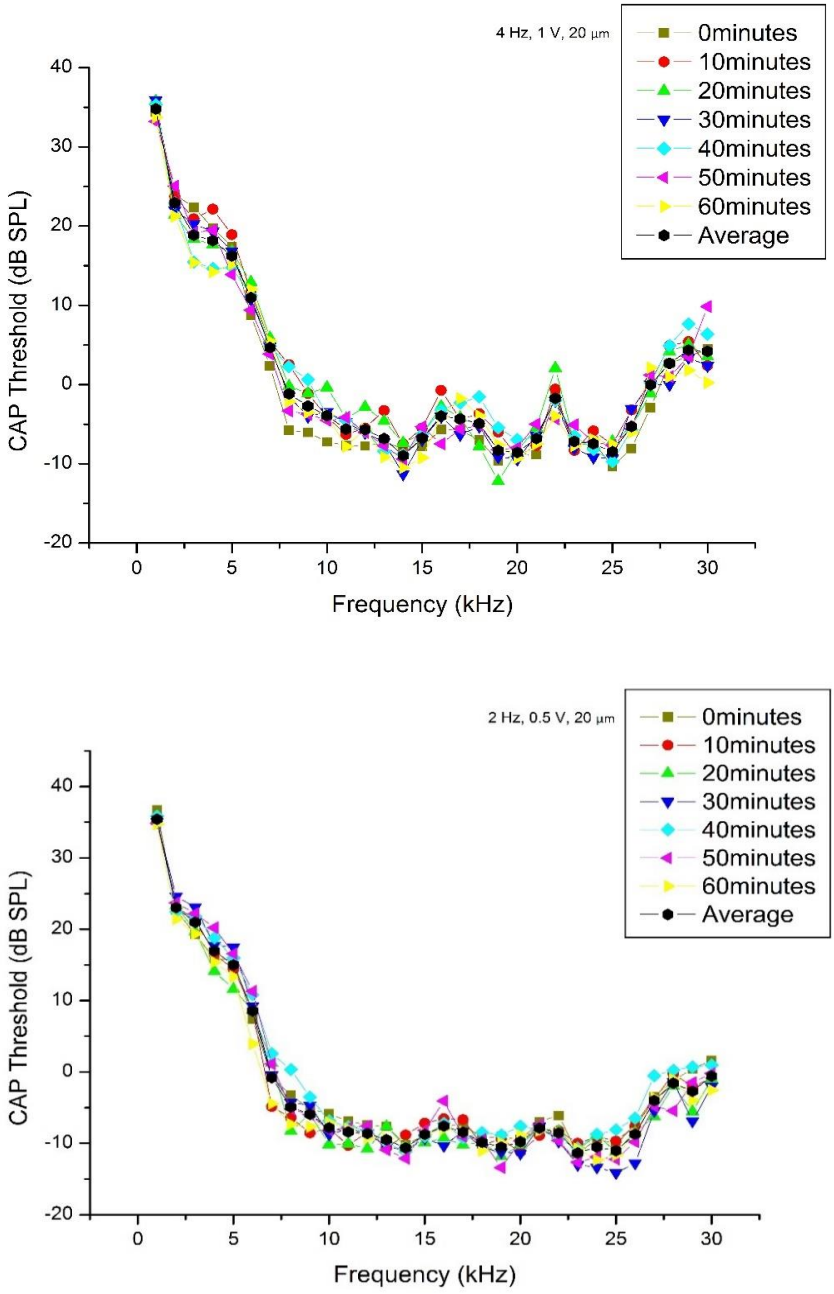

Figure 5.1. The effect of continuous RWM probe vibrations on CAP thresholds without the application of salicylate solution as a function of acoustic stimulus frequency. Frequency and amplitude of RWM probe vibrations is indicated for each graph. Corresponding duration of vibrations is indicated by curves with different colours/ symbols. Each curve represents averaged data for 4 preparations (mean value, SD is not indicated for clarity). Solid black curves indicate averaged data (mean value) for all times presented on each graph. Vibration time indicated corresponds to the beginning of each individual CAP threshold curve measurements. It took less than a minute to record the CAP threshold curve for the entire frequency range 1-30 kHz.

The ability of RWM micro vibrations to enhance drug distribution along the cochlear spiral was demonstrated in our experiments with the application of salicylate to the RWM. CAP threshold elevation measurements, caused by salicylate at different frequencies of acoustic stimulation, which, due to cochlear tonotopicity, corresponds to different distances from the RWM, were recorded (Greenwood, 1990). Thus, through measuring the CAP threshold elevations, the diffusion of salicylate along the cochlea spiral could be monitored, when applied to the RWM.

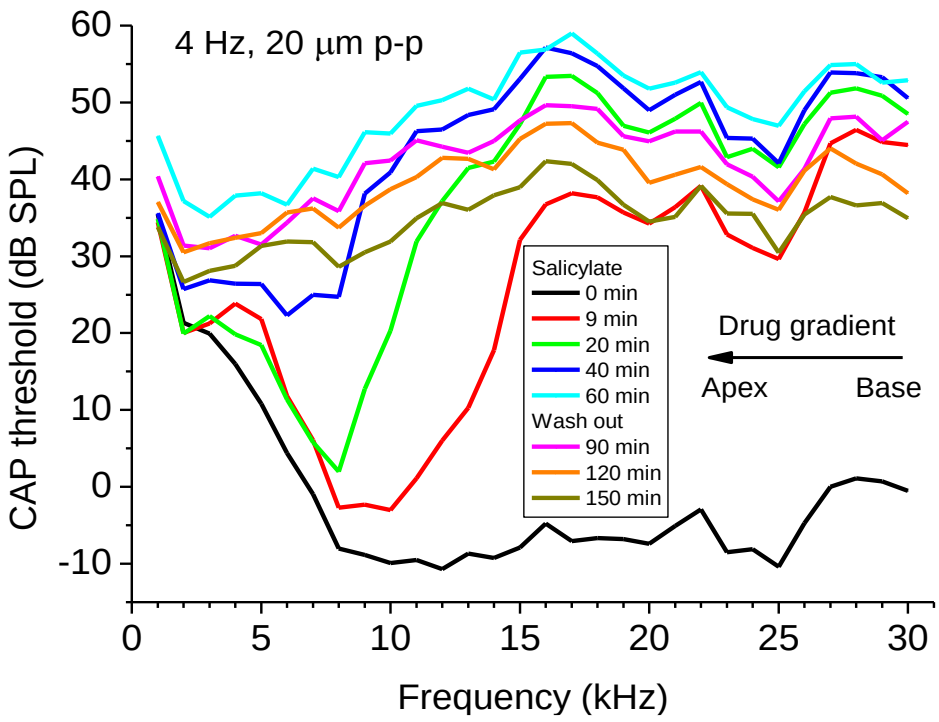

Figure 5.2. The Effect of combined application of 5 µl 100 mM/l salicylate solution and continuous RWM probe vibrations at frequency of 4 Hz as a function of acoustic stimulus frequency. Salicylate was applied at time zero and RWM probe vibrations started at the same time. The total salicylate application time was 60 minutes. Salicylate was washed out from the RWM after that. CAP thresholds for different times of salicylate application/RWM vibrations (colour coded curves) as a function of acoustic stimulus frequency (mean values, SDs are not shown for clarity, N=6).

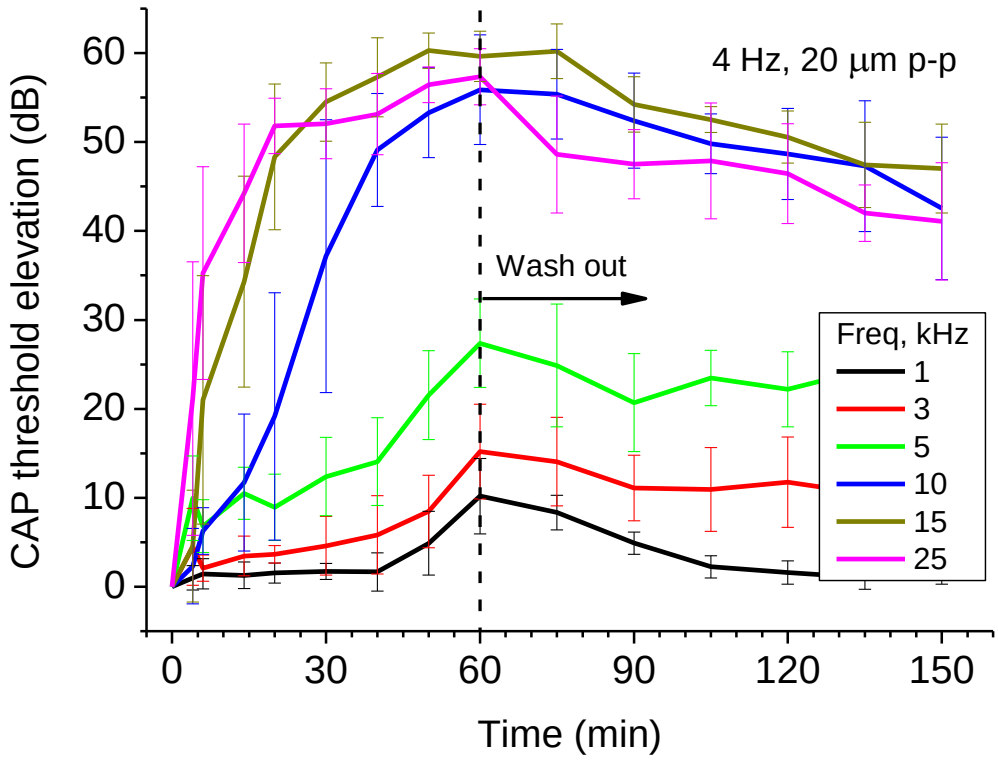

Figure 5.3. The Effect of combined application of 5 µl 100 mM salicylate solution and continuous RWM probe vibrations at frequency of 4 Hz as a function of acoustic stimulus frequency. The CAP threshold elevations relative to the thresholds before salicylate application (time zero) for six acoustic stimulus frequencies (colour coded curves) which correspond to different locations along the cochlea (mean ± SD, N = 6). Salicylate was applied at time zero and RWM probe vibrations started at the same time. The total salicylate application time was 60 minutes. Salicylate was washed out from the RWM after that as indicated on the graph.

When 5 µl of 100 mM salicylate solution was applied to the RWM (figure 5.2, 5.3), it caused a rapid increase followed by saturation of CAP thresholds for high frequency tones with the characteristic frequency place situated below and close to the RWM (e.g., 25 kHz, figure 5.2, 5.3). Over time, CAP threshold elevation gradually spreads to lower frequencies (figure 5.2) indicating salicylate diffusion into the cochlear apex. Salicylate did not cause elevation of the CAP threshold responses for frequencies below 5 kHz, which corresponds to about 45% of the total cochlear length from the base, when diffusing through the cochlea passively (Sadreev et al., 2019). The calculated gradient of base-to-apex salicylate concentration was approximately

13 orders of magnitude. When, however, placement of salicylate solution on the RWM was followed by RWM probe vibrations at frequencies of 2 Hz and 4 Hz, the CAP threshold was elevated throughout the entire 1–30 kHz frequency range tested. The CAP threshold elevation did not saturate and was still rising for frequencies below 5 kHz (Figure 5.3, 5.5) indicating continuous increase in salicylate concentration in this cochlear region even after 60 minutes of the probe vibration. This corresponds to about 75% of the total cochlear length from the base (Greenwood, 1990). Partial recovery of the CAP thresholds during wash out of salicylate from the RWM after 60 minutes of its application provided confirmation that the integrity of the sensory cells was preserved and the CAP threshold elevation after joint salicylate application and RWM probe vibrations was not caused by the later.

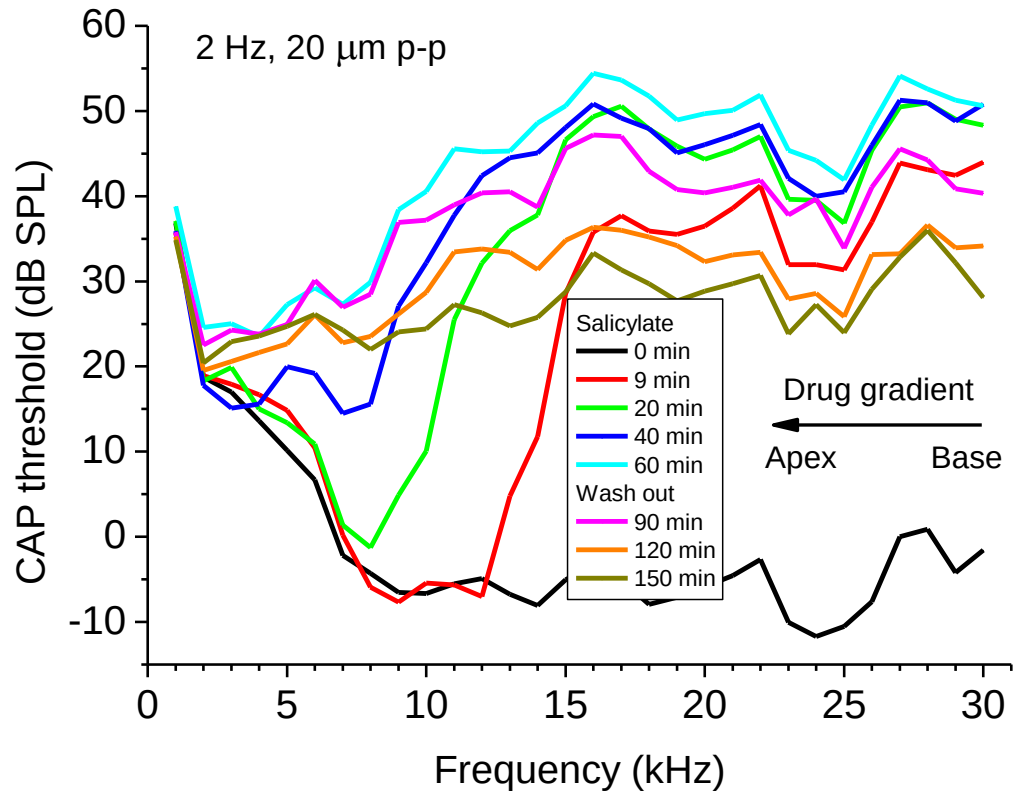

Figure 5.4. The Effect of combined application of 5 µl 100 mM salicylate solution and continuous RWM probe vibrations at a frequency of 2 Hz as a function of acoustic stimulus frequency. Salicylate was applied at time zero and RWM probe vibrations started at the same time. The total salicylate application time was 60 minutes. Salicylate was washed out from the RWM after that. CAP thresholds for different times of salicylate application/RWM vibrations (colour coded curves) as a function of acoustic stimulus frequency (mean values, SDs are not shown for clarity, N=6).

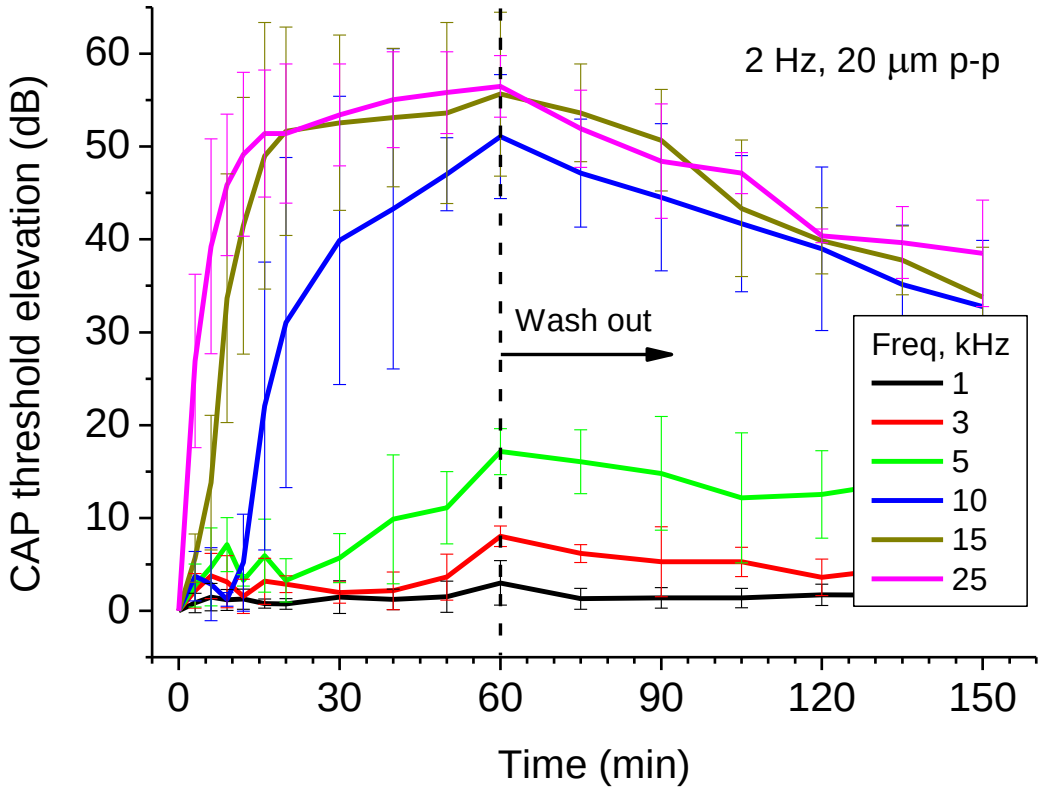

Figure 5.5. The Effect of combined application of 5 µl 100 mM salicylate solution and continuous RWM probe vibrations at frequency of 2 Hz as a function of acoustic stimulus frequency. The CAP threshold elevations relative to the thresholds before salicylate application (time zero) for six acoustic stimulus frequencies (colour coded curves) which correspond to different locations along the cochlea (mean ± SD, N = 6). Salicylate was applied at time zero and RWM probe vibrations started at the same time. The total salicylate application time was 60 minutes. Salicylate was washed out from the RWM after that as indicated on the graph.

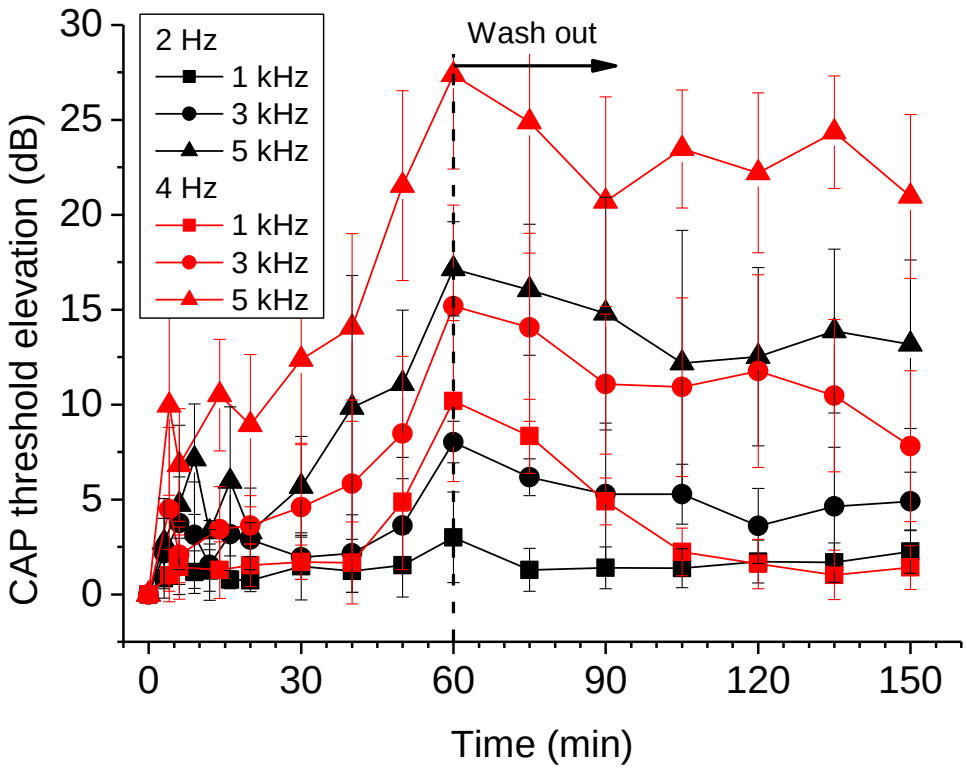

Figure 5.6. Effect of combined application of 5 µl 100 mM salicylate solution and continuous RWM probe vibrations at frequencies of 4 Hz and 2 Hz as a function of acoustic stimulus frequency. The CAP threshold elevations relative to the thresholds before salicylate application (time zero) for acoustic stimulus frequencies (different symbols) corresponding to apical half of the cochlea (mean ± SD, N = 6 and 4 for 4 Hz and 2 Hz of probe vibrations respectively). Statistically significant ($p < 0.05$, unpaired t test) differences between the threshold elevations for probe vibrations at 4 Hz and 2 Hz are observed after 60 minutes of salicylate application/RWM vibrations.

The CAP threshold elevations during combined application of salicylate solution to the RWM and RWM probe vibrations were frequency dependent (figure 5.4, 5.5) and increase with a higher frequency of the RWM probe vibrations. This is particularly evident for the lowest frequencies of acoustic stimulation (figure 5.6). For the same acoustic frequencies (i.e., cochlear locations), the total CAP threshold elevations after 60 minutes of combined salicylate application and RWM probe vibrations at 4 Hz were significantly higher ($p < 0.05$, unpaired t test) than the threshold elevations observed during probe vibrations at 2 Hz. This frequency dependence confirms that increase in the CAP thresholds at frequencies which correspond to

more apical cochlear locations and, hence, enhanced diffusion of salicylate to the cochlear apex, was not due to placement of the probe alone and probe vibrations were required to observe the effect.

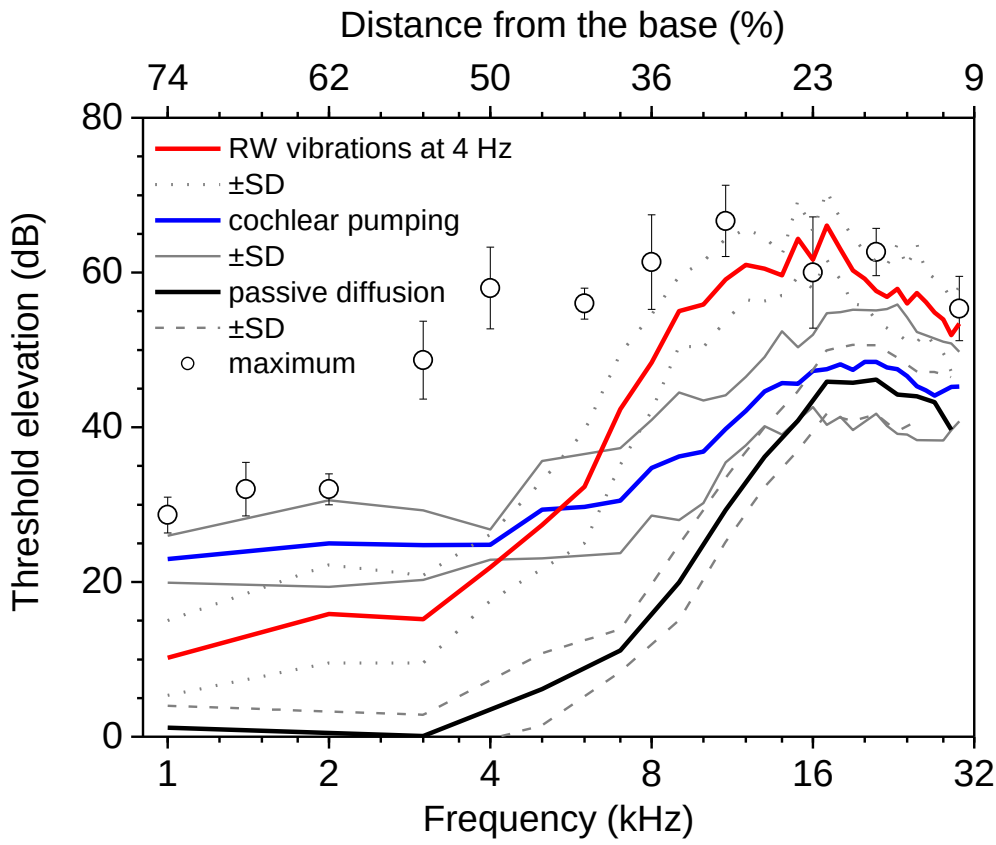

Figure 5.7. Comparison between different techniques of drug delivery through the RWM. Frequency dependence of the CAP threshold elevation after 60 min of 5µl 100 mM/l salicylate solution application for passive diffusion (black line, mean ± SD, N = 5, Lukashkin et al., 2020), during cochlear pumping (35 min of the total pumping time) (blue line, mean ± SD, N = 5, Lukashkin et al., 2020) and continuous RWM probe vibrations (red line, mean ± SD, N = 6) are shown. Open circles show maximal increase of the CAP thresholds after complete block of the cochlear amplifier by application of 5 µl 1 M salicylate solution to the RWM (mean ± SD, N = 3) (Sadreev et al., 2019).

When 5 µl of 100 mM salicylate solution was applied to the RWM and salicylate is allowed to diffuse passively along the cochlea, it does not cause CAP threshold elevations for frequencies of acoustic stimulation below 5 kHz (figure 5.7, black line; Sadreev et al., 2019). This

effectively means that salicylate is not able to reach apical 50% of the cochlea at any profound concentrations. Combined application of salicylate and low-frequency (4 Hz) pressure oscillations to the ear canal (cochlear pumping), which causes large amplitude (80 µm peak-to-peak), movement of the stapes and reciprocal movement of the RW, causes elevation of CAP thresholds within the entire frequency range tested (figure 5.7, blue line; Lukashkin et al., 2020). This indicates ability of the cochlear pumping to distribute salicylate evenly along the entire cochlea. Joint application of salicylate and RWM probe vibrations (4 Hz, 20 µm peak-to-peak amplitude) reported in this work causes CAP threshold elevations for the frequencies corresponding to the cochlear apex (figure 5.7, red line) indicating enhanced drug diffusion during the RWM vibration. The threshold elevations at the cochlear apex (below 5 kHz) were smaller than observed during cochlear pumping, probably because of the smaller RWM probe vibration amplitude (20 µm peak-to-peak) compared to the stapes vibration amplitude (80 µm peak-to-peak). However, the CAP threshold elevations for the basal half of cochlea (frequency of acoustic stimulation above 5 kHz) observed during the RWM probe vibrations exceed those recorded during both passive salicylate diffusion and cochlear pumping. These high-frequency thresholds elevations during the RWM vibrations are, in fact, close to the maximum threshold elevations after complete block of the cochlear amplifier by application of 1 M salicylate solution (figure 5.7, circles; Sadreev et al., 2019). Therefore, the RWM probe vibrations not only promote drug diffusion into the cochlea apex but also enhance salicylate passage through the RWM.

To gain insight into the mechanism of enhanced drug diffusion with RWM vibrations, an experiment was designed to compare the speed of passive, molecular diffusion of Lucifer yellow along water filled straight pipes and its diffusion assisted by micro vibrations of a membrane covering one end of the pipes (Figure 5.8 A, B). The pipes were water filled to ~ 30 mm from the membrane and their internal cross-sectional area was ~ 1.02 mm^2 which corresponds to the length and average cross-sectional area of the human ST, respectively (Thorne et al., 1999). Fluorescence intensity profiles, obtained immediately after injection of 0.2 µl of the dye, were closely similar in all experiments (Figure 5.8 C), indicating the initial conditions remained constant for all sets of measurements. Small, 40 µm peak-to-peak vibration of the membrane at 10 Hz over 60 minutes enhanced dye distribution compared to passive diffusion (Figure 5.8 D). The additional spread of the diffusion front was small (about 1.7 mm for fluorescence intensity of 150 AU, green arrow in Figure 5.8 D). However, due to nonlinear dispersion of the diffusion front, this small additional spread led to a statistically

significant increase (unpaired *t*-test for 0.5 mm bins, $p<0.05$) in the fluorescence intensity, i.e., dye concentration, over a much wider range of 9 mm (blue horizontal bar, Figure 5.8 D).

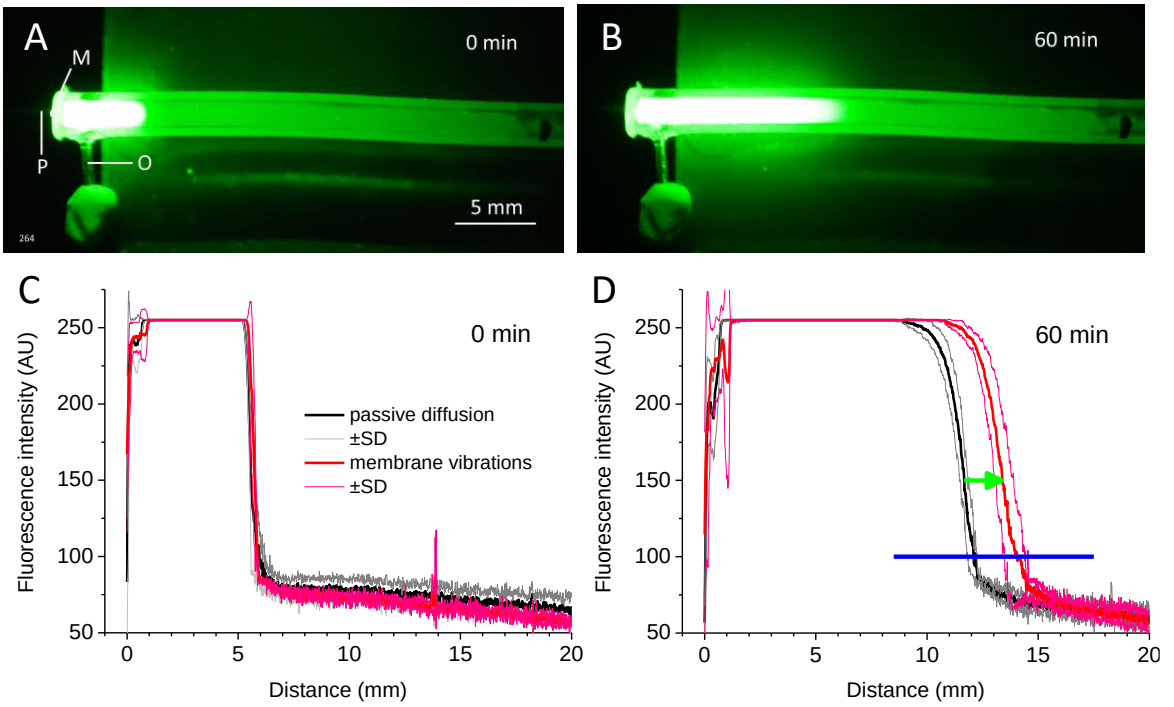

Figure 5.8. Distribution of Lucifer yellow in a straight pipe during passive diffusion and during vibrations of a membrane at a pipe end. (**A**). Fluorescence immediately after injections of 0.2 µl of 5% Lucifer yellow water solution into the pipe through outlet O. M – latex membrane; P – carbon probe. (**B**). Fluorescence after 60 minutes of membrane vibrations at 10 Hz with 40 µm peak-to-peak carbon probe movements. (**C**). Overlapping fluorescence intensity profiles measured along the pipe axis for all passive diffusion (black line, mean ± SD, N = 3) and membrane vibration (red line, mean ± SD, N = 3) experiments indicating the same initial conditions immediately after the dye injection. (**D**). Fluorescence intensity profiles after 60 minutes of passive dye diffusion (black line, mean ± SD, N = 3) and membrane vibrations (red line, mean ± SD, N = 3). The same experiments as in C. Green arrow indicates additional spread of the diffusion front during membrane vibrations. Blue horizontal bar indicates the spread of statistically significant increase (unpaired *t*-test for 0.5 mm bins, $p<0.05$) in the fluorescence intensity/dye concentration which is observed during membrane vibrations.

5.4 Discussion

This work is a proof-of-concept report which demonstrates that vibrating the partially occluded RWM at low frequencies of 2 and 4 Hz, with an amplitude of 10 µm, facilitates drug distribution along the cochlear spiral. Finding optimal and safe parameters for the RWM vibrations was outside the study's scope. However, the data supports that, for the range of stimulation parameters used, and within the timeframe of experiments, drug diffusion was enhanced with increasing RWM stimulus frequency without affecting neural thresholds. This frequency dependence of drug distribution also indicates that placement of the RWM probe did not rupture the RWM. At the same time, the enhanced effect on the CAP threshold elevation in the basal half of the cochlea, produced by the RWM vibrations (figure 5.7) compared to passive diffusion (Sadreev et al., 2019) and cochlear pumping (Lukashkin et al., 2020), suggests that RWM drug permeability for salicylate was increased during direct mechanical stimulation of the RWM.

RWM vibration stimulation alone did not elicit electrical responses which could be recorded at the RWM, including CAPs associated with afferent fibre/inner hair cell excitation or cochlear microphonic potentials dominated by basal turn OHC mechanoelectrical transducer currents (Patuzzi et al., 1989; Cheatham et al., 2011). Previously, very large cochlear microphonic potentials in response to 5 Hz acoustic stimulation were recorded from the cochlear apex but not from the cochlear base in guinea pigs, suggesting excitation of the OHCs in this tonotopic frequency place (Salt et al., 2013). It is demonstrated here, however, that excitation of sensory hair cells due to the low-frequency RWM vibrations was minimal in these experimental configurations. The RWM probe diameter (0.5 mm) and its cross-sectional area (0.2 mm^2) were much smaller than the dimensions and area of the RWM in guinea pigs (Ghiz et al., 2001; Wysocki & Sharifi, 2005), and the probe covered only a small part of the RWM. Under these conditions, most of the pressure relief during the probe movement was through the RWM area not occluded by the probe (Weddell et al., 2014) and the average alternating far-field pressure, P_M, generated within the cochlea was small. This was confirmed by the absence of stapes responses, which were below the measurement noise floor (~0.1 nm) during probe vibrations at the RWM at either 2 or 4 Hz. The magnitude of P_M will depend on the stiffness, S, of the freely moving area, A_R, of the RWM and its volume velocity, q, as (Weddell et al., 2014)

$$P_{\mathrm{M}} = \frac{Sq}{i\omega {A_{\mathrm{R}}}^2}$$

Even if a small far-field pressure was generated in these experiments due to finite stiffness, S, of the RWM, which did not generate measurable stapes vibrations, then it still would not lead to a significant excitation of the BM. The frequencies of 2 and 4 Hz used in this experimental design are below the helicotrema cut-off frequency in guinea pigs (Marquardt et al. 2007) and will be filtered out by the helicotrema, preventing BM excitation at these frequencies and damage to the cochlear sensory cells during the RWM probe stimulation. The role of the cochlear aqueduct in pressure relief at frequencies of 2 and 4 Hz, used to vibrate the RWM in these experiments, should be small because the time constant for inner ear pressure relaxation due to the cochlear aqueduct is in the order of seconds (Thalen et al., 2002; Feijen et al., 2004). The potential influence of mass and viscosity of the relatively large volume of fluid placed on the RWM in these experiments should also be small. Dai *et* al. demonstrated that cochlear impedance remains stiffness-dominated at low frequencies even when the middle ear is filled with fluid. i.e., when the RWM is loaded with fluid. Dai *et al*. did not make measurements at frequencies as low as the 2 and 4 Hz used in these experiments but asymptotic behaviour of their magnitude transfer functions at low frequencies clearly indicates stiffness dominated responses.

Vibrations of the partially occluded RWM at acoustic frequencies excite the BM with conventional travelling waves. A jet-like, near-field component, P_{N}, of a complex pressure field near the RWM is the proposed mechanism of stimulation (Weddell et al., 2014). P_{N} is proportional to the fluid density, ρ, and to the acceleration of the probe, $i\omega q$, and an indicative overall magnitude of P_{N} can then be defined as:

$$P_{\mathrm{N}} \propto i\omega\rho q.$$

This work suggests that the guinea pig BM is not excited at frequencies of 2 and 4 Hz used in our experiments, which resulted in lack of excitation of the cochlea sensory apparatus by this pressure component, and the lack of any probe induced hearing loss even for relatively large 20 µm probe displacement.

RWM vibrations with the carbon probe did not evoke any cochlear microphonic potentials from the basal OHCs that could be detected by the RWM electrode (Patuzzi et al., 1989; Cheatham et al., 2011). This near-field component did not excite the basilar membrane at frequencies of 2 and 4 Hz used in these experiments, which also resulted in a lack of excitation of the cochlear sensory apparatus and the absence of any probe induced hearing loss, even for relatively large 20 μm peak-to-peak RW probe displacements. It is worth noting that the near-field pressure, P_N , increases with increasing frequency, which is demonstrated by the higher efficiency of 4 Hz RWM vibrations compared to 2 Hz (figure 5.6), if the near-field pressure component is the main factor facilitating enhanced drug diffusion during vibration of the partially occluded RWM.

The question is how this short acting jet-like, near-field pressure component, can facilitate drug distribution along the entire cochlea, which is an order of magnitude longer than the near-field pressure spread (Weddell et al., 2014). The fluorescent dye experiments (figure 5.8), while being different from the RWM stimulation experiments in two important aspects, provide an insight into the underlying physical mechanisms. Firstly, the latex membrane stiffness was much larger than the RWM stiffness. Pressure relief in this case was through the open pipe end and a large far-field pressure component was generated within the fluid-filled pipe leading to movement of the entire fluid column. Taylor dispersion (Taylor, 1953) of solvents is observed during oscillatory pipe flows which lead to additional spread of solvents compared to molecular diffusion alone (Aris, 1960; Watson, 1983). It has been demonstrated experimentally that for small-stroke fluid oscillatory movements and dimensions of the human cochlea this effect is small (Dasgupta, 2015), which is confirmed by lack of changes in the diffusion front in our experiments (Figure 5.8). However, when a physical body vibrates in confined spaces, which resembles the geometry of these experiments, the jet-like fluid movement is transformed into steady fluid streaming which forms vortexes in the vicinity of the vibrating body, even at low frequencies (Costalonga et al., 2015). The vortexes can facilitate fluid mixing close to the vibrating body, which is the inner surface of the vibrating membrane in these experiments. Thus, in the fluorescent dye experiments, this mixing should change the boundary condition at the closed pipe end and lead to additional spread of the diffusion front without changing its dispersion (Figure 5.8 D). The diffusion front dispersion over the same time is larger for substances with larger diffusion coefficients. Therefore, it be can predicted that the effective range of increased concentration should be larger for salicylate used in these experiments (salicylate diffusion coefficient is 9.59×10^{-4} mm^2/s (Lide (2002)) and for dexamethasone, the

most frequently used drug for intratympanic treatment of hearing disorders (dexamethasone diffusion coefficient calculated from Stokes-Einstein equation which, however, underestimates experimental values, is 6.82×10^{-4} mm^2/s), than we observed for Lucifer yellow (diffusion coefficient is 3.1×10^{-4} mm^2/s (Brink & Ramanan, 1985)).

The second major difference between our *in vivo* and fluorescent dye experiments is in the amount of material available for diffusion. The amount of dye was limited by its initial injection. A relatively large volume of 5 µl of salicylate solution was placed on the outer surface of the RWM *in vivo*. Hence, an additional amount of salicylate could enter the ST down its concentration gradient when the salicylate concentration in the immediate vicinity of the inner surface of the RWM dropped due to enhanced mixing because of the vortex formation described above and because the RWM permeability increased during its mechanical stimulation (e.g., Park & Moon, 2014; Liao et al., 2020). This facilitated additional influx of salicylate could increase its concentration at the cochlear base, which is indicated by higher basal CAP threshold elevations observed in these experiments (Figure 5.7). The increase in salicylate concentration changes the diffusion boundary condition and promotes diffusion of salicylate to the cochlear apex. It should be noted that salicylate was utilized in this study due to its well documented physiological effects. However, it is a difficult drug to distribute along the cochlea because it is cleared rapidly from the ST (Sadreev et al., 2019). It is anticipated that drugs, which are better retained in the ST, will be redistributed along the cochlea even more quickly and efficiently (Salt & Ma, 2001; Sadreev et al., 2019).

Considerations of the effect of RWM vibration frequency on the distribution of salicylate solution within the cochlea were explored. Probe diameter and peak-to-peak displacement remained constant throughout this work. For future studies, probe size and maximum displacements should be considered, which will potentially result in greater drug distribution. A larger probe diameter was attempted however, due to the anatomical restrictions of the bulla and round window niche, it was not possible to place a larger probe size onto the RWM in this experimental model without causing damage to the middle ear and thus, introducing increased fluid aspiration into the round window niche. It should be noted that the guinea pig stapes is limited to a maximum displacement of ~80 µm due to the crista stapedius (Lukashkin *et al*., 2020). The concentration of salicylate solution was constant throughout this work and should be a consideration in further work. The concentration of salicylate used in this experiment was 100 mM to illustrate the effect of micro vibrations on the distribution of the drug. Larger drug

concentrations would improve drug diffusion however it is known passive diffusion alone cannot provide uniform drug delivery along the cochlea (Sadreev *et al*., 2019).

This work is a proof-of-concept study and it remains to be demonstrated that RWM micro vibrations can promote distribution of substances for cochleae of the human cochlea's size and for stimulation parameters that are safe for human cochlear function. If this drug delivery method is effective in human patients, it could be used to deliver and distribute drugs along the cochlea when cochlear pumping (Lukashkin et al., 2020) cannot be applied. For example, when ossicular functionality is absent or impeded, e.g., after injection of high concentrations of hydrogel formulations into the middle ear (e.g., Piu et al., 2011; Schilder et al., 2019). Cochlear drug delivery utilizing micro vibrations of the RWM could be particularly useful in patients with RW vibroplasty (e.g., Beltrame et al., 2014) if a part of the RWM is left available for drug diffusion from the middle ear. In this case a vibrator is already present at the RWM and any additional interventions required are minimal.

To advance this work and strengthen the claims made, perilymph sampling experiments that look to directly measure perilymph salicylate concentrations at the cochlear apex, at set time points post micro-vibrations, should be completed. This experiment should have the exact same design as the one here to ensure consistency but would also allow perilymph concentrations to be correlated with elevated CAP threshold data. Perilymph sampling at the cochlear apex has been demonstrated by Salt *et al* (2006). Furthermore, it would be beneficial to perform the fluorescent dye experiments (figure 5.8) *in vivo* and use imaging techniques to accurately determine the diffusion path of a free dye or a dye bound to salicylate. Ayoob *et al* (2019) achieved this in the guinea pig cochlea. With further data to support the claim that micro-vibrations at the RWM enhance intracochlear drug diffusion, it would be interesting to modify a vibrating device clinically used for RW vibroplasty surgeries, to fit the parameters outlined in this work. With the modified device, further fluorescent experiments could be conducted *in vitro*, with a set up similar to the fluorescent dye experiments performed here, or with pharmacological drugs in clinic. A limitation of this study is the use of only one drug. It is imperative to this work that different drugs be tested while using RWM micro vibrations. Experiments that look to determine RWM drug permeability, during RWM micro vibrations, should utilise drugs that can diffuse through the RWM but also drugs that normally cannot. It could be possible that RWM vibrations enable the diffusion of larger molecules.

Chapter Six
Conclusions

This thesis explores novel advancements in the challenge to provide effective rehabilitation to patients with conductive, sensorineural and mixed hearing loss. A quantified model to determine arbitrary substance passive diffusion through the RWM and along the cochlear spiral was used to further strengthen the necessity of bioengineering intervention for inner ear drug delivery. From this, an original method of effective drug delivery to the entire cochlea was designed. The efficiency of RWM stimulation was explored using probes which partially occlude the RWM and without the requirement of ossicular chain functionality.

The data presented in chapter three quantifies the findings of a significant drug concentration gradient within the cochlea when drugs passively diffuse through the RWM and along the cochlear spiral (Saijo and Kimura, 1984; Imamura and Adams, 2003; Hargunani *et al*., 2006; Grewal *et al*., 2013). Based on the experimental findings described, the calculated base-to-apex salicylate concentration gradient was 12 orders of magnitude smaller at the apex than at the base in this guinea pig model. For the same substance, it is further predicted that the concentration gradient would be 16 orders of magnitude smaller at the apex than the base in the human cochlea, due to the larger size of the human cochlea. This was confirmed by the lack of CAP threshold elevation at 5 kHz, due to salicylate diffusion, and below which is equal to 55% of the guinea pig cochlea. Our findings further describe the parameters which determine the base-to-apex concentration gradient, such as better drug retention in the ST (higher kd/kc ratio). The significance of this work is to aid in the development of further drug delivering technologies (nanoparticles) and also improvements to drug delivery methods. A nanoparticle drug carrier which can readily diffuse through the RWM, be assisted by an external device (magnets, cochlear pumping, micro vibrations), and release its payload along the entire cochlear spiral is desirable (Glueckert *et al*., 2018).

Salicylate was used in this study due to its well characterised inhibitory effect on OHC functionality allowing for direct quantification of passive diffusion. It would be interesting to determine how substances with a higher kd/kc ratio behave within the cochlea and whether the base-to-apex concentration gradient is as predicted – a smaller base-to-apex concentration gradient but traded for a considerably longer time to reach steady-state concentrations in the cochlear apex. The permeability of the RWM was not considered in this study as it is well

documented that salicylate readily diffuses through the RWM. Such considerations should be explored in further work to determine the effect on passive diffusion of larger molecules. It must be noted that RWM perforation should be avoided and the cochlea remain intact.

The data presented in chapter four provides evidence that RWM stimulation of the cochlea can be optimised to a point at which cochlear excitation is maximum but also allowing for effective simultaneous pressure relief through the RWM. This would be specific to the device-RWM coupling interface in which, the portion of the RWM occluded is optimal and the exposed region is sufficient to allow intracochlear pressure relief. Our data further supports claims that partial RWM stimulation does not require ossicular chain functionality (Weddell *et al*., 2014).

Ossicular chain mobility is not necessary for this mechanism of cochlear excitation to be effective, which is supported by the data in this work. In further work, the ossicular chain should be entirely immobilised and the effect on recorded CAP thresholds be determined during RWM stimulation with a partially occluding hearing device. It can be predicted that there would be no change, due to the findings described here, where decreasing the ossicular chain response by 20 dB which did not affect CAP thresholds during RWM cochlear excitation. Placement of the probe onto the RWM was challenging at first and the recordings were not always repeatable. Factors such as probe placing location on the RWM (i.e., deviation from the centre), RWM loading (applying greater pressure on the RWM) and damage to the surrounding round window niche can affect CAP threshold recordings. In 1 preparation, the probe damaged the RWM and fluid aspiration was seen. This was later determined to be due to the angle of approach of the probe in which the probe footplate was not completely perpendicular to the RWM surface. During minor positioning alterations, the slight ‘hook’ design of the probe pulled on the RWM and made a small opening. Experiments were ended if any physical damage occurred to the RWM or the animal showed severe hearing loss. In total, 5 experiments were ended due to these factors.

The significance of the findings described in chapter four supports the argument that complete occlusion of the RWM may not be the most efficient method of RWM stimulation. Most, if not all, groups working on this mechanism of cochlear excitation block the RWM entirely (Liu *et al*., 2019; Tian *et al*., 2015; Yang *et al.,* 2015; Schraven *et al.,* 2011; Zhang and Gan, 2011; Arnold *et al.,* 2010) and explore improved RWM coupling techniques. Also, by not entirely occluding the RWM, the surgical implications of fitting a RWM displacing hearing device are less difficult. The surgeon will not be required to form a ‘seal’ between the hearing device and

the RWM using tissue or other materials. A further significant conclusion is the ability to efficiently excite the cochlea without ossicular chain mobility. This reduces the requirements during patient selection in which, patients who previously suffered from osteosclerosis, for example, and would normally find a RWM stimulating hearing device non effective, would now be eligible for such a device.

Chapter five explores the possibility of using a RWM displacing device to enhance drug distribution along the cochlear spiral.

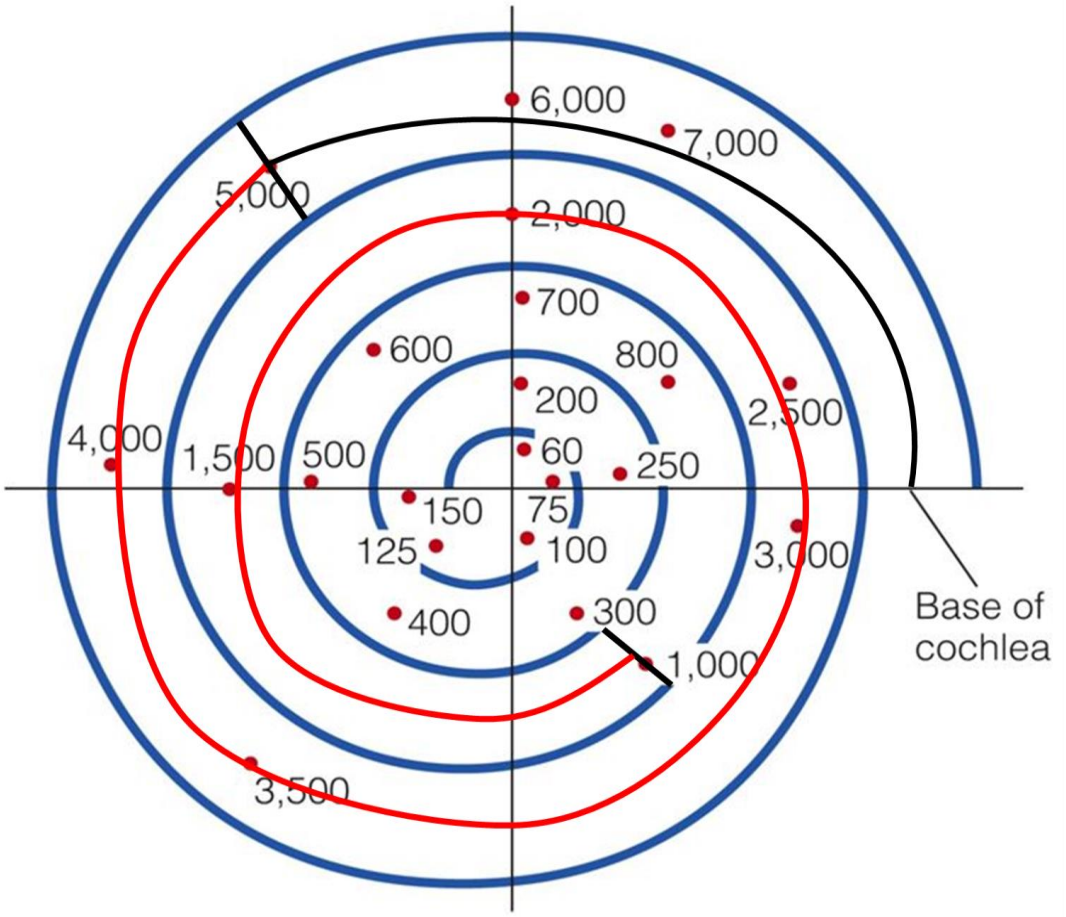

Figure 6.1. A guinea pig cochlea frequency map illustrating the diffusion pathway of a substance from the base to the apex determined via the CAP threshold elevations recorded when salicylate diffused through the RWM. Values at red dots display the cochlear frequency regions in Hz. The black line from the base of the cochlea to 5000 Hz is the diffusion pathway by passive cochlea drug diffusion. The black line (from the base to 5000 Hz) and the red line (from 5000 Hz to 1000 Hz) illustrates the diffusion pathway of salicylate in the cochlea when assisted by RWM micro vibrations as demonstrated in this work. (Adapted from Culler *et al*., 1943).

The diagram in figure 6.1 aids to visualise the issue of passive drug diffusion along the cochlear spiral. RWM micro vibrations demonstrated drug diffusion along the entire frequency range tested without damaging the cochlea. Due to the low frequency of the micro vibrations and no stapes displacement recordings above the noise floor of the laser interferometer, this method of drug delivery would not require ossicular chain functionality. Intracochlear pressure is effectively shunted through the RWM region that was not occluded by the probe as seen in chapter four and Weddell *et al* (2014). Low-frequency micro vibrations of the stapes would provide similar drug distribution if the experimental design were similar as proposed here (Liu *et al*., 2019).

It is proposed that ossicular chain functionality would not be required for effective drug distribution along the cochlear spiral during RWM micro vibrations. Due to the nature of these experiments, it was not possible to increase ossicular chain impedance as this would directly affect the CAP threshold recordings, preventing drug distribution to be accurately determined. In future work, the use of a dye which passes through the RWM, as readily as salicylate, during micro vibrations without ossicular chain functionality would confirm this claim. Furthermore, perilymph sampling experiments post RWM micro-vibrations would support the claims of this work. A restriction to a maximum RWM occlusion diameter of 0.5 mm, due to the design of the carbon probe set up and the anatomical layout of the guinea pig round window niche, was a limitation in this work. It would be interesting to see whether a larger occlusion to exposure ratio would further improve the efficiency of the drug distribution described in this work. The findings in chapter four suggests that a larger probe diameter would further enhance drug-perilymph mixing. Peak-to-peak probe displacement in our work was constant at 20 μm for both 4 Hz and 2 Hz RWM micro vibrations. A larger displacement would be possible and a maximum value of ~80 μm due to the crista stapedius plausible, although complications may arise (Lukashin *et al*., 2020). Tympanic cochlear pumping provided stapes displacement amplitudes of 80 μm and subsequent displacement at the RWM without elevating CAP thresholds without drug application (Lukashin *et al*., 2020). The RWM was displaced for 60 minutes to determine the effectiveness this time frame would have on the distribution of salicylate. It is unclear whether steady state concentrations were met at the apical regions of the cochlear spiral and thus, increased time periods may further enhance drug distribution.

The significance of the findings discussed in chapter five is a proof of concept that vibrating the RWM enhances drug distribution along the cochlear spiral. RWM micro vibration drug delivery is not optimised and does not operate at its most efficient, however, effective drug

distribution along the cochlea is still observed. With optimisation, the implications of this work are vast. Current hearing devices could be modified to enable the parameters discussed to allow effective drug delivery to the cochlea post intratympanic injection. New drug loaded hearing devices could be developed which sit in the round window niche, release a substance and displace the RWM. The main downside of this mechanism of drug delivery is the requirement for surgical intervention. Although, if effective drug delivery to the entire cochlear spiral at therapeutic concentrations is possible, without the need for ossicular chain functionality, the need for surgery may be a plausible trade-off for patients.

References

Albuquerque AAS, Rossato M, De Oliveira JAA, Hyppolito MA. Understanding the anatomy of ears from guinea pigs and rats and its use in basic otologic research. Rev Bras Otorrinolaringol. 2009; 75(1):43-9.

del Amo, E. M., Rimpelä, A. K., Heikkinen, E., Kari, O. K., Ramsay, E., Lajunen, T., ... and Subrizi, A. Pharmacokinetic aspects of retinal drug delivery. Prog. Retin. Eye Res. 2017; 57, 134-185.

Angeli S, Lin X, Liu XZ. Genetics of hearing and deafness [published correction appears in Anat Rec (Hoboken). 2015 Nov; 298(11):1815]. Anat Rec (Hoboken). 2012; 295(11):1812–1829.

Aris R. On the dispersion of a solute in pulsating flow through a tube. Proc R Soc A 1960; 259:370–6.

Arnold A, Stieger C, Candreia C, Pfiffner F, Kompis M. Factors Improving the Vibration Transfer of the Floating Mass Transducer at the Round Window, Otology & Neurotology. 2010; 31 (1): 122-128.

Ashmore JF. A fast-motile response in guinea-pig outer hair cells: the cellular basis of the cochlear amplifier. J Physiol (Lond) 1987; 388:323–347.

Asma A, Ubaidah MA, Hasan SS, et al. Surgical outcome of bone anchored hearing aid (baha) implant surgery: a 10 years' experience. Indian J Otolaryngol Head Neck Surg. 2013; 65(3):251–254.

Assad JA, Corey DP. An active motor model for adaptation by vertebrate hair cells. J. Neurosci. 1992; 12:3291–3309.

Ayoob AM, Peppi M, Tandon V, Langer R, Borenstein JT. Intracochlear drug delivery: Fluorescent tracer evaluation for quantification of distribution in the cochlear partition. Eur J Pharm Sci. 2019; (1) 126:49-58.

Barrs DM. Intratympanic corticosteroids for Meniere's disease and vertigo. Otolaryngol Clin North Am, 2004; 37: 955-972.

Bas E, Bohorquez J, Goncalves S, et al. Electrode array-eluted dexamethasone protects against electrode insertion trauma induced hearing and hair cell losses, damage to neural elements, increases in impedance and fibrosis: a dose response study. Hear Res. 2016; 337:12–24.

Beltrame AM, Martini A, Prosser S, Giarbini N, Streitberger C. Coupling the Vibrant Soundbridge to cochlea round window: auditory results in patients with mixed hearing loss. Otol Neurotol. 2009 ;30(2):194-201.

Beltrame AM, Todt I, Sprinzl G, et al. Consensus statement on round window vibroplasty. Ann Otol Rhinol Laryngol 2014; 123:734–40.

Bento RF, Kiesewetter A, Ikari LS, Brito R. Bone-anchored hearing aid (BAHA): indications, functional results, and comparison with reconstructive surgery of the ear. Int Arch Otorhinolaryngol. 2012; 16(3):400–405.

Békésy GV. Experiments in Hearing, McGraw-Hill, New York, NY, USA, 1960.

Borkholder, DA, Zhu, X, and Frisina, RD. Round window membrane intracochlear drug delivery enhanced by induced advection. J. Control. Release. 2014; 174, 171-176.

Borkholder, D. A., Zhu, X., Hyatt, BT., Archilla, AS., Livingston III, WJ, and Frisina, RD. Murine intracochlear drug delivery: reducing concentration gradients within the cochlea. Hear. Res. 2010; 268, 2-11.

Borrmann A, Arnold W. Non-syndromal round window atresia: an autosomal dominant genetic disorder with variable penetrance? Eur. Arch. Otorhinolaryngol. 2007; 264, 1103–1108

Bowe, SN, and Jacob, A. Round window perfusion dynamics: implications for intracochlear therapy. Curr. Opin. Otolaryngol. Head Neck Surg. 2010; 18, 377-385.

Bledsoe SC., Bobbin, RP., and Puel, JL. Neurotransmission in the inner ear, in Physiology of the Ear, edited by AF Jahn, and J Santos-Sacchi (Raven Press, New York). 1988; 385–406.

Brink PR, Ramanan SV. A model for the diffusion of fluorescent probes in the septate giant axon of earthworm. Axoplasmic diffusion and junctional membrane permeability. Biophys J. 1985; 48(2):299-309.

Brookes GB. Vitamin D deficiency – a new cause of cochlear deafness. J Laryngol Otol. 1983; 97:405–420.

Brownell WE, Bader CR, Bertrand D, de Ribaupierre Y. Evoked mechanical responses of isolated cochlear outer hair cells. Science. 1985; 227:194–196.

Brown MC, Nuttall AL, Masta RI, Lawrence M. Cochlear inner hair cells: Effects of transient asphyxiaon intracellular potentials. HearRes 9:131-144, 1983.

Buckiová D, Ranjan, S, Newman, TA, Johnston, AH, Sood, R, Kinnunen, PK, Popelář, J, Chumak T, and Syka J. Minimally invasive drug delivery to the cochlea through application of nanoparticles to the round window membrane. Nanomedicine 2012; 7, pp.1339-1354.

Carpenter AM, Muchow D, Goycoolea MV. Ultrastructural studies of the human round window membrane. Arch. Otolaryngol. Head Neck Surg. 1989; 115:585–590.

Cervo DG, Mansur SS, Vieira EDR. Flow over rough surfaces. Proceedings of the 22nd International Congress of Mechanical Engineering (COBEM 2013), 3-7, 2013, RibeirãoPreto Brazil (2013), 5966-5976.

Cheatham MA, Naik K, Dallos P. Using the cochlear microphonic as a tool to evaluate cochlear function in mouse models of hearing. J Assoc Res Otolaryngol. 2011;12(1):113-125

Chen, Z., Kujawa, S. G., McKenna, M. J., Fiering, J. O., Mescher, M. J., Borenstein, J. T., Swan, E. E. L. and Sewell, W. F. (2005). Inner ear drug delivery via a reciprocating perfusion system in the guinea pig. J. Control. Release 2005; 110, 1-19.

Cheung EL, Corey DP. Ca2+ changes the force sensitivity of the hair-cell transduction channel. Biophys J. 2006; 90:124–139.

Colletti V, Carner M, Colletti L. TORP vs round window implant for hearing restoration of patients with extensive ossicular chain defect. ACTA Otolaryngol. 2009; 129:449–520

Colletti V, Soli SD, Carner M, et al. Treatment of mixed hearing losses via implantation of a vibratory transducer on the round window. Internat Journal of Audiology. 2006; 45:600–608.

Crawford AC, Fettiplace R. The mechanical properties of ciliary bundles of turtle cochlear hair cells. J. Physiol., 1985: 364: 359-379.

Creber, N. J., Eastwood, H. T., Hampson, A. J., Tan, J., and O'Leary, S. J. A comparison of cochlear distribution and glucocorticoid receptor activation in local and systemic dexamethasone drug delivery regimes. Hear. Res. 2018; 368, 75-85.

Culler E, Coakley J, Lowy K, Gross N. A Revised Frequency-Map of the Guinea-Pig Cochlea. The American Journal of Psychology, 1943; 56 (4): 475-500.

Culler E, Finch G, Girden E. Function of the round window in hearing. Am. J. Physiol. 1935; 111, 416–425.

Dahl D, Kleinfeldt D. Method for measuring the viscosity of the perilymph in the guinea pig cochlea under physiological conditions. Arch Klin Exp Ohren Nasen Kehlkopfheilkd. 1970;197(1):31-40.

Dai C, Wood MW, Gan RZ. Combined effect of fluid and pressure on middle ear function. Hear Res. 2008; 236 (1-2): 22-32.

Dallos P, Cheatham MA. Cochlear hair cell function reflected in intracellular recordings in vivo. Soc Gen Physiol Ser. 1992; 47:371–393

Dallos, P., and Cheatham, M. A. Production of cochlear potentials by inner and outer hair cells. J. Acoust. Soc. Am. 1976; 60, 510–512.

Dasgupta S. (2015). An experimental study of dispersion in oscillating flows in cylindrical tubes [thesis]. Rochester Institute of Technology. Accessed at: https://scholarworks.rit.edu/theses/8762

Davids T, Gordon K A, Clutton D, Papsin B C. Bone-anchored hearing aids in infants and children younger than 5 years. Arch Otolaryngol head neck surg. 2007; 133:51–55.

Davis H. An active process in cochlear mechanics. Hear. Res. 1983; 9: 79–90.

De Paolis A, Watanabe H, Nelson JT, Bikson M, Packer M, Cardoso L. Human cochlear hydrodynamics: A high-resolution μCT-based finite element study. J Biomech. 2017; 50:209-216.

Devare, J., Gubbels, S., and Raphael, Y. Outlook and future of inner ear therapy. Hear. Res. 2018; 368, 127-135.

Douchement D, Terranti A, Lamblin J, et al. Dexamethasone eluting electrodes for cochlear implantation: Effect on residual hearing. Cochlear Implants Int. 2015; 16:195–200.

Drake, RL, Vogl W, Mitchell, AWM, Gray H. Gray's anatomy for students. Philadelphia, Elsevier/Churchill Livingstone. 2005.

Drexl, M., Überfuhr, M., Weddell, T. D., Lukashkin, A. N., Wiegrebe, L., Krause, E., and Gürkov, R. Multiple indices of the ‘bounce’ phenomenon obtained from the same human ears. J. Assoc. Res. Otolaryngol. 2014; 15, 57-72.

van Drunen WJ, Mueller M, Glukhovskoy A, et al. Feasibility of Round Window Stimulation by a Novel Electromagnetic Microactuator. Biomed Res Int. 2017; 2017:6369247.

Dumon T, Zennaro O, Aran JM, Bébéar JP. Piezoelectric middle ear implant preserving the ossicular chain. Otolaryngol Clin North Am. 1995; 28:173–187.

El Kechai, N., Agnely, F., Mamelle, E., Nguyen, Y., Ferrary, E., and Bochot, A. Recent advances in local drug delivery to the inner ear. Int. J. Pharm. 2015; 494, 83-101.

Ersner MS, Spiegel EA, Alexander MH. Transtympanic injection of anesthetics for the treatment of Meniere's syndrome. AMA Arch Otolaryngol, 1951; 54: 43-52.

Eshraghi AA, Adil E, He J, Graves R, Balkany TJ, Van de Water TR. Local dexamethasone therapy conserves hearing in an animal model of electrode insertion trauma-induced hearing loss. Otol Neurotol. 2007; 28:842–849

Evans EF, Klinke R. The effects of intracochlear and systemic furosemide on the properties of single cochlear nerve fibres in the cat. J Physiol 331:409-427, 1982.

Farhadi M, Jalessi M, Salehian P, et al. Dexamethasone eluting cochlear implant: histological study in animal model. Cochlear Implants Int. 2013; 14:45–50.

Feijen RA, Segenhout JM, Albers FW, Wit HP. Cochlear aqueduct flow resistance depends on round window membrane position in guinea pigs. J Assoc Res Otolaryngol. 2004;5(4):404-10.

Fettiplace R. Hair Cell Transduction, Tuning, and Synaptic Transmission in the Mammalian Cochlea. Compr Physiol. 2017;7(4):1197-1227.

Fettiplace R, Ricci AJ. Adaptation in auditory hair cells. Curr Opin Neurobiol. 2003; 13:446–451.

Ghiz AF, Salt AN, DeMott JE, Henson MM, Henson O, Gewalt SL. Quantitative anatomy of the round window and cochlear aqueduct in guinea pigs. Hear. Res. 2001; 162: 105-112.

Glueckert, R., Chacko, L. J., Rask-Andersen, H., Wei, L., Handschuh, S., and Schrott-Fischer, A. Anatomical basis of drug delivery to the inner ear. Hear. Res. 2018; 368, 10-27.

Gluth M. B., Eager K. M., Eikelboom R. H., et al. Long-term benefit perception, complications, and device malfunction rate of bone-anchored hearing aid implantation for profound unilateral sensorineural hearing loss. Otol Neurotol. 2010; 31: 1427–1434.

Goodhill V. Sudden deafness and round window rupture. Laryngoscope 1971; 81, 1462–1474.

Gold T. The physical basis of the action of the cochlea. Proc R Soc Lond B Biol Sci. 1948; 135:492–498.

Goycoolea MV, Carpenter AM, Muchow D. Ultrastructural studies of the round-window membrane. Arch Otolaryngol Head Neck Surg. 1987; 113:617–624.

Goycoolea MV, Lundman L. Round window membrane. Structure function and permeability: a review. Microsc Res Tech. 1997; 36(3):201–211.

Goycoolea MV, Muchow D, Schachern P. Experimental studies on round window structure: function and permeability. The Laryngoscope. 1988 Jun;98(6 Pt 2 Suppl 44):1–20.

Grati M, Kachar B. Myosin VIIa and sans localization at stereocilia upper tip-link density implicates these Usher syndrome proteins in mechanotransduction. Proc Natl Acad Sci U S A. 2011; 108:11476–11481.

Greenwood, D. D. A cochlear frequency-position function for several species--29 years later. J. Acoust. Soc. Am. 1990; 87, 2592-2605.

Grewal, A. S., Nedzelski, J. M., Chen, J. M., and Lin, V. Y. Dexamethasone uptake in the murine organ of Corti with transtympanic versus systemic administration. J. Otolaryngol.-Head N. 2013; 42, 19.

Haghpanahi, M., Gladstone, M. B., Zhu, X., Frisina, R. D., and Borkholder, D. A. Noninvasive technique for monitoring drug transport through the murine cochlea using micro-computed tomography. Ann. Biomed. Eng. 2013; 41, 2130-2142.

Hahn H, Salt AN, Biegner T, Kammerer B, Delabar U, Hartsock JJ, Plontke SK. Dexamethasone levels and base-to-apex concentration gradients in the scala tympani perilymph after intracochlear delivery in the guinea pig. Otol Neurotol. 2012; 33:660–665.

Hallowell D and Silverman SR (Ed.). Hearing and Deafness. Holt, Rinehart and Winston. 1970 3rd ed.

Hallworth, R. Modulation of outer hair cell compliance and force by agents that affect hearing. Hear. Res. 1997; 114, 204-212.

Hao J and Li SK. Inner ear drug delivery: Recent advances, challenges, and perspective. Eur. J. Pharm. Sci. 2019; 126, 82-92.

Hargunani, CA, Kempton, JB, DeGagne, JM., and Trune, DR. Intratympanic injection of dexamethasone: time course of inner ear distribution and conversion to its active form. Otol. Neurotol. 2006; 27, 564-569.

Hasko JA, Richardson GP. The ultrastructural organisation and properties of the mouse tectorial membrane matrix. Hear Res. 1988; 35:21–38.

He DZ, Jia S, Dallos P. Prestin and the dynamic stiffness of cochlear outer hair cells. J Neurosci. 2003; 23:9089–9096. The stiffness of the outer hair cell changes with electromotility, and is modulated by chloride and acetylcholine

Himeno C, Komeda M, Izumikawa M, Takemura K, Yagi M, Weiping Y, Doi T, Kuriyama H, Miller JM, Yamashita T. Intra-cochlear administration of dexamethasone attenuates aminoglycoside ototoxicity in the guinea pig. Hear Res. 2002; 167:61–70.

Horie RT, Sakamoto T, Nakagawa T et al. Stealth-nanoparticle strategy for enhancing the efficacy of steroids in mice with noise-induced hearing loss. Nanomedicine 2010; 5: 1331–1340.

Howard J, Hudspeth AJ. Mechanical relaxation of the hair bundle mediates adaptation in mechanoelectrical transduction by the bullfrog's saccular hair cell. Proc Natl Acad Sci U S A. 1987; 84:3064–3068.

Howard J, Ashmore JF. Stiffness of sensory hair bundles in the sacculus of the frog

Hear. Res.1986: 23: 93-104.

Hudspeth AJ, Jacobs R. Stereocilia mediate transduction in vertebrate hair cells (auditory system/cilium/vestibular system). Proceedings of the National Academy of Sciences of the United States of America. 1979; 76(3):1506-1509.

Hudspeth AJ. Hair-bundle mechanics and a model for mechanoelectrical transduction by hair cells. Soc. Gen. Physiol. Ser. 1992; 47:357–370.

Ikeda K, Kobayashi T, Kusakari J, Takasaka T, Yumita S, Furukawa Y. Sensorineural hearing loss associated with hypoparathyroidism. Laryngoscope. 1987; 97:1075–1079.

Imamura, SI and Adams JC. Distribution of gentamicin in the guinea pig inner ear after local or systemic application. J. Assoc. Res. Otolaryngol. 2003; 4, 176-195.

Jaramillo F, Hudspeth AJ. Displacement-clamp measurement of the forces exerted by gating springs in the hair bundle. Proc. Natl. Acad. Sci. USA. 1993; 90:1330–1334.

Jones GP. Acoustic sensitivity of the vestibular system and mechanical analysis of the tectorial membrane in mammals. Doctoral, University of Sussex. 2012.

Jones, GP, Lukashkina, VA, Russell, IJ, Elliott, SJ. and Lukashkin, AN. Frequency-dependent properties of the tectorial membrane facilitate energy transmission and amplification in the cochlea. Biophys. J. 2013; 104, 1357–1366.

Johnstone JR, Johnstone BM. Origin of Summating Potential. The Journal of the Acoustical Society of America. 1966; 40, 1405-1413.

Johnstone BM and Sellick PM. The peripheral auditory apparatus. Quart. Revs Biophys. 1972; 5, 1-57.

Kachar B, Brownell WE, Altschuler R, Fex J. Electrokinetic shape changes of cochlear outer hair cells. Nature. 1986; 322:365–368

Kachar B, Parakkal M, Kurc M, Zhao Y, Gillespie PG. High-resolution structure of hair-cell tip links. Proc Natl Acad Sci U S A. 2000; 97:13336–13341

Kamalov, MI, Đặng, T, Petrova, NV, Laikov, AV, Luong, D, Akhmadishina, RA, Lukashkin, AN. and Abdullin, TI. Self-assembled nanoformulation of methylprednisolone succinate with carboxylated block copolymer for local glucocorticoid therapy. Colloids Surf. B Biointerfaces 2018; 164, 78-88.

Karimi, M., Sahandi Zangabad, P., Baghaee-Ravari, S., Ghazadeh, M., Mirshekari, H., and Hamblin, M. R. (2017). Smart nanostructures for cargo delivery: uncaging and activating by light. J. Am. Chem. Soc. 2017; 139, 4584-4610.

Karimi, M., Sahandi Zangabad, P, Ghasemi, A, Amiri, M, Bahrami, M, Malekzad, H., Hambilin, MR. (2016). Temperature-responsive smart nanocarriers for delivery of therapeutic agents: applications and recent advances. ACS Appl. Mater. Interfaces 2016; 8, 21107-21133.

Kemp DT. Stimulated acoustic emissions from within the human auditory system. J Acoust Soc Am. 1978; 64:1386–1391.

Kho ST, Pettis RM, Mhatre AN, Lalwani AK. Cochlear microinjection and its effects upon auditory function in the guinea pig. Eur Arch Otorhinolaryngol. 2000; 257:469–72.

Kiang NY, Sachs MB, Peake WT. Shapes of tuning curves for single auditory-nerve fibres. J Acoust Soc Am. 1967 Dec; 42(6):1341-2.

Kiefer J, Arnold W, Staudenmaier R. Round window stimulation with an implantable hearing aid (Soundbridge) combined autogenous reconstruction of the auricle- a new approach. ORL. 2006; 68:378–385.

Kirk, DL, Moleirinho, A., and Patuzzi, RB. Microphonic and DPOAE measurements suggest a micromechanical mechanism for the ‘bounce’ phenomenon following low-frequency tones. Hear. Res. 1997; 112, 69–86.

Koka K, Holland NJ, Lupo JE, Jenkins HA, Tollin DJ. 2010. Electrocochleographic and mechanical assessment of round window stimulation with an active middle ear prosthesis. Hear. Res. 263, 128–137.

Krenzlin S, Vincent C, Munzke L, et al. Predictability of drug release from cochlear implants. J Control Release. 2012; 159:60–68.

Lahav A & Skoe E. An acoustic gap between the NICU and womb: A potential risk for compromised neuroplasticity of the auditory system in preterm infants. Frontiers in neuroscience. 2014; 8. 381.

Lalwani AK, Gürtler N. Sensorineural hearing loss, the aging inner ear, and hereditary hearing impairment. In: Lalwani AK, editor. CURRENT diagnosis & treatment in otolaryngology—head & neck surgery. 2. New York: McGraw-Hill; 2008. pp. 683–704.

Legan PK, Lukashkina VA, Goodyear RJ, Kössi M, Russell IJ, Richardson GP. A targeted deletion in alpha-tectorin reveals that the tectorial membrane is required for the gain and timing of cochlear feedback. Neuron. 2000;28(1):273-85.

Lenarz T. Cochlear implant - state of the art. GMS Curr Top Otorhinolaryngol Head Neck Surg. 2018;16: Doc04.

Leng Y, Liu B., Zhou R., Liu J., Liu D., Zhang S.L., Kong W.J. Repeated courses of intratympanic dexamethasone injection are effective for intractable Meniere's disease. Acta Otolaryngol. 2017;137(2):154–160.

Li L, Chao T, Brant J, O'Malley Jr, B, Tsourkas, A, and Li, D. Advances in nano-based inner ear delivery systems for the treatment of sensorineural hearing loss. Adv. Drug Deliv. Rev. 2017; 108, 2-12.

Liao AH, Wang CH, Weng PY, Lin YC, Wang H, Chen HK, Liu HL, Chuang HC, Shih CP. Ultrasound-induced microbubble cavitation via a transcanal or transcranial approach facilitates inner ear drug delivery. JCI Insight. 2020;13;5 (3): e132880.

Liberman MC, Gao J, He DZ, Wu X, Jia S, Zuo J. Prestin is required for electromotility of the outer hair cell and for the cochlear amplifier. Nature. 2002; 419:300–304.

Lide, DR. CRC Handbook of Chemistry and Physics, 83rd edn. Boca Raton, FL: CRC Press. 2002.

Linder TE, Ma F, Huber A. Round window atresia and its effect on sound transmission. Otol. Neurotol. 2003; 24, 259–263.

Liu H, Zhao Y, Yang J, Rao Z. The Influence of Piezoelectric Transducer Stimulating Sites on the Performance of Implantable Middle Ear Hearing Devices: A Numerical Analysis. Micromachines 2019; 10: 782.

Liu H, Zhang H, Yang J, Huang X, Liu W, Xue L. Influence of ossicular chain malformation on the performance of round-window stimulation: A finite element approach. Proc Inst Mech Eng H. 2019 May;233(5):584-594.

Liu YC, Chi FH, Yang TH, Liu TC. Assessment of complications due to intratympanic injections. World J Otorhinolaryngol Head Neck Surg. 2016;2(1):13-16.

Lukashkin, AN., and Russell, IJ. Analysis of the f2− f1 and 2f1− f2 distortion components generated by the hair cell mechanoelectrical transducer: Dependence on the amplitudes of the primaries and feedback gain. J. Acoust. Soc. Am. 1999; 106, 2661-2668.

Lukashkin, AN., Lukashkina, VA., and Russell, IJ. One source for distortion product otoacoustic emissions generated by low- and high-level primaries. J. Acoust. Soc. Am. 2002; 111, 2740-2748.

Lukashkin AN, Bashtanov ME, Russell IJ. A self-mixing laser-diode interferometer for measuring basilar membrane vibrations without opening the cochlea. J. Neurosci. Methods 2005; 148, 122–129.

Lupo JE, Koka K, Holland NJ, Jenkins HA, Tollin DJ. 2009. Prospective electrophysiologic findings of round window stimulation in a model of experimentally induced stapes fixation. Otol. Neurotol. 30, 1215–1224.

Lusting LR. et al.Hearing Rehabilitation using the BAHA bone-anchored hearing aid: results in 40 patients. Otology & Neurotology. 2001; 22:328–334

Lyon RF. Automatic gain control in cochlear mechanics. in The Mechanics and Biophysics of Hearing, P. Dallos, C. D. Geisler, J. W. Matthews, M. A. Ruggero, and C. R. Steele, Eds., Springer, Berlin, Germany, 1990

Lyon RF and Mead CA. Cochlear hydrodynamics demystied. Caltech Computer Science Technical Report, California Institute of Technology, Pasadena, Calif, USA, 1988

Macherey O, Carlyon RP. Cochlear implants. Science Direct. 2014; 24(18): 878- 884.

Mansour S., Magnan J., Nicolas K., Haidar H. Chronic Suppurative Otitis Media (CSOM): A Middle Ear Mucosal Disease. In: Middle Ear Diseases. Springer, Cham. 2018.

Marquardt T, Hensel J, Mrowinski D, Scholz G. Low-frequency characteristics of human and guinea pig cochleae. J Acoust Soc Am. 2007; 121 (6):3628-38.

Martin C, Tringali S, Bertholon P, Pouget JF, Prades JM. Isolated congenital round window absence. Ann. Otol. Rhinol. Laryngol. 2002; 111, 799–801

McCabe BF. Autoimmune inner ear disease: therapy, Am. J. Otol. 1989; 10: 196–197.

McCall AA, Leary Swan EE, Borenstein JT, Sewell WF, Kujawa SG, McKenna MJ. Drug Delivery for Treatment of Inner Ear Disease: Current State of Knowledge. Ear and hearing. 2010; 31(2):156-165.

Meaud J and Grosh, K. Effect of the attachment of the tectorial membrane on cochlear micromechanics and two-tone suppression. Biophys. J. 2014; 106, 1398-1405.

Medical Advisory Secretariat. Bone anchored hearing aid: an evidence-based analysis. Ont Health Technol Assess Ser. 2002;2(3):1-47.

Moskowitz D, Lee KJ, Smith HW. Steroid use in idiopathic sudden sensorineural hearing loss. Laryngoscope. 1984; 94:664–666.

Mountain, DC, Hubbard, AE, and McMullen, TA. "Electromechanical processes in the cochlea," in Mechanics of Hearing, eds. E. de Boer and M. A. Viergever (Dordrecht: Springer), 1983; 119-126.

Muallem D, Ashmore J. An anion antiporter model of prestin, the outer hair cell motor protein. Biophys J. 2006; 90:4035–4045

Mudry A, Tjellström A. Historical background of bone conduction hearing devices and bone conduction hearing aids. Adv Otorhinolaryngol. 2011; 71:1–9.

Mynatt, R, Hale, SA, Gill, RM., Plontke, SK, and Salt, AN. Demonstration of a longitudinal concentration gradient along scala tympani by sequential sampling of perilymph from the cochlear apex. J. Assoc. Res. Otolaryngol. 2006; 7, 182-193.

Ni, G, Elliott, SJ, and Baumgart, J. Finite-element model of the active organ of Corti. J. R. Soc. Interface 2016; 13, 20150913.

Niedermeyer HP, zahneisen G, Luppa p, et al. Cortisol levels in the human perilymph after intravenous administration of prednisolone. Audiol Neurootol. 2003; 8:316–321.

Nolte. The Human Brain 3rd Ed. Fig. 1993; 9-34A, p.213.

Nordang L, Linder Birgitta Anniko M. Morphologic changes in the round window memebrane after topical hydrocortisone and dexamethasone treatment. Otology and Neurotology. 2003; 24:339–43.

Nuttall AL, Ricci AJ, Burwood G, Harte JM, Stenfelt S, Cayé-Thomasen P, Ren T, Ramamoorthy S, Zhang Y, Wilson T, and Lunner T. A mechanoelectrical mechanism for detection of sound envelopes in the hearing organ. Nat. Commun. 2018; 9, 4175.

Ohmori H. Mechano-electrical transduction currents in isolated vestibular hair cells of the chick. J Physiol. 1985; 359:189–217.

Ohyama K, Salt AN, and Thalmann R. Volume flow rate of perilymph in the guinea-pig cochlea. Hear. Res. 1988; 35, 119-129.

Okuno H, Sando I. Anatomy of the round window. A histopathological study with a Graphic reconstruction method. Acta Otolaryngol 1988; 106:55–63.

Oliver D, He DZ, Klocker N, et al. Intracellular anions as the voltage sensor of prestin, the outer hair cell motor protein. Science. 2001; 292:2340–2343.

Pararas EE, Borkholder DA, Borenstein JT. Microsystems technologies for drug delivery to the inner ear. Adv Drug Deliv Rev. 2012;64(14):1650-1660.

Park SH, Moon IS. Round window membrane vibration may increase the effect of intratympanic dexamethasone injection. Laryngoscope. 2014; 124(6):1444-51.

Parnes LS, Sun AH, Freeman DJ. Corticosteroid pharmacokinetics in the inner ear fluids: an animal study followed by clinical application, Laryngoscope. 1999; 109: 1–17.

Patuzzi RB, Yates GK, Johnstone BM. Outer hair cell receptor current and sensorineural hearing loss. Hear Res. 1989;42(1):47-72.

Pickles JO. An Introduction to the Physiology of Hearing, Academic Press. 2008

Piu F, Wang X, Fernandez R, Dellamary L, Harrop A, Ye Q, Sweet J, Tapp R, Dolan DF, Altschuler RA, Lichter J, LeBel C. OTO-104: a sustained-release dexamethasone hydrogel for the treatment of otic disorders. Otol Neurotol. 2011; 32(1):171-9

Plontke, SK., Biegner, T, Kammerer, B, Delabar, U, and Salt, AN. Dexamethasone concentration gradients along scala tympani after application to the round window membrane. Otol. Neurotol. 2008; 29, 401-406.

Plontke SK, Götze G, Rahne T, Liebau A. Intracochlear drug delivery in combination with cochlear implants. HNO. 2017;65(Suppl 1):19-28.

Plontke, SK, Mynatt, R, Gill, RM, Borgmann, S, and Salt, AN. Concentration gradient along the scala tympani after local application of gentamicin to the round window membrane. Laryngoscope, 2007a; 117, 1191-1198.

Plontke, SK., Siedow, N, Wegener, R, Zenner, HP, and Salt, AN. Cochlear pharmacokinetics with local inner ear drug delivery using a three-dimensional finite-element computer model. Audiol. Neurotol. 2007b; 12, 37-48.

Poe D, Pyykkö I, Valtonen H. et al. Analysis of eustachian tube function by video endoscopy. Am. J. Otol. 2000; 21, 602–660.

Ramaswamy, B, Roy, S, Apolo, AB., Shapiro, B, and Depireux, DA. Magnetic nanoparticle mediated steroid delivery mitigates cisplatin induced hearing loss. Front. Cell. Neurosci. 2017; 11, 268.

Rhode WS. “Observations of the vibration of the basilar membrane in squirrel monkeys using the Mössbauer technique,” Journal of the Acoustical Society of America, vol. 49, no. 4, Article ID 1218, 1971.

Ricci AJ, Wu YC, Fettiplace R. The endogenous calcium buffer and the time course of transducer adaptation in auditory hair cells. J Neurosci. 1998; 18:8261–8277.

Richardson GP, Lukashkin AN, Russell IJ. The tectorial membrane: one slice of a complex cochlear sandwich. Curr Opin Otolaryngol Head Neck Surg. 2008; 16(5):458-64.

Rivera, T, Sanz, L, Camarero, G, and Varela-Nieto, I. Drug delivery to the inner ear: strategies and their therapeutic implications for sensorineural hearing loss. Curr. Drug Deliv. 2012; 9, 231-242.

Robles L, Ruggero MA. Mechanics of the mammalian cochlea. Physiol Rev. 2001; 81:1305–1352.

Ruggero MA, Rich NC. Furosemide alters organ of corti mechanics: Evidence for feedback of outer hair cells upon the basilar membrane. JNeurosci 11:1057-1067, 1991.

Ruggero, MA, Narayan, SS, Temchin, AN, and Recio, A. Mechanical bases of frequency tuning and neural excitation at the base of the cochlea: comparison of basilar-membrane vibrations and auditory-nerve-fiber responses in chinchilla. Proc. Natl. Acad. Sci. USA 2000 97, 11744-11750.

Russell IJ, Legan PK, Lukashkina VA, Lukashkin AN, Goodyear RJ, Richardson GP. Sharpened cochlear tuning in a mouse with a genetically modified tectorial membrane. Nat Neurosci. 2007; 10:215–23.

Russell IJ, Sellick P. Intracellular studies of hair cells in the mammalian cochlea. The Journal of physiology. 1978; 284, 261-290.

Russell IJ and Schauz C. Salicylate ototoxicity: Effects on stiffness and electromotility of outer hair cells isolated from the guinea pig cochlea. Auditory Neurosci. 1995; 1, 309-319.

Rybalchenko V, Santos-Sacchi J: Cl-flux through a non-selective, stretch-sensitive conductance influences the outer hair cell motor of the guinea pig. J Physiol 2003.

Sade J, Ar A. Middle ear and auditory tube: middle ear clearance, gas exchange and pressure regulation. Otolaryngol. Head Neck Surg. 1997; 116, 499-524.

Sáenz J, Aguilera A, Ordaz V, Rodríguez V, Rentería A., Castãneda C. Eustachian tube dysfunction in allergic rhinitis. Otolaryngol Head Neck Surg. 2005; 132, 626-631.

Sahni RS, Paparella MM, Schachern PA, Goycoolea MV, Le CT. Thickness of the human round window membrane in different forms of otitis media. Arch Otolaryngol Head Neck Surg. 1987; 113:630–4.

Saijo, S, and Kimura, RS. Distribution of HRP in the inner ear after injection into the middle ear cavity. Acta Otolaryngol. 1984; 97, 593-610.

Salt AN. Pharmacokinetics of Drug Entry into Cochlear Fluids. Volta Rev. 2005;105(3):277-298.

Salt, AN, and Hirose, K. Communication pathways to and from the inner ear and their contributions to drug delivery. Hear. Res. 2018; 362, 25-37.

Salt AN, et al. Radial communication between the perilymphatic scalae of the cochlea. II: Estimation by bolus injection of tracer into the sealed cochlea. Hear Res. 1991; 56:37–43.

Salt AN, Kellner, C, Hale, S. Contamination of perilymph sampled from the basal cochlear turn with cerebrospinal fluid. Hear. Res. 2003; 182, 24–33

Salt AN, Lichtenhan JT, Gill RM, Hartsock JJ. Large endolymphatic potentials from low-frequency and infrasonic tones in the guinea pig. J Acoust Soc Am. 2013;133(3): 1561-71.

Salt AN, and Ma, Y. Quantification of solute entry into cochlear perilymph through the round window membrane. Hear. Res. 2001; 154, 88-97.

Salt AN, and Plontke, SK. Local inner-ear drug delivery and pharmacokinetics. Drug Discov Today. 2005;10(19):1299-1306. doi:10.1016/S1359-6446(05)03574-9

Salt, AN and Plontke SK. Principles of local drug delivery to the inner ear. Audiol. Neurotol. 2009; 14, 350-360.

Salt, AN and Plontke, SK. Pharmacokinetic principles in the inner ear: influence of drug properties on intratympanic applications. Hear. Res. 2018; 368, 28-40.

Santos-Sacchi J. Asymmetry in voltage-dependent movements of isolated outer hair cells from the organ of Corti. J Neurosci. 1989; 9:2954–2962.

Santos-Sacchi J, Dilger JP. Whole cell currents and mechanical responses of isolated outer hair cells. Hear Res. 1988; 35:143–150.

Schilder AGM, Su MP, Blackshaw H, Lustig L, Staecker H, Lenarz T, Safieddine S, Gomes-Santos CS, Holme R, Warnecke A. Hearing Protection, Restoration, and Regeneration: An Overview of Emerging Therapeutics for Inner Ear and Central Hearing Disorders. Otol Neurotol. 2019; 40(5):559-570.

Schraven SP, Hirt B, Goll E, Heyd A, Gummer AW, Zenner HP, Dalhoff E. 2012. Conditions for highly efficient and reproducible round-window stimulation in humans. Audiol. Neurotol. 17, 133–138.

Schuknecht, HF. Ablation therapy for the relief of Meniere's disease. Laryngoscope 1956; 66, 859-859.

Sendowski I, Abaamrane L, Raffin F, Cros A, Clarencon D. Therapeutic efficacy of intra-cochlear administration of methylprednisolone after acoustic trauma caused by gunshot noise in guinea pigs. Hear Res. 2006; 221:119–127.

Serra L, Novanta G, Sampaio AL, Augusto Oliveira C, Granjeiro R, Braga SC. The Study of Otoacoustic Emissions and the Suppression of Otoacoustic Emissions in Subjects with Tinnitus and Normal Hearing: An Insight to Tinnitus Etiology. International Archives of Otorhinolaryngology. 2015; 19(2):171-175.

Shimizu Y, Puria S, Goode RL. The Floating Mass Transducer on the Round Window versus Attachment to an Ossicular Replacement Prosthesis. Otology & neurotology: official publication of the American Otological Society, American Neurotology Society [and] European Academy of Otology and Neurotology. 2011; 32(1):98-103.

Shin DH, Cho JH. Piezoelectric Actuator with Frequency Characteristics for a Middle-Ear Implant. Sensors (Basel). 2018;18(6):1694.

Schultz, Michael & Baumhoff, Peter & Maier, Hannes & Teudt, Ingo & Krüger, Alexander & Lenarz, Thomas & Kral, Andrej. Nanosecond laser pulse stimulation of the inner ear— A wavelength study. Biomedical optics express. 2012. 3. 3332-45.

Skarzynski H, Olszewski L, Skarzynski PH et al. Direct round window stimulation with the Med-El Vibrant Soundbridge: 5 years of experience using a technique without interposed fascia. Eur Arch Otorhinolaryngol 271, 477–482 (2014).

Spindel JH, Corwin JT, Ruth RA, Lambert PR: The basis for a round window electromagnetic implantable hearing aid. Proc Ann Int Conf IEEE 1991; 13:1891–1892.

Spindel JH, Lambert PR, Ruth RA: The round window electromagnetic implantable hearing aid approach. Otolaryngol Clin North Am 1995; 28:189–205.

Sprinzl GM, Wolf-Magele A, Schnabl J, Koci V. The active middle ear implant for the rehabilitation of sensorineural, mixed and conductive hearing losses. Laryngo-Rhino-Otologie. 2011;90(9):560–572.

Takagi, M, Taki, Y, Sakane, T, Nadai, T, Sezaki, H, Oku, N, and Yamashita, S. A new interpretation of salicylic acid transport across the lipid bilayer: implications of pH-dependent

but not carrier-mediated absorption from the gastrointestinal tract. J. Pharmacol. Exp. Ther. 1998; 285, 1175-1180.

Takemura K, Komeda M, Yagi M, Himeno C, Izumikawa M, Doi T, Kuriyama H, Miller JM, Yamashita T. Direct inner ear infusion of dexamethasone attenuates noise-induced trauma in guinea pig. Hear Res. 2004; 196:58–68

Tasaki I. Nerve impulses in individual auditory nerve fibers of guinea pig. J Neurophysiol. 1954; 17:97–122.

Tanaka Y, Asanuma A, Yanagisawa K. Potentials of outer hair cells and their membrane properties in cationic environments. Hear Res. 1980; 2:431–438.

Tanaka K, Motomura S. Permeability of the labyrinthine window in guinea pigs. Arch Otorhinolaryngol. 1981; 233:67–75.

Taylor GI. Dispersion of soluble matter in solvent flowing slowly through a tube. Proc R Soc A 1953; 219:186–203.

Temchin, AN, Rich, NC, and Ruggero, MA. Threshold tuning curves of chinchilla auditory-nerve fibers. I. Dependence on characteristic frequency and relation to the magnitudes of cochlear vibrations. J. Neurophysiol. 2008; 100, 2889-2898.

Thalen E, Wit H, Segenhout H, Albers F. Inner ear pressure changes following square wave intracranial or ear canal pressure manipulation in the same guinea pig. Eur Arch Otorhinolaryngol. 2002 ;259 (4) :174-9

Thorlabs. CTN003603-S01, Rev B data sheet. 2020

Thorne M, Salt AN, DeMott JE, Henson MM, Henson Jr OW and Gewalt SL. Cochlear fluid space dimensions for six species derived from reconstructions of three-dimensional magnetic resonance images. Laryngoscope 1999; 109, 1661–1668.

Tian J, Huang X, Rao Z, Ta N, Xu L. Finite element analysis of the effect of actuator coupling conditions on round window stimulation. Journal of Mechanics in Medicine and Biology. 2015;15(4):19.

Tos M, Salomon G. Bonding P. Implantation of electromagnetic ossicular replacement device. Ear Nose Throat J. 1994; 73:92–103.

Veldmann JE, Hanada T, Meeuwsen F. Diagnostic and therapeutic dilemmas in rapidly progressive sensorineural hearing loss and sudden deafness. Acta Otolaryngol. 1993; 113:303–306.

Visaton. K 16 - 8 Ohm. Art. No. 2815 data sheet. 2015.

Wangemann P. Supporting sensory transduction: Cochlear fluid homeostasis and the endocochlear potential. J Physiol. 576:11-21, 2006.

Watson EJ. Diffusion in oscillatory pipe flow. J Fluid Mech 1983; 133:233–44.

Weaver SP, Schweitzer L. A radial gradient of fibril density in the gerbil tectorial membrane. Hear Res. 1994; 76:1–6.

Weddell TD. Mechanisms of excitation and amplification in the mammalian cochlea. In Pharmacy and Biomolecular Sciences. 2013; 182.

Weddell TD, Yarin YM, Drexl M, Russell IJ, Elliott SJ, Lukashkin AN. A novel mechanism of cochlear excitation during simultaneous stimulation and pressure relief through the round window. J. R. Soc. Interface 2014; 11: 20131120.

Wei BPC, Mubiru S, O'Leary. Steroids for idiopathic sudden sensorineural hearing loss. Cochrane Database of Systematic Reviews. 2009; 1.

White HJ, Helwany M, Peterson DC. Anatomy, Head and Neck, Ear Organ of Corti. [Updated 2020 Oct 27]. In: StatPearls [Internet]. Treasure Island (FL): StatPearls Publishing; 2020.

Who.int. Deafness and Hearing Loss. 2020 [online] Available at: <https://www.who.int/news-room/fact-sheets/detail/deafness-and-hearing-loss> [Accessed 15 December 2020].

Wilk M, Hessler R, Mugridge K, et al. Impedance Changes and Fibrous Tissue Growth after Cochlear Implantation Are Correlated and Can Be Reduced Using a Dexamethasone Eluting Electrode. PLOS ONE. 2016;11: e0147552.

Wilson WR, Byl FM, Laird N. The efficacy of steroids in the treatment of idiopathic sudden hearing loss. A double-blind clinical study. Arch Otolaryngol. 1980; 106:772–776.

Wu, T, Lv, P, Kim, HJ, Yamoah, EN, and Nuttall, AL. Effect of salicylate on KCNQ4 of the guinea pig outer hair cell. J. Neurophysiol. 2010; 103, 1969-1977.

Wysocki, jarosław & Sharifi, Mansoor. Measurements of selected parameters of the guinea pig temporal bone. Folia morphologica. 2005; 64. 145-50.

Yang S, Xu D, Liu X. Evaluation of Round Window Stimulation Performance in Otosclerosis Using Finite Element Modelling. Computational and Mathematical Methods in Medicine. 2016; 2016.

Yates, GK. Basilar membrane nonlinearity and its influence on auditory nerve rate-intensity functions. Hear. Res. 1990; 50, 145-162.

Yener HM, Sarı E, Aslan M, Yollu U, Gözen ED, İnci E. The Efficacy of Intratympanic Steroid Injection in Tinnitus Cases Unresponsive to Medical Treatment. J Int Adv Otol. 2020;16(2):197-200. doi:10.5152/iao.2020.7588

Yuan, A, Huan, W, Liu, X., Zhang, Z, Zhang, Y, Wu, J, and Hu, Y. NIR light-activated drug release for synergetic chemo-photothermal therapy. Mol. Pharm. 2017; 14, 242-251.

Zhang X, Gan RZ. A comprehensive model of human ear for analysis of implantable hearing devices. IEEE Transactions on Biomedical Engineering. 2011;58(10):3024–3027.

Zhang X, Gan RZ. Dynamic properties of human round window membrane in auditory frequencies running head: dynamic properties of round window membrane. Med Eng Phys. 2013;35(3):310-318.

Zou, J, Sood, R., Zhang, Y, Kinnunen, PK, and Pyykkö, I. Pathway and morphological transformation of liposome nanocarriers after release from a novel sustained inner-ear delivery system. Nanomedicine 2014; 9, 2143-2155.

Zurek PM. Spontaneous narrowband acoustic signals emitted by human ears. J. Acoust. Soc. Am. 1981; 69: 514–523.

Appendix

Only diffusion along the long axis x of the tube of decreasing diameter is considered (Figure 3.1A). The concentration c within each cross-section for a fixed instance *t* is assumed to be constant, i.e. $c = c(x,t)$ is independent to the$y$axis. If the area of the cross-section is $S(x)$, then the flux J along the$x$axis is given by:

$$J(x,t) = -S(x) \cdot k_d \cdot \frac{dc(x,t)}{dx}, \tag{A20}$$

where k_d is the diffusion coefficient.

At the same time the clearing of salicylate from the tube of length Δx, its perimeter $P(x)$ and with an area of surface $P(x)\Delta x$, can be described as:

$$Cl(x,t) = c(x,t) \cdot k_c \cdot P(x) \cdot \Delta x, \tag{A21}$$

where k_c is the clearing coefficient.

The balance of fluxes and clearing in the volume between x_0 and x_1 can be described as:

$$S(x) \cdot \Delta x \cdot \frac{dc(x,t)}{dt} = S(x_1) \cdot k_d \cdot \frac{dc(x_1,t)}{dx} - S(x_0) \cdot k_d \cdot \frac{dc(x_0,t)}{dx} - c(x,t) \cdot k_c \cdot P(x) \cdot \Delta x, \tag{A22}$$

where $\Delta x = x_1 - x_0$ is positive and x is in $[x_0, x_1]$.

Divide both sides of Eq (A22) by Δx and rearrange it as follows:

$$S(x) \cdot \frac{dc(x,t)}{dt} = \frac{S(x_1) \cdot k_d \cdot dc(x_1,t)/dx - S(x_0) \cdot k_d \cdot dc(x_0,t)/dx}{\Delta x} - c(x,t) \cdot k_c \cdot P(x). \tag{A23}$$

Take the limit of Δx converging to zero and divide by $S(x)$, the following is obtained:

$$\frac{dc(x,t)}{dt} = \frac{1}{S(x)} \cdot \frac{d}{dx}\left(S(x) \cdot k_d \cdot \frac{dc(x,t)}{dx}\right) - c(x,t) \cdot L(x), \tag{A24}$$

where $L(x) = k_c \cdot \frac{P(x)}{S(x)}$ is an integral coefficient of clearing.

The perimeter is

$$P(x) = 2\pi \cdot (mx + a) \tag{A25}$$

and the area is

$$S(x) = \pi \cdot (mx + a)^2, \tag{A26}$$

where $m = (b - a)/l$.

The integral coefficient can be written as:

$$L(x) = k_c \cdot \frac{P(x)}{S(x)} = \frac{2k_c}{r(x)}. \quad \text{(A27)}$$

Thus, the diffusion can be described by the following partial differential equation

$$\frac{dc(x,t)}{dt} = \frac{1}{S(x)} \cdot \frac{d}{dx}\left(S(x) \cdot k_d \cdot \frac{dc(x,t)}{dx}\right) - c(x,t) \cdot \frac{2k_c}{r(x)}, \quad \text{(A28)}$$

with the boundary conditions

$$c(0,t) = c_{rw}, \quad \text{(A29)}$$

$$k_d \frac{dc(l,t)}{dx} = 0 \quad \text{(A30)}$$

and initial conditions

$$c(0,0) = c_{rw}; x = 0, \quad \text{(A31)}$$

$$c(x,0) = 0; x > 0. \quad \text{(A32)}$$

Equation (A28) can be rewritten in the following non-dimensional form

$$\frac{du(\chi,\tau)}{d\tau} = \frac{1}{((b-a)\chi+a)^2} \cdot \frac{d}{d\chi}\left(((b-a)\chi + a)^2 \cdot \frac{du(\chi,\tau)}{d\chi}\right) - u(\chi,\tau) \cdot \frac{2l^2/ratio}{(b-a)\chi+a}, \quad \text{(A33)}$$

with the boundary conditions

$$u(0,\tau) = 1, \quad \text{(A34)}$$

$$ratio \cdot \frac{du(1,\tau)}{d\chi} = 0 \quad \text{(A35)}$$

and the initial conditions

$$c(0,0) = 1; \chi = 0, \quad \text{(A36)}$$

$$c(\chi,0) = 0; \chi > 0, \quad \text{(A37)}$$

where $u = c/c_{rw}$, $\tau = t \cdot k_d/l^2$ and $\chi = x/l$.